ENVIRONMENTALLY MEDIATED TRANSMISSION MODELS FOR INFLUENZA AND THE RELATIONSHIPS WITH METEOROLOGICAL INDICES

by

Sheng Li

A dissertation submitted in partial fulfillment
of the requirements for the degree of
Doctor of Philosophy
(Epidemiological Science)
in The University of Michigan
2011

Doctoral Committee:

Associate Professor Joseph N. Eisenberg, Co-Chair
Professor James S. Koopman, Co-Chair
Professor Mark L. Wilson
Associate Professor Edward L Ionides
Senior Research Scientist Rick Riolo

For the most inspirational teachers of my life:

My parents

My committee members, particularly my co-chairs

ACKNOWLEGEMENTS

I have been extremely fortunate to work with generous and highly skilled colleagues and mentors. I would particularly like to thank my dissertation committee: Mark Wilson, Edward Ionides, Rick Riolo, and my co-advisors, Jim Koopman and Joe Eisenberg. They have always provided outstanding intellectual and emotional supports. Their instruction and suggestions have fundamentally shaped and improved the work here in complementary ways.

The greatest privilege has been the opportunity to watch and learn from two most inspiring epidemiologists in the modeling field, Jim Koopman and Joe Eisenberg. I am inspired by their enthusiasm, professionalism, creativity and talent. I thank Jim for introducing me to transmission modeling research field and supervising most of my work. I thank Joe for his extensively mentoring me through the most difficult time during my research. I would like to thank Mark Wilson specially for inspiring me to conduct more practical epidemiology research for the benefit of public health. I thank Rick for his patience and feedback in complex system scientific issues. I would also like to thank Ed for providing constructive suggestions on statistical methods and theory.

Many thanks go to all my peer colleagues in Jim/Joe's lab group, including Ian Ispickna, Josep M. Serra, Jijun Zhao, Nottasorn, and Bryan Mayers. Specifically, I thank Ian for working closely in the same project and co-authorships. Jijun Zhao constructively assisted with agent based model analysis. I am also grateful for having been surrounded by gracious and skilled fellow doctoral students, including TW Chuang, Ethan, Jong-

Hoon Kim, and Megan. They have provided an intellectually stimulating environment in the infectious disease Epidemiology program.

My special thanks should finally go to my families in China, and my wife, Dr. Xiaorong Yan. Without their support, I could not go this far along my journey.

I would like to acknowledge the financial support of this work. This work was supported by the US EPA STAR Program, and US DHS University Programs grant R83236201 to Drs. Joe Eisenberg and Jim Koopman.

A paper of "Dynamics and Control of Infections Transmitted from Person to Person through the Environment" based on the essential findings of Chapter 2 has been published in *American Journal of Epidemiology* in May 2009. Portions of Chapter 3 and Chapter 4 were prepared and will be submitted to scientific journals.

TABLE OF CONTENTS

LIST OF TABLES

LIST OF FIGURES

ABSTRACT

ENVIRONMENTALLY MEDIATED TRANSMISSION MODELS FOR INFLUENZA AND THE RELATIONSHIPS WITH METEOROLOGICAL INDICES

By

Sheng Li

Co-Chairs: Joseph N.S. Eisenberg and James S. Koopman

High public health concerns for future influenza pandemics and ongoing avian influenza emerging outbreaks need extended studies on influenza. In this dissertation, the impact of environmental factors on human influenza transmission was explored by using multiple modeling approaches.

An environmental infection transmission system (EITS) compartmental model that describes the dynamics of human interaction with pathogens in the environment was developed. Its environmental parameters include: the pathogen elimination rate, μ; and the rate humans pick up pathogens, ρ, and deposit them, α. The ratio, $\rho N / \mu$, (N equals population size) indicates whether transmission is density dependent (low ratio) or frequency dependent (high ratio), or in between. The environmental contamination ratio, α / γ, where γ is the recovery rate, reflects total agent deposition per infection and outbreak probability.

The temporal dynamics of the relative importance of different influenza transmission modes over the course of epidemics were further studied in an EITS agent-

based model. The temporal variation of the relative importance of different influenza transmission modes is primarily attributable to the environmental dissemination and persistence effects of influenza virus particles in air and on surfaces. Some model parameters, including movement rate, virus die off rate and surface touching rate, significantly alter the temporal dynamics of the relative importance of different influenza transmission modes.

A second smaller or equal-sized summer epidemic was identified in 9 of 11 years of study period in Hong Kong, China. We found that a new dominant subtype strain is commonly associated with this second peak. Multiple local weather variables and global climatic indices are statistically significantly associated with the influenza virus positive proportion of virus isolates, and the proportion of Influenza-like illness (ILI) case among all patients who visit influenza surveillance network clinics. We found that the correlations between influenza morbidity and absolute humidity are the strongest among all weather variables. The significant negative absolute humidity anomaly two weeks prior to the onset of influenza epidemics was identified.

These findings will provide theoretical contexts to examine the role of the environment in influenza transmission and scientific suggestions for improving public health surveillance.

CHAPTER 1

INTRODUCTION TO INFLUENZA, INFLUENZA TRANSMISSION MODELS, AND THE RELATIONSHIPS BETWEEN CLIMATE AND INFLUENZA

Influenza is a major cause of acute respiratory disease among humans and is associated with global pandemics and annual epidemics. Influenza poses a serious public health threat and causes significant morbidity, mortality, and economic burden globally. In the United States, influenza is estimated to cause more than 200,000 hospitalizations and 36,000 deaths annually (1). In European countries, influenza can cause similar heath impacts (2, 3). In Asian regions, influenza is significantly related to respiratory and cardiovascular disease hospitalization (4).

The global spread of a new swine influenza H1N1 strain in 2009 and ongoing spread of H5N1 avian influenza strains reveal the necessity of extended studies on influenza. The influenza virus is transmitted among humans through air and fomite mediated contact. In this work, the impact of environment factors was explored by using multiple modeling approaches. Deterministic compartmental and agent-based modeling approaches were applied to develop environmental mediated influenza transmission models in chapter 2 and chapter 3. Lagged correlation test and time series analysis were used to examine the relationship between meteorological factors and influenza in chapter 4. New findings about temporal dynamics of influenza dominant transmission mode and absolute humidity were achieved. These findings capture previously under-recognized or

under-estimated perspectives which are important for population influenza transmission. We expect the results from this research will contribute to building a better theoretical basis for influenza research and intervention.

INFLUENZA VIROLOGY AND EPIDEMIOLOGY

Virology of Influenza Virus

Influenza is caused by RNA viruses of the family orthomyxoviridae (5). There are three main types, influenza A, B, and C. Type A influenza virus is subdivided into sub-serotypes based on two surface antigens: hemagglutinin (H) and neuraminidase (N). There are total of sixteen hemagglutinin (H) and nine neuraminidase (N) surface antigens (1, 6). Some confirmed subtypes in humans include H1N1, H2N2, H3N2, H5N1 and H9N2. Type A influenza virus can infect birds and mammals, and is the most virulent in humans, causing moderate to severe illness in all age groups. Subtype H3N2 is commonly associated with greater and quicker clinical incidence peaks (3). Type B virus almost exclusively infects humans and can cause milder epidemics (7). Type C virus can infection humans, dogs, and pigs, but is less common than other types in humans (8, 9).

Influenza virus constantly evolves by mutation or reassortment (10). Mutations can result in minor changes in H and N and in similar antigens. This is called antigenic drift. In contrast, reassortment causes major changes in H and N resulting in completely new antigens, which is called antigenic shift. Antigenic drift might cause epidemics but people who were previously infected by the parent strain might still be immune to the novel strain (11). Antigenic shift might cause pandemics because all people are susceptible to the novel strain (12).

Influenza virus strains can be very contagious, and some studies have shown that as few as 0.67 TCID50 (50% Tissue Culture Infective Dose) unit of influenza virus may cause infection in healthy adults (13). Influenza viruses cannot multiply outside of live cells but can survive in the air and on environmental surfaces. Both temperature and humidity influence its survivability (14).

Influenza Infection Clinical Characteristics

Clinical manifestations of influenza infection include fever, chills, sore throat, coughing, muscle pains, headache, and fatigue. Coughs, sore throat, and fever are the most frequent symptoms. Influenza is almost clinically undistinguishable from many other acute respiratory infections. Influenza infection has an average 1 to 2 day incubation period, followed by clinical symptoms usually lasting 3-7 days (1). Infectious people shed virus from the second to the eighth day, and the virus peaks at the third day after infection (15). The majority of infected people develops one or more symptoms and completely recovers without serious complication or long-term health effects (16). The very young, the elderly, and immune-compromised persons may have complications (1), and therefore are the target population of annual influenza vaccination.

In clinical settings, diagnosis commonly is based on clinical symptoms and not on laboratory tests. All age groups are susceptible to novel strains, though adults might be immune to previously circulated virus strains. Influenza infection can recur throughout the whole lifetime of a person due to consistent novel strains from viral mutation and reassortment.

Influenza Transmission Mode among Humans

Previous studies have suggested evidence of multiple transmission modes for influenza transmission. Some research suggests the possibility of respirable air transmission dominance (17, 18). Other research finds that large droplet transmission could be the primary influenza transmission mode (19, 20). Contact mediated transmission might be also dominant in some contexts (21). Understanding the mode dominance and potential temporal dynamics of mode dominance is of great public health significance. The most effective intervention strategies could be determined only based on this knowledge.

Influenza Infection Burden Measurements

In ongoing influenza surveillance system, because of the high prevalence among all human age groups and the economic and technologic impracticality of etiologic diagnosis in reality, Influenza morbidity and mortality are commonly only examined among a fraction of patients who visit surveillance sentinel clinics/hospitals. Influenza morbidity and mortality measurements are based on Influenza-like illness (ILI) cases and pneumonia and influenza (P&I) deaths respectively from influenza surveillance system. ILI is defined as high fever $\geq 38\ ^{0}C$ plus cough or sore throat. The proportion of outpatients who are diagnosed as ILI from influenza surveillance sentinel clinics and hospitals is common influenza morbidity indicator. The P&I death rate or the proportion of deaths attributed to P&I are common influenza mortality indictor.

Typical ILI is defined as a clinical presentation consisting of the sudden onset of fever $>37.8\ ^{0}C$, plus cough or sore throat (22). Other common symptoms include

headache, nasal congestion, watering eyes, body aches, muscle pain, and fatigue. Various etiological agents can cause ILI, including influenza virus, respiratory syncytial virus (RSV), streptococcus pneumoniae, haemophilus influenzae, and others (23). ILI symptoms, except fever, could not reliably distinguish influenza infections from those caused by other etiologies (24). P&I deaths could be also attributed to other etiologies besides influenza viruses. Therefore, the major complication of influenza ILI and P&I indicators are sensitivity and specificity issues. This problem can only be resolved by extensive viral detection from patients. However, combinations of the ILI symptoms could present influenza with relative good sensitivity. For example, more than 79% of influenza can be predicted by combination of fever and cough (25). Commonly, influenza mortality and morbidity burden temporal patterns were estimated based on statistical models (26).

Influenza Surveillance System and Seasonality

The WHO global influenza surveillance network was established in 1952. As of 2010, there are 135 national surveillance centers (NICs) from 105 countries and six WHO collaborating centers (WHO CCs) from Australia, China, Japan, United Kingdom, and United States. NICs sample ILI patients and submit representative isolates to WHO CCs for antigenic and genetic analyses. On average, 175,000 ILI patients and 2,000 viral isolates are submitted annually from this surveillance network (27). In temperate regions of developed countries, such as North America, Europe and Australia, influenza sentinel surveillance systems have been implemented for decades (28). In most tropical and sub-

tropical countries, however, influenza surveillance systems have only recently been developed or remain non-existent.

In the United States, the Center for Disease Control and Prevention (CDC) influenza surveillance system components include outpatient ILI surveillance, viral surveillance, mortality surveillance, and hospitalization surveillance. The ILI surveillance network consists of more than 3,000 healthcare providers from 1,800 outpatient care sites across the United States reporting more than 25 million patient visits each year. Viral surveillance network includes 80 U.S. WHO collaborating laboratories and 60 National Respiratory and Enteric Virus Surveillance System (NREVSS) laboratories. Vital statistics offices from 122 U.S. cities are on the mortality surveillance network. U.S. influenza surveillance system reports weekly ILI, virus isolation, influenza-associated hospitalization and death (29).

China, particularly southern China, has long been referred to as one of the possible global influenza epidemic centers based on influenza virus transmission among birds, pigs and humans (30). Two of the three recorded influenza pandemics in human history, the "Asian Flu" caused by H2N2 in 1957-58 and the "Hong Kong Flu" caused by H3N2 strain in 1968-69, first emerged or were detected in Hong Kong and adjacent regions in China (31). Hong Kong is an important component in the WHO global influenza surveillance network. Hong Kong enhanced and extended its pre-existing influenza sentinel surveillance system after the first human H5N1 outbreak in 1997 (32). The Hong Kong influenza surveillance system consists of 50 private practitioners and 42 sentinel clinics covering a population of 6.8 million. The surveillance system reports weekly ILI and virus isolation year around.

Influenza seasonality in temporal regions is relatively well-identified, where annual influenza epidemics occur in winter months for both north and south hemispheres (33-36). In the U.S., the flu season usually starts in October or November and peaks some time from December to March (34). Influenza seasonality in tropic/sub-tropic regions is still poor defined. Annual and biannual influenza epidemics were identified in some years in Hong Kong (37, 38). Although many efforts have been made the mechanisms underlying seasonality is not clear. However, the obvious correlation between influenza seasonality and environmental effects and population behaviors were observed. These factors include weather, pollution, and seasonal human activities (28). Accurate prediction of the shape of future influenza seasons based on previous data and current knowledge is unavailable.

Influenza and Climate

Awareness of relationships between influenza and weather reaches back to early twentieth century in the United States (28). In a medical book published before 200 AD in China, Zhang Zhongjing, one of the most famous traditional Chinese Medicine healers argued that what we now consider influenza-like illness is caused by cold environmental conditions, one of six major disease causalities (wind, coldness, hotness, humidity, dryness, fire) (39).

The associations between climate and human influenza transmission are highly complex. Some evidence suggests that upper respiratory tract epidemics, including influenza, might be associated with rapid change in temperature and sudden cold weather (40). Rainfall has been associated with subtype B influenza in Singapore and a German

study demonstrated that air pressure is also an importance factor (41). A recent laboratory study on animals showed that both temperature and relative humidity (RH) are associated with influenza virus survivability and transmissibility, however, absolute humidity (AH) might be more important than RH (42, 43). The association between AH and influenza related mortality has been demonstrated in regions of the Americas (44). But the relationship between AH and influenza morbidity in tropic/subtropic regions has not been examined.

In addition to local weather or climatic indices, several recent studies have linked large-scale global climate indices to influenza seasonal variability. Viboud et al. examined the influence of global climate on influenza activities from 1979-2000 in France. Associations between a global climatic index, the Multivariable ENSO Index (MEI), influenza-related mortality and ILI were found (2). Greene et al. examined both local and global climatic indices in relation to P&I mortality in different climate regions in the United States, and found that temperature and West Pacific index were weakly associated with P&I in some climate regions (45).

The underlying mechanisms by which climate variability affects influenza seasonal variation still remain poorly understood, especially in the tropical and sub-tropical regions. The potential confounders such as environmental factors, human social behavior, and influenza clinical classification contribute to this problem (28). We explored associations between AH, global climate indices and ILI rate and virus positive proportion in subtropic metropolitan region, the city of Hong Kong in Chapter 4. The work in chapter 4 is not intended to explore the underlying mechanisms, but rather to

describe the observed relationships between weather and influenza morbidity in tropic/subtropic regions.

TRANSMISSION MODELS FOR INFLUENZA

Mathematical Models for Influenza Infection

Bio-mathematicians and infectious diseases epidemiologists commonly use deterministic compartmental models that assume instantaneous contacts with instantaneously thorough mixing to explore infection transmission dynamics and to develop public health policy (46-48). Compartmental models can provide insight into transmission dynamics and policy making, and is computationally efficient. For example, Chowell et al. developed a compartment model to assess the hypothetical intervention efficacy in the influenza pandemic of 1918 in Switzerland (49). The popularity of using these models is primarily due to the availability of simple and powerful analytical tools. However, compartmental models use major model assumptions to reduce systematic complexity. These assumptions commonly include homogeneity of individual contagiousness and susceptibility, homogeneous instantaneous contact process for individuals, instantaneous mixing, unlimited dividable population, and constant contagiousness and recovery. These model assumptions rarely hold for infectious diseases including influenza. The physical environment is often not explicitly explored in non-vector born infections such as influenza. Population infection transmission is normally a complex system, where population demography, individual immunity, individual social status and social connections, microbial contagiousness, survivability, dispersion, dose-response relationship, environmental contamination, and

temperature all are important (50). Previous influenza transmission modeling studies normally formulated infection transmission processes as a simple probability while ignoring the detailed physical environmental contact processes (49). Recent studies showed the environment mediates influenza transmission process from one person to another, and provides points for infection control (51-56). The rational of inclusion of environmental mediating process in infectious disease models is to simulate more realistic infection transmission and to pursue intervention strategies that require activity via environment.

Environmental mediation plays a very important role in human infection transmission. The authors of one of the major text on infection transmission risks has argued that majority of human infections were acquired through the environment (e.g. food, water, air, fomites) and only small part of infection were acquired by direct contact, such as kissing, skin to skin transfer, and sexual activity (57). Traditionally, environmental microbiologists have detected microbes from environmental samples and environmental health and environmental engineering scientists have simulated infectious pathogens spreading in environments by using various equation-based methods. For example, computational fluid dynamics (CFD) based on different equations has been widely used to simulate how pathogens spread in hospital settings. Monte Carlo simulation methods have been applied to simulate air fluidity with pathogens in enclosed health care settings (58).

These methods commonly only explain the instantaneous “direct risk” of environmental microbes at the individual level. Population system dynamics and secondary transmissions caused by other infectious individuals are often not considered

in these models. Influenza pathogens transmitted through the environment cause risks both at the individual level and at the population level. Environmental microbial contaminations have direct effects on exposed individuals, but transmissible pathogens may also have indirect effects on population infection levels due to secondary transmission. Various factors like environmental contamination level, person-environment contact patterns can modify the real risk effect [52]. The generalizability of these purely direct effect models to realistic epidemic scenarios is limited because subsequent circulation of infection may be more important than those initially contaminated for most transmissible pathogens.

Traditionally population transmission modeling and environmental modeling have their own refined systematic theories, and have not been integrated into a systems science capable of dealing with environmental factors associated with population infection transmission. In Chapter 2, we integrate the compartmental deterministic transmission model with an environmental model to explicitly explore environment effects in the influenza transmission process. The compartment models can specify media contamination, agent survival and media uptake. The data of environmental microbes provides more accurate scientific information for epidemiological modeling. This population infection transmission system modeling using approaches that integrate diverse model forms might strengthen infection disease epidemiological theory.

Agent Based Modeling for Influenza Infection

Agent-based models (ABM) have been widely used in ecology, social science, politics, economics and molecular biology (59, 60). The rational behind ABM is that

individual entities interact with one another or with the external environment. The local, possibly stochastic individual interactions influence global system-wide dynamics and patterns. This rationale makes it suitable to study population infection transmission where individual heterogeneity and spatial interactions are critical. ABM is a bottom-up approach to mimic greater details that normally cannot be captured by compartmental modes. The ABM approach allows each individual and each interaction between individuals to be unique and can specify contact duration and connection patterns between individuals, which are not possible using compartmental models. Practically, an ABM approach builds a computational model of individual agents and simulates the system dynamics according to certain rules. A complete ABM model includes data collection, model building, exploration of the model behavior, the collection of statistics, and validation of the model.

ABM is a complementary to equation-based modeling (EBM) for exploring the complexity of a system and is more intuitive to non-mathematicians. Especially in infectious disease epidemiology, we view population infection transmission as a complex process involving spatial and temporal organization and interactions of numerous elements. ABM has been introduced to epidemiology in the 1960's, however, it became more popular and was used more frequently after the 2001 anthrax bioterrorism event. For example, Stephen Eubank et al. developed a highly resolved agent-based simulation model (EpiSims) with realistic population mobility to gain insights of infectious diseases outbreaks (61). Joshua M. Epstein et al. applied an ABM to simulate smallpox epidemic in county level and test the potential for different control strategies (62). Longini et al.

constructed an AMB to test influenza control strategies (63). All these models do not include detailed human and physical environment interactions.

There is clear a shortage of knowledge regarding environmentally mediated influenza transmission due to individual heterogeneity. A system of models that can explore more realistic human environment contact in a population is urgently needed when preparing for future influenza pandemics. To effectively control influenza epidemics, it is critical that we consider it as a dynamic, heterogeneous, and environmentally-mediated process. Heterogeneity during population transmission process comes from multiple sources, for example, difference in pathogens' intrinsic infectivity and virulence; variability in individual exposure, individual disease pattern in incubation, severity and duration, differences in population level movement patterns, herd immunity level, population environmental exposures; and difference in venue characteristics. These heterogeneities affect influenza infection risk from an environmental microbial exposure.

There is a trade-off between the model complexity and the parameter identifiability based on available real world measurements. An overly complex model is difficult to analyze, and some variables may not be measured and some parameters may not be identifiable. On the other hand, an overly simple model may miss some important biological mechanisms and make incorrect inferences that are not robust to realistic relaxation of simplifying assumptions. An ideal model should be simple enough to incorporate available data and complex enough to capture important mechanisms and not lead to numerous inferences that would be changed in important ways if the model had more realistic details.

In the chapter 3, we developed an agent-based transmission model which integrates environmental factors. Population characteristics, social connections, pathogen features, and environmental factors were explicitly studied. Temporal variation of the relative importance of different transmission modes were explored, which could not have been effectively pursued using a deterministic compartmental model. Compartmental models are easier to analyze, but ABMs are a natural extension of compartmental models and can deal with population heterogeneity and environmental interaction better in influenza transmission. This model will help test effectiveness of alternative control strategies in more realistic settings.

OBJECTIVES AND HYPOTHESES

Our overall objective is to explore the importance of environmental mediation process and environmental relevant factors in influenza population transmission. In the second chapter, we evaluate the hypothesis that environmental effects can significantly alter population transmission processes and intervention efficacies using a deterministic compartmental model. The third chapter's hypothesis is that the dominant transmission mode of influenza is inconsistent during epidemics, and that an environmental dispersion effect and a persistence effect contribute to the temporal dynamics. Reaching that inference required the use of an agent based model. It is hypothesized in the fourth chapter that influenza morbidity is associated with local weather variables and global climate indices. The fifth chapter summarizes the major outcomes in chapter two to four, and outlines potential limitations and future research directions.

Software Tools

In this work, Berkeley-Madonna was used to build compartmental deterministic models. This software is designed to numerically solve differential equations and has many useful functions for drawing parameter figures and processing sensitivity analysis. JAVA was the primary programming language for agent based model and stochastic compartmental model development. R package was used in all statistical analysis and is free open source statistical software.

REFERENCES

1. CDC. Flu in the United Staes. National Center for Infectious Disease. http://ww.cdc.gov/flu/. Access in 2009.

2. Viboud C, Pakdaman K, Boe¨lle PY, Wilson ML, Myers MF, et al. Association of influenza epidemics with global climate variability. *Eur J Epidemiol* 2004;19:1055–1059.

3. Fleming DM, Zambon M, Bartelds AI, de Jong JC. The duration and magnitude of influenza epidemics: A study of surveillance data from sentinel general practices in England, Wales and The Netherlands. *Eur J Epidemiol* 1999; 15: 467–473.

4. Chit Ming Wong, Lin Yang, King Pan Chan, Gabriel M. Leung, Kwok H. Chan, Yi Guan, Tai Hing Lam, Anthony Johnson Hedley, Joseph S. M. Peiris. Influenza-Associated Hospitalization in a Subtropical City. *PLoS Medicine*. 2006: Volume 3, Issue 4, e121, P485-491.

5. Kilbourne ED: Influenza New York: Plenum Press; 1987.

6. Fouchier RAM, Munster V, Wallensten A, Bestebroer TM, Herfst S, Smith D, et al. Characterization of a novel influenza A virus hemagglutnin subtype (H16) obtained from black-headed gulls. *J Virol* 2005;79(5):2814-2822.

7. Hay, A, Gregory V, Douglas A, Lin Y. "The evolution of human influenza viruses. *Philos Trans R Soc Lond B Biol Sci*, 2001;356(1416):1861–70. doi:10.1098/rstb.2001.0999.

8. Matsuzaki, Y; Sugawara K, Mizuta K, Tsuchiya E, Muraki Y, Hongo S, Suzuki H, Nakamura K. Antigenic and genetic characterization of influenza C viruses which caused two outbreaks in Yamagata City, Japan, in 1996 and 1998. *J Clin Microbiol* 2002;40 (2): 422–9. doi:10.1128/JCM.40.2.422-429.

9. Matsuzaki, Y; Katsushima N, Nagai Y, Shoji M, Itagaki T, Sakamoto M, Kitaoka S, Mizuta K, Nishimura H. Clinical features of influenza C virus infection in children. *J Infect Dis* 2006;193 (9):1229–35. doi:10.1086/502973

10. Hay, A; Gregory V, Douglas A, Lin Y. "The evolution of human influenza viruses". *Philos Trans R Soc Lond B Biol Sci*. 2001;356 (1416): 1861–70. doi:10.1098/rstb.2001.0999

11. Wolf, Yuri I, Viboud, C, Holmes, EC, Koonin, EV, Lipman, DJ. Long intervals of stasis punctuated by bursts of positive selection in the seasonal evolution of influenza A virus. *Biol Direct* 2006;1(1):34. doi:10.1186/1745-6150-1-34.

12. Parrish, C; Kawaoka Y. The origins of new pandemic viruses: the acquisition of new host ranges by canine parvovirus and influenza A viruses. *Annual Rev Microbiol* 2005;59:553–86. doi:10.1146/annurev.micro.59.030804.121059

13. Alford RH, Kasel JA, Gerone PJ, et al. Human influenza resulting from aerosol inhalation. *Proc Soc Exp Biol Med*. 1996;122(3):800-804.

14. RM Epan, RF Epan. The thermal denaturation of influenza virus and its relationship to membrane fusion. *Biochem. J.,* 2002;365:841-848

15. Murphy BR, Chalhub EG, Nusinoff SR, et al. Temperature-sensitive mutants of influenza virus. 3. Further characterization of the ts-1(e) influenza A recombinant (H3N2) virus in man. *J Infect Dis.* 1973;128:479-487.

16. Frederick G. Hayden, R. Scott Fritz, Monica C. Lobo, W. Gregory Alvord, Warren Strober, and Stephen E. Straus. Local and Systemic Cytokine Responses during Experimental Human Influenza A: Virus Infection Relation to Symptom Formation and Host Defense. *JCI.* 1998;Volume 101, Number 3, 643–649.

17. Raymond Tellier. Review of aerosol transmission of influenza a virus. *Emerg Infect Dis.* 2006;Vol. 12, No. 11.

18. Samira Mubareka, Anice C. Lowen, John Steel, et al. Transmission of influenza virus via aerosols and fomites in the guinea pig model. *J Infect Dis.* 2009; 199:858–65.

19. Brankston G, Gitterman L, Hirji Z, Lemieux C, Gardam M Transmission of influenza A in human beings. *Lancet Infect Dis* 2007;7: 257-265. doi:10.1016/S1473-3099(07)70029-4

20. Carolyn Buxton Bridges, Matthew J. Kuehnert, and Caroline B. Hall. Transmission of Influenza: Implications for Control in Health Care Settings. *Clin Infect Dis* 2003; 37:1094–1101.

21. Spicknall IH, Koopman JS, Nicas M, Pujol JM, Li S, et al. Informing Optimal Environmental Influenza Interventions: How the Host, Agent, and Environment Alter Dominant Routes of Transmission. *PLoS Comput Biol* 2010;6(10): e1000969. doi:10.1371/journal.pcbi.1000969.

22. CDC. Influenza activity – United States, 2001-2002 season. *JAMA* 2002;287(1):35-40.

23. D S Hui, J Woo,1, E Hui, A Foo,1 M Ip, K-W To, E Cheuk, W-Y Lam, A Sham, P K S Chan. Influenza-like illness in residential care homes: a study of the incidence, aetiological agents, natural history and health resource utilization. *Thorax* 2008;63:690–697. doi:10.1136/thx.2007.090951.

24. Navarro-Mari JM, Perez-Ruiz M, Cantudo-Munoz P, Petit-Gancedo C, Jimenez-Valera M, et al. Influenza-like illness criteria were poorly related to laboratory-confirmed influenza in a sentinel surveillance study. *J Clin Epidemiol* 2005;58: 275–279.

25. Monto AS, Gravenstein S, Elliott M, Colopy M, Schweinle J. Clinical signs and symptoms predicting influenza infection. *Arch Intern Med* 2000;160:3243–3247.

26. Cowling BJ, Wong IO, Ho LM, Riley S, Leung GM. Methods for monitoring influenza surveillance data. *Int J Epidemiol.* 2006;35:1314–21. DOI: 10.1093/ije/dyl162

27. Thompson WW, Shay DK, Weintraub E, Brammer L, Cox N, Anderson LJ, et al. Mortality associated with influenza and respiratory syncytial virus in the United States. *JAMA* 2003;289(2):179-186.

28. WHO. http://www.who.int/csr/disease/influenza/surveillance/en/index.html. WHO Global Surveillance Network. Access 2010.

29. David N. Fisman. Seasonality of Infectious Diseases. Annu. *Rev. Public Health*. 2007;28:127-143.

30. CDC. http://www.cdc.gov/flu/weekly/overview.htm. Overview of Influenza Surveillance in the United States. Access 2010.

31. Kennedy F. Shortridge. Is China an influenza epicenter? Chinese Medical Journal 1997;110(8):637-641.

32. Stuart-Harris CH, Schild GC, Oxford JS. Influenza. The Viruses and the Disease. pp. 118–38. Victoria, Can.: Edward Arnold. 2nd ed. 1985.

32. Center for Health Protection. Sentinel Surveillance. Available: http://www.chp.gov.hk/. Accessed 2006 Dec 11.

33. Brammer TL, Murray EL, Fukuda K, Hall HE, Klimov A, Cox NJ. Surveillance for influenza--United States, 1997-98, 1998-99, and 1999-00 seasons. *MMWR Surveill Summ.*. 2002;51(7):1-10.

34. Fleming DM, Zambon M, Bartelds AI, de Jong JC. The duration and magnitude of influenza epidemics: A study of surveillance data from sentinel general practices in England, Wales and The Netherlands. *Eur J Epidemiol* 1999;15: 467–473.

35. Cox NJ, Subbarao K. Global Epidemiology of Influenza: Past and Present. *Ann Rev Med* 2000;51:407–421.

36. Viboud C, Alonso WJ, Simonsen L. Influenza in Tropical Regions. *PLoS Med.* 2006;3(4):e89.

37. Julian W. Tang1, Karry L. K. Ngai1, Wai Y. Lam1, Paul K. S. Chan. Seasonality of Influenza A(H3N2) Virus: A Hong Kong Perspective (1997–2006). *PLoS ONE.* 2008;3(7):e2768.

38. Brian S. Finkelman1, Cecile Viboud, Katia Koelle, Matthew J. Ferraril, Nita Bhartil, Bryan T. Grenfell. Global Patterns in Seasonal Activity of Influenza A/H3N2, A/H1N1, and B from 1997 to 2005: Viral Coexistence and Latitudinal Gradients. *PLoS ONE* 2007;2(12): e1296. doi:10.1371/journal.pone.0001296.

39. http://zh.wikipedia.org/張仲景. Access, July 2010.

40. Eccles R. An explanation for the seasonality of acute upper respiratory tract viral infections. *Acta Otolaryngol* 2002;122:183-191.

41. Babin SM. Weather and Climate effects on disease background levels. *Johns Hopkins Appl. Technical. Digest* 2003;24(1):343-348.

42. Lowen AC, Mubareka S, Steel J, Palese P. Influenza virus transmission is dependent on relative humidity and temperature. *PLoS Pathog* 2007;3:1470–1476.

43. Jeffrey Shaman, and Melvin Kohn. Absolute humidity modulates influenza survival, transmission, and seasonality. *PNAS.* 2009;vol.106;9:3243–3248.

44. Jeffrey Shaman1, Virginia E. Pitzer, Ce´ cile Viboud, Bryan T. Grenfell, Marc Lipsitch. Absolute humidity and the seasonal onset of influenza in the continental United States. *PLoS Biology*. 2010;Volume 8;Issue 2.

45. Sharon Greene. Influenza-associated mortality in the united states: spatio-temporal patterns related to climate and virus subtype. Doctoral dissertation. Ann Arbor, University of Michigan. 2008.

46. Anderson RM, May RM. Infectious Diseases of Humans Dynamics and Control. Oxford University Press; 1992.

47. Diekmann O, Heesterbeek JAP. Mathematical Epidemiology of Infectious Diseases. Wiley John & Sons. Inc.; 2000.

48. D.J. Daley & J. Gani. Epidemic Modelling: An Introduction. Cambridge Univ. Press 1999.

49. G. Chowell, C.E. Ammonb, N.W. Hengartnera, J.M. Hyman. Transmission dynamics of the great influenza pandemic of 1918 in Geneva, Switzerland: Assessing the effects of hypothetical interventions. *J. Theor. Biol.* 2006;241;193–204.

50. Jim Koopman. Modeling infection transmission. *Annu. Rev. Public Health*. 2004;25:303-26.

51. Sheng Li, Joseph N. S. Eisenberg, Ian H. Spicknall and James S. Koopman. Dynamics and Control of Infections Transmitted From Person to Person Through the Environment. *Am J Epidemiol* 2009;170 (2): 257-265. doi: 10.1093/aje/kwp116.

52. Ian H. Spicknall, James S. Koopman, Mark Nicas, Josep M. Pujol, Sheng Li, Joseph N. S. Eisenberg. Informing Optimal Environmental Influenza Interventions: How the Host, Agent, and Environment Alter Dominant Routes of Transmission. *PLoS Comput Biol* 2010;6(10): e1000969. doi:10.1371/journal.pcbi.1000969.

53. Joseph N.S. Eisenberg, Bryan L. Lewis, Travis C. Porco, Alan H. Hubbard, and John M Colford, Jr.. Bias due to Secondary Transmission in Estimation of Attributable Risk From Intervention Trials. *Epidemiology*. 2008;Volume 14, Number 4, 442-50.

54. Joseph N.S. Eisenberg, et al.. Disease Transmission Models for Public Health Decision Making: Analysis of Epidemic and Endemic Conditions Caused by Waterborne Pathogens. *Environ Health Perspect*, 2002;110(8):783:90.

55. C. J. Noakes, C. B. Beggs, P. A. Sleigh and K. G. Kerrs. Modeling the transmission of airborne infections in enclosed spaces. *Int. J. Tuberc. Dis*. 2003;7(11):1015–1026.

56. Richard I. Joh, HaoWang, Howard Weiss, Joshua S. Weitz. (2009) Dynamics of Indirectly Transmitted Infectious Diseases with Immunological Threshold. *Bull Math Biol.* 2009;71: 845–862. DOI 10.1007/s11538-008-9384-4.

57. Charles P. Gerba. Fate and Transport of Pathogens in the Environment. CAMRA 2006 Summer Institute.

58. Charles N. Haas, Joan B. Rose and Charles P. Gerba. Quantitative Microbial Risk Assessment. P41 and P260-312. Wiley John & Sons. Inc.; 1999.

59. Zoltán Toroczkai and Stephen Eubank. Agent-based Modeling as a Decision Making Tool: How to Halt a Smallpox Epidemic. Cutting-Edge Research in Engineering. The bridage. 2005;Vol 35; number 4.

60. V. Grimm, Ten years of individual-based modeling in ecology: what have we learned and what could we learn in the future, *Ecol. Model.* 1999;115:129–148.

61. Stephen Eubank, Hasan Guclu, V. S. Anil Kumar, Madhav V. Marathe, Aravind Srinivasan, Zolta´n Toroczkai & Nan Wang. Modelling disease outbreaks in realistic urban social networks. *Nature.* 2004;Vol429:180-183.

62. Joshua M. Epstein, Derek A. T. Cummings, Shubha Chakravarty, Ramesh M. Singa, and Donald S. Burke. Toward a Containment Strategy for Smallpox Bioterror: An Individual-Based Computational Approach. Brookings Institution Press c. 55pp. 2004.

63. Ira M. Longini, Jr., et al. Containing Pandemic Influenza at the Source. *Science* 2005;309:1083 DOI: 10.1126/science.1115717.

CHAPTER 2

DYNAMICS AND CONTROL OF INFECTIONS TRANSMITTED FROM PERSON TO PERSON THROUGH THE ENVIRONMENT

INTRODUCTION

Human infections that pass from one person to another commonly do so through environmental media such as air, fomites, food, hands, and water. Infection transmission models for non-vector borne infections, however, rarely specify the mode of transmission or the vehicle that carries infection from one person to another. Instead, most models assume that the dynamic details of environmental transmission can be approximated by a point contact process (1-5). With the exception of sexually transmitted diseases, however, the environment often plays a major role in transmission, espaecially for enteric and respiratory diseases. Moreover these environmental processes provide important points of intervention. To promote a transmission system framework that explicitly accounts for environmental process dynamics, we present a transmission model with environmental components that mediate transmission. We call this an environmental infection transmission system (EITS) model.

A number of approaches have been presented for incorporating environmental processes of non-vectorborne infections in transmission models. One approach is to collapse across environmental dynamics resulting in a static description of the

environment (6). Another approach is to explicitly formulate environmental pathogen dynamics. This has been done for water mediated transmission in deterministic (7-11) and stochastic (12) formulations, as well as for air and fomite mediated transmission of influenza (13). We both generalize and abstract these approaches in our EITS framework.

Much of the previous work on defining transmission rates in this area has focused on the household to define contact and to estimate transmission probabilities (14-17). Other attempts to define contact have relied on conversational encounters (3, 18, 19), direct touching (3), or simultaneous presence in a room (4, 5). Conversational contact is likely relevant to airborne transmission. Direct touching could transmit environmentally acquired pathogens. Simultaneous presence of both transmission modes could generate vastly different transmission probabilities in different venues depending upon environmental conditions, human behaviors in those venues, the survival characteristics of the agent as it transits in air or on fomites, and the dose required to initiate infection. By explicitly modeling environmental processes that mediate transmission, our EITS models differentiate air, water, and fomite pathways of transmission (and even different classes of fomite transmission). We will demonstrate how this framework provides paths to: 1) Developing transmission parameters that can be independently measured in environmental field studies, including survival rates of pathogens in the environment, transfer coefficient from fomites to hands, and many more; 2) Formulating transmission processes specific for air, water, food, and fomites in a manner that facilitates assessment of potential environmental control effects and the interpretation of environmental pathogen measurements; and 3) Developing mechanistic theory on environmentally-

based transmission rates, analogous to how vector borne transmission rates are largely defined by entomological factors that are easily measured in the field.

MATERIALS AND METHODS

Model Assumptions

We present a basic EITS model with the following assumptions:

(1) All individuals are identical except that one is either *S* (completely susceptible), *I* (infected and infectious), or *R* (completely immune);

(2) The total population size is constant;

(3) The environment is a single, fixed-size, homogeneous compartment;

(4) Humans are the only source of pathogens and individuals are uniformly exposed to pathogens in the environment;

(5) In the environment, pathogens instantaneously and thoroughly mix, and do not replicate;

(6) Once picked up from the environment, pathogens can instantaneously infect S at a rate that is independent of prior pathogen pick up;

(7) Pathogen levels in the environment diminish via first order dynamics through pick up of pathogens by humans, die off, and environmental decontamination.

EITS Deterministic Compartmental Model

As shown in Figure 1, our EITS deterministic compartmental model includes two types of state entities: 1) humans, which are divided into *S*, *I*, and *R* states, and 2) live pathogens in the environment, *E*. The model is based on the following ordinary differential equations (ODEs):

$$\begin{aligned}
\frac{dS}{dt} &= -S\rho\pi E \\
\frac{dI}{dt} &= S\rho\pi E - \gamma I \\
\frac{dR}{dt} &= \gamma I \\
\frac{dE}{dt} &= \alpha I - E((S+I+R)\rho + u)
\end{aligned} \qquad \text{(Equation 1)}$$

ρ is the fraction of *E* picked up by each person per unit time; π is the probability that a susceptible individual becomes infectious per pathogen *E* picked up; γ is the rate per individual and per unit time of recovery from and acquisition of immunity to infection; α is the number of pathogens per unit time deposited into the environment by an infectious individual; and μ is the rate at which pathogens are eliminated from the environment by any means (naturally dying, being killed by decontamination processes, or being cleaned or otherwise removed from the environment).

Berkeley Madonna is used to numerically solve the ODEs in Equation 1 (20).

Stochastic Compartmental Model

Our EITS stochastic model is Markovian. All state entities and transmission rates are defined similarly to those in EITS deterministic compartmental model. One difference is that the state variables (*S, I, R, E*) are discrete integers in the stochastic

model rather than continuous as in the deterministic compartmental model. Our stochastic models only allow for a single event to occur at any given time; the specific event is randomly determined by the transition rates (Table 1). In deterministic compartmental models, on the other hand, events happen continuously and simultaneously. The output of these two model structures converge as initial number of infected individuals and environmental pathogens are large. As these initial values decrease, the chance of stochastic die out increases. This phenomenon does not occur in a deterministic model.

The Gillespie algorithm (21) is applied to simulate the stochastic transmission process and to randomly execute a single event at variable time steps on a continuous time scale. This model was coded and run in JAVA.

Choice of Parameter Values

To illustrate the behavior of the EITS, we chose to parameterize our model for influenza (Table 2) such that the environment corresponds to either 1) frequently touched fomites that are touched by many different individuals such as door handle; 2) infrequently touched fomites such as floors or ledges; or 3) air inside a building. Any real situation might incorporate all three of these pathways simultaneously. We isolated these three conditions for the sake of clarifying the dynamics related to each condition separately. The population size N, ($N = S + I + R$), represents the number of people in a public indoor venue. We used a point estimate for the recovery rate derived from previous influenza models (22, 23). Except for the recovery rate, γ, all parameters vary by route of transmission. Infectivity, π, differs between air and fomite because the

different routes of infection, inhalation for air and touched membrane for fomites, have different dose response characteristics as illustrated from empirical studies (24-26). Estimates on environmental elimination rates, μ, are based on experimental studies in air (27) and on non-porous surfaces (28). Considering the particle size distribution of excretions, only the smaller particles stay suspended in air and are respirable, whereas larger particles rapidly settle onto surfaces where they may be picked up; thus there is a route specific deposit rate, α, for each pathway. We assume that frequently touched fomites have smaller surface areas than infrequently touched fomites, and therefore receive proportionally less contamination. The deposit rate is governed by physical and behavioral factors such as sneezing or cough rates, deposition and aerosolization fractions, among others that are derived from a variety of empirical studies (29-35). Analogously, the pick up rate, ρ, is governed by physical and behavioral factors such as breathing, touching rates, and transfer efficiencies between surfaces, hands, and membranes (36-41). In order to compare across the three scenarios, scenarios were parameterized to have the same R_0. For more parameterization details see the supplemental materials.

RESULTS

Mathematical Analysis of EITS Model Structure and Behavior

In the EITS model, pathogens are picked up by humans at a rate, ρN, and eliminated from the environment at a rate, μ. The fraction of live environmental pathogens picked up by humans, therefore is

$$f_E = \frac{\rho N}{\rho N + \mu} \qquad \text{(Equation 2)}$$

This fraction ranges from near zero when elimination is much larger than the pick up to near 1 if the pick up is much larger than elimination. Another important metric is the average time pathogens persist in the environment, t_E.

$$t_E = \frac{1}{\rho N + \mu} \qquad \text{(Equation 3)}$$

For our three environmental transmission pathways (air, frequently touched fomites, infrequently touched fomites), the parameter values defined in Table 2 generate fractions of live environmental pathogens picked up by humans of 0.01%, 99.04%, 0.50%, respectively. They generate average persistence times of 0.115, 0.003, 0.345 days. These values reflect the fact that frequently touched fomites are picked up at a high rate, and therefore have a low environmental persistence time compared to infrequently touched fomites. Air is more similar to infrequently touched fomites with respect to persistence and fractional pick up. The specific relationship between these two transmission routes depend on pathogen and environment specific factors.

The basic reproductive number, R_0, represents the expected number of secondary cases caused by introducing a single primary case into a totally susceptible population. As shown in supplemental materials, R_0 can be written as

$$\frac{\alpha}{\gamma} * \frac{\rho N}{\rho N + \mu} * \pi \qquad \text{(Equation 4)}$$

R_0 can be considered as the product of: 1) total pathogens deposited by an infectious individual during his/her contagious period, $\frac{\alpha}{\gamma}$; 2) the proportion of pathogens picked up while still alive, $\frac{\rho N}{\rho N + \mu}$; and 3) infectivity of pathogens, π. Based on parameter values presented in Table 2, R_0 = 1.8 for the three model scenarios.

When the total pickup rate is much larger than the elimination rate ($\rho N >> \mu$), R_0 approaches $\alpha * \frac{\pi}{\gamma}$ and is independent of population size *N*. This results in a frequency dependent mass action formulation, and corresponds to a frequently touched fomite like a door handle or a frequently used workspace. When total pickup rate is much smaller than elimination rate ($\rho N << \mu$), R_0 approaches $\alpha * \frac{\rho N}{\mu} * \frac{\pi}{\gamma}$ and is proportional to the population size *N*. This corresponds to a density dependent mass action formulation, such as either: 1) airborne transmission with rapid thorough mixing of air; or 2) surface contamination where individuals infrequently touch the surface and the majority of agents die or are disinfected before next person touches it. This density dependent formulation is similar to the case addressed by Noakes in an airborne transmission model (6). Therefore, according to the ratio, $\rho N / \mu$, the EITS model can characterize airborne or fomite mediated transmission, and within fomite mediated transmission, either frequently or non-frequently touched surfaces. Multiple pathways can be also be modeled, each with unique parameterizations.

By rearranging Equation 4, we get

$$R_0 = \pi \cdot \left(\frac{\alpha}{\gamma} \right) \cdot \left(\frac{\frac{\rho N}{\mu}}{\frac{\rho N}{\mu} + 1} \right) \qquad (5)$$

This reformulation of R_0 brings out two important ratios: $(\rho N) / \mu$, environmental persistence ratio, an indicator of the importance of pick-up compared to environmental elimination pathogens from the environment; and α / γ, contamination ratio, a measure of the pathogen deposition magnitude from an infectious individual. The condition $\rho N / \mu >> 1$ corresponds to frequently touched fomites. Under this condition environmental contamination, α / γ, is more likely to be picked up than to die off. The condition $\rho N / \mu << 1$ corresponds to infrequently touched fomites. Under this condition environmental processes attenuate pathogen levels before humans are exposed.

These frequency and density dependent relationships can also be appreciated by transforming our EITS model into an instantaneous contact model corresponding to the classic Kermack-McKendrick SIR model (42). To this end, we assume that the dynamics of E can be ignored, such that dE / dt = 0. Under these conditions:

$$E = \frac{\alpha I}{(S + I + R)\rho + \mu}$$

Substituting E into Equation (1) we have

$$\begin{aligned} \frac{dS}{dt} &= -\frac{\alpha \pi \rho}{\rho N + \mu} SI \\ \frac{dI}{dt} &= \frac{\alpha \pi \rho}{\rho N + \mu} SI - \gamma I \\ \frac{dR}{dt} &= \gamma I \end{aligned} \qquad (6)$$

the term $\frac{\alpha \pi \rho}{\rho N + \mu}$ is equivalent to the single transmission rate parameter in the classic SIR model. The R_0 of this instantaneous contact SIR model is

$$R_0 = N\left(\frac{\alpha \pi \rho}{\rho N + \mu}\right)\left(\frac{1}{\gamma}\right) \qquad (7)$$

This is the same as that derived previously from our EITS model with environmental dynamics. The Kermack-McKendrick SIR model is formulated as density dependent contact, and its R_0 is proportional to the population size. As in the EITS model, the formulation of this instantaneous contact SIR model can be considered as either density or frequency dependent contact based on the environmental persistence ratio, $\rho N/\mu$.

Analyses of Dynamics of the EITS Model

Figure 2 compares the influenza dynamics for the three EITS model scenarios (air, frequently touched fomites, and infrequently touched fomites) with the SIR model configuration shown in Equation 6. The final cumulative incidence is similar for all three EITS transmission pathways and the SIR configuration, reflecting that they were all parameterized to have the same R_0 (Figure 2A). The SIR configuration dynamics are the fastest, although frequently touched fomite transmission exhibits similar dynamics. Air transmission dynamics are slower and the infrequently touched fomite transmission is even slower.

These dynamic differences are reflected in the different environmental persistence times, $\frac{1}{\rho N + \mu}$, for the three EITS model scenarios. Environmental persistence time is greatest for the infrequently touched fomites and therefore time to peak infection prevalence is longer than for the other scenarios (Figure 2B). On the other hand, pathogen environmental persistence time is short in the case of the frequently touched fomites, so the time to peak infection prevalence is the shortest.

The specific timing and dynamics will vary by the specific parameterization. For example, decreasing the pick up rate and elimination rate by the same fraction ($\rho N / \mu$ remains constant) results in slower dynamics, lower peak prevalence, and unchanged final cumulative incidence. However, the general features of the EITS model are that: 1) environmental pathogen dynamics will slow the epidemic curve; 2) environmental transmission will attenuate peak incidence and prevalence; and 3) different routes of environmental transmission will exhibit different dynamics.

Intervention Effects in the EITS Deterministic Compartment Model

To gain insights into environment infection control dynamics, we assess two types of interventions. The first affects the elimination rate parameter, μ, which corresponds to environmental decontamination. The second affects the pathogen pick-up rate parameter, ρ. The pick up rate, ρ, has no simple intervention analog, but could be thought of as either a behavioral change that decreases environmental contact, an altered transfer efficiency, or a dilution of the environmental surface area to be touched. To illustrate intervention effectiveness in different scenarios and how interventions impact dynamics and risk, we examine two simple scenarios: 1) increasing the elimination rate, μ, by 25%; and 2) reducing the pathogen pick up rate, ρ, by 25%. As shown in Figure 3, both interventions have little effect on the dynamics of epidemics for the frequently touched fomite scenario. Frequently touched objects, such as doorknob handles, have a high pick-up rate, so that a small increase in the elimination rate or decrease in the pick-up rate will have very little impact on transmission. This can be also explained by noting that R_0 for frequently touched fomites is approximately independent of both the elimination and pick-up rates. For the air and the infrequently touched fomite scenarios, however, these

two interventions can lead to lower cumulative incidence, slower dynamics, and a smaller peak of live pathogens in the environment. Although reducing pathogen pick up is more effective than environmental decontamination, the efforts required by these two interventions will affect the choice of intervention. The reason these two interventions are effective for air and infrequently touched fomites is that the elimination rate and pickup rate are approximately proportional to R_0 in these two scenarios.

Stochastic Model Analyses

The EITS stochastic model was first analyzed to explore how an environmental contamination event affects the probability of an outbreak. To this end, we varied the initial level of environmental contamination to assess its impact on the probability of an outbreak occurring, defined as the proportion of simulations that resulted in attack rates > 0.05 (simulation details defined in Figure 4). The relationship between the outbreak probability and $E_{(t=0)}$ is sigmoidal; *i.e.*, above a threshold contamination level, there is a region in which the probability of an epidemic increases exponentially with $E_{(t=0)}$At higher initial contamination levels the probability of an outbreak levels off. Using the probability of outbreak as an additional risk measure in microbial risk assessments may be an important complement to the currently used measures that generally rely on mean values.

We also explored the influences of human contamination, through shedding from infectious individuals, on the dynamics of epidemics (simulation details defined in Figure 5). An infectious individual sheds on average $\frac{\alpha}{\gamma}$ pathogens into the environment during his/her contagious period. As shown in Figure 5, when fixing R_0 and the initial

conditions, increasing the contamination ratio, $\frac{\alpha}{\gamma}$, results in an increase in the probability of an outbreak. The relationship in Figure 5 holds for any proportional change in the elimination rate, pick up rate, and infectivity parameter values where R_0 remains constant, suggesting that as long as R_0 is constant these three parameters do not have significant influence on the probability of an outbreak. The reason that the contamination ratio can affect the probability of an outbreak, even when R_0 is constant, is that when infectious individuals excrete fewer pathogens into the environment, reflected by a small contamination ratio, $\frac{\alpha}{\gamma}$, this smaller number of environmental pathogens have a higher chance of extinction, preventing the initiation of an outbreak.

Figure 4 and 5 results also hold for both the infrequently touched fomite and air scenarios (data not shown).

DISCUSSION

Commonly, the mechanisms of transmission through the environment are not explicitly formulated in non-vector borne infectious disease population dynamic models, except some models that focus on enclosed hospital settings (31) or water-borne outbreaks (7-12). In this paper, we present a basic conceptual framework of environmentally mediated population infection transmission for non-vector borne infectious diseases by incorporating environmental mechanisms into epidemic models.

Using the EITS framework presented here, the transmission rate and R_0 are formulated by well defined and measureable environmental factors, similar to how

vector-borne transmission is formulated using entomological factors. Although we focus on air and fomite transmission, a potential generalization of this framework would be incorporating pathogen dynamics within different environmental settings, such as other vectors, food, and water.

The adoption of an EITS framework provides a theoretical basis for understanding and modeling intervention efficacy in realistically detailed situations involving diverse venues where transmission takes place. The parameters of the EITS model reflect physical events on which data can be readily gathered using newly developed methodologies and for which a considerable body of data and theory already exists. In contrast, contact rates and transmission probabilities in specific venues are abstract and not feasibly measurable in most situations except in uniform places with repeated and prolonged contact like households.

The EITS framework also helps identify and relax unrealistic mass action assumptions, such as no time passing between pathogens leaving one person and reaching another. It also provides a way to conceptualize the extent to which transmission is a density or frequency dependent contact process (1, 2). In reality, most transmissions occur between these two extremes and the EITS formulation reflects this. As the environmental persistence ratio, $\rho N/\mu$, increases transmission becomes more density dependent and as this ratio decreases it becomes more frequency dependent.

Another theoretically valuable focus is found in the contamination ratio, α / γ, a measure of the total amount of pathogens shed by infectious individuals. This ratio and the magnitude of a contamination event are both indicators of the probability that an

outbreak will occur, suggesting that stochastic die-out is more likely when environmental contamination is low.

EITS models will eventually help us define the role of different transmission modes in sustaining or amplifying transmission. Multiple transmission modes have been recognized for many other infections than those in our example, such as cholera, hepatitis A, and cryptosporidiosis (43-45). The EITS model framework provides leverage for using detailed environmental data and well established parameters reflecting pathogen characteristics to analyze different transmission modes and the role they play in endemic and epidemic situations.

While including more realistic details than classic SIR models, the EITS models presented here are abstract in order to serve heuristic purposes. Future EITS models will relax current model assumptions. The specific choices on which assumptions to relax will depend on the research question. For example, with only a single environmental compartment, our models may not accurately capture contact patterns or pathogen dynamics in the environment. In fact, our preliminary analysis pointed out that a key way to relax the homogeneous environment assumption is to distinguish frequently touched fomites from infrequently touched fomites. Additionally, a more refined understanding of transmission patterns might require model structure that accounts for detailed contact patterns between people and the environment.

Our simple EITS models identify key elements and important data gaps of the environmental infection transmission system. They provide an initial step in motivating improved environmental measurements that would complement human case data and might be more informative and more cost-effective to gather than such data. EITS

models incorporating more realistic details than those presented here can be used to help design future environmental data collection efforts. They also can provide a basis for analyzing focused environmental based interventions such as decontamination of specific surfaces, water, or air, as well as hygiene and sanitation efforts.

Table 2.1 Event and transition rates for the EITS stochastic model

Event	Result	Transition rate
Infection	(S, I, R, E)→(S-1, I+1, R, E)	$S*\rho * E*\pi$
Removal	(S, I, R, E)→(S, I-1, R+1, E)	$I*\gamma$
Depositing	(S, I, R, E)→(S, I, R, E+1)	$I*\alpha$
PathogenDecrease	(S, I, R, E)→(S, I, R, E-1)	$E*(\rho *(S+I+R)+\mu)$

Table 2.2 Parameter values for an influenza EITS model based on data from the literature

Parameter		Parameter Estimates			Notes*
		Air	Frequently Touched Fomite	Infrequently Touched Fomite	
Recovery rate (1/day)	γ	0.2	0.2	0.2	Based on empirical probability distribution
Infectivity	π	0.0517	0.0000693	0.0000693	Based on exponential dose response model. Route of transmission: air = inhalation; Fomite = membrane.
Elimination rate (1/day)	μ	8.64	2.88	2.88	Loss in air comes from die-off and loss on fomite reflects loss on non-porous surface.
Deposit rate (pathogens / infected / day)	α	693	5,244	1040,177	Contamination based on cough and sneezing rates. Deposition based on size distribution from sneezing where pre-evaporative particle diameter < 20 μm are assumed to remain in air.
Pickup (1 / person / day)	ρ	0.0000877	0.297	0.0000145	Based on breathing rates and touching rates. Exposure duration is assumed to be 8 hr/day.

* References for model parameterization are in supplemental materials.

Table 2.3 Initial conditions and basic statistics for the EITS models

Parameter		**Airborne**	**Frequently touched fomite**	**Infrequently touched fomite**
Total population	N	1,000	1,000	1,000
Initial S	S_0	999	999	999
Initial I	I_0	1	1	1
Initial R	R_0	0	0	0
Initial E	E_0	0	0	0
Basic reproductive number	R_0	1.80	1.80	1.80
Environmental persistence time	t_E	0.115	0.003	0.345
Fraction of pickup from environment	f_E	0.010	0.990	0.005

Figure 2.1 A schematic representation of flow of individual (solid lines) among states and the flow of pathogens in the environment (dotted lines) for the EITS model

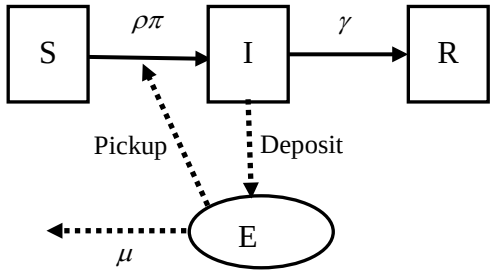

Figure 2.2 Cumulative incidence (A) and prevalence (B) using the EITS deterministic compartmental model. EITS model scenarios include transmission through infrequently touched fomite (dashed line), air (doted line), and frequently touched fomite (solid line with square mark). Corresponding instantaneous contact SIR model (solid line with triangle mark) is shown for comparison, and is close to EITS frequently touched fomite. R_0 = 1.8 and simulations are seeded with one infectious individual. Parameter values are shown in Table 2.2

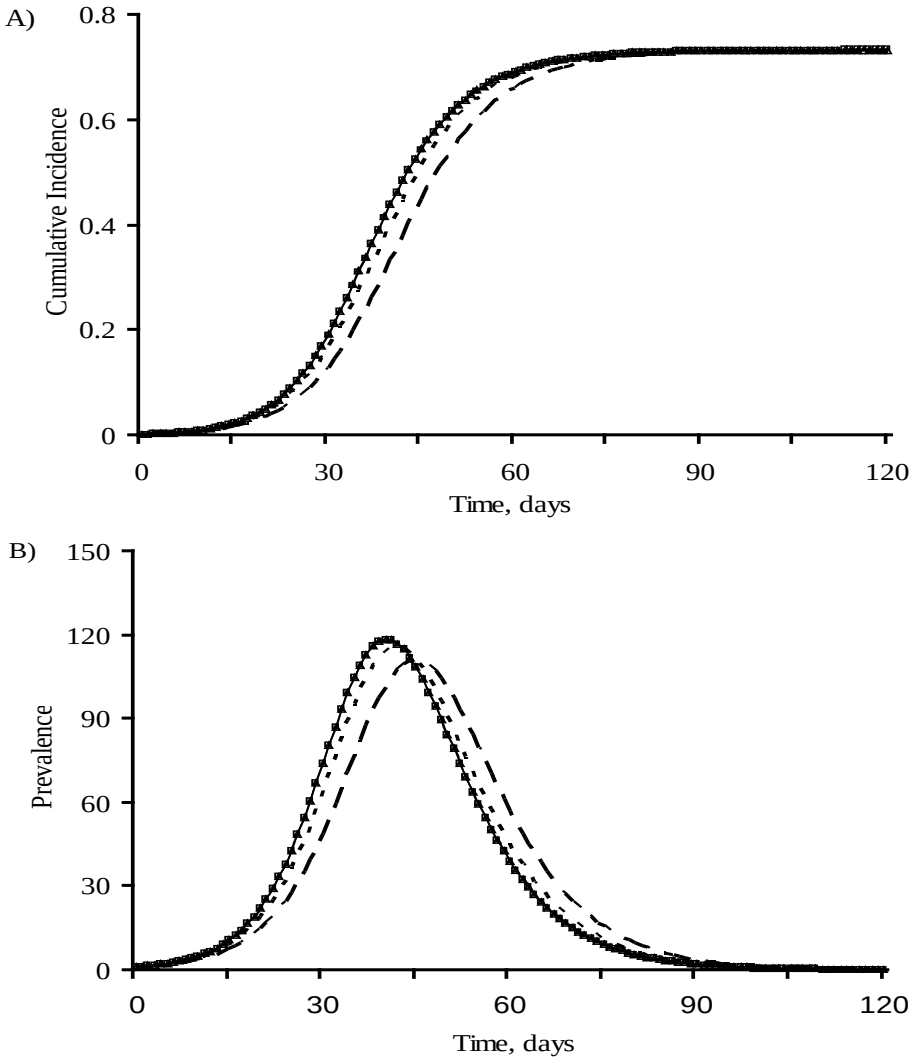

Figure 2.3 Comparing the effectiveness of environmental decontamination (dotted line), decreasing environment contact (dashed line), and no intervention (solid line) using the EITS deterministic compartmental model for air (A), frequently touched fomite (B), and infrequently touched fomite (C) scenarios. Parameter values for the "no intervention" scenario are shown in Table 2. Environmental decontamination corresponds to increasing the elimination rate by 25%. Decreasing environmental contact corresponds to decreasing the pick up rate by 25%.

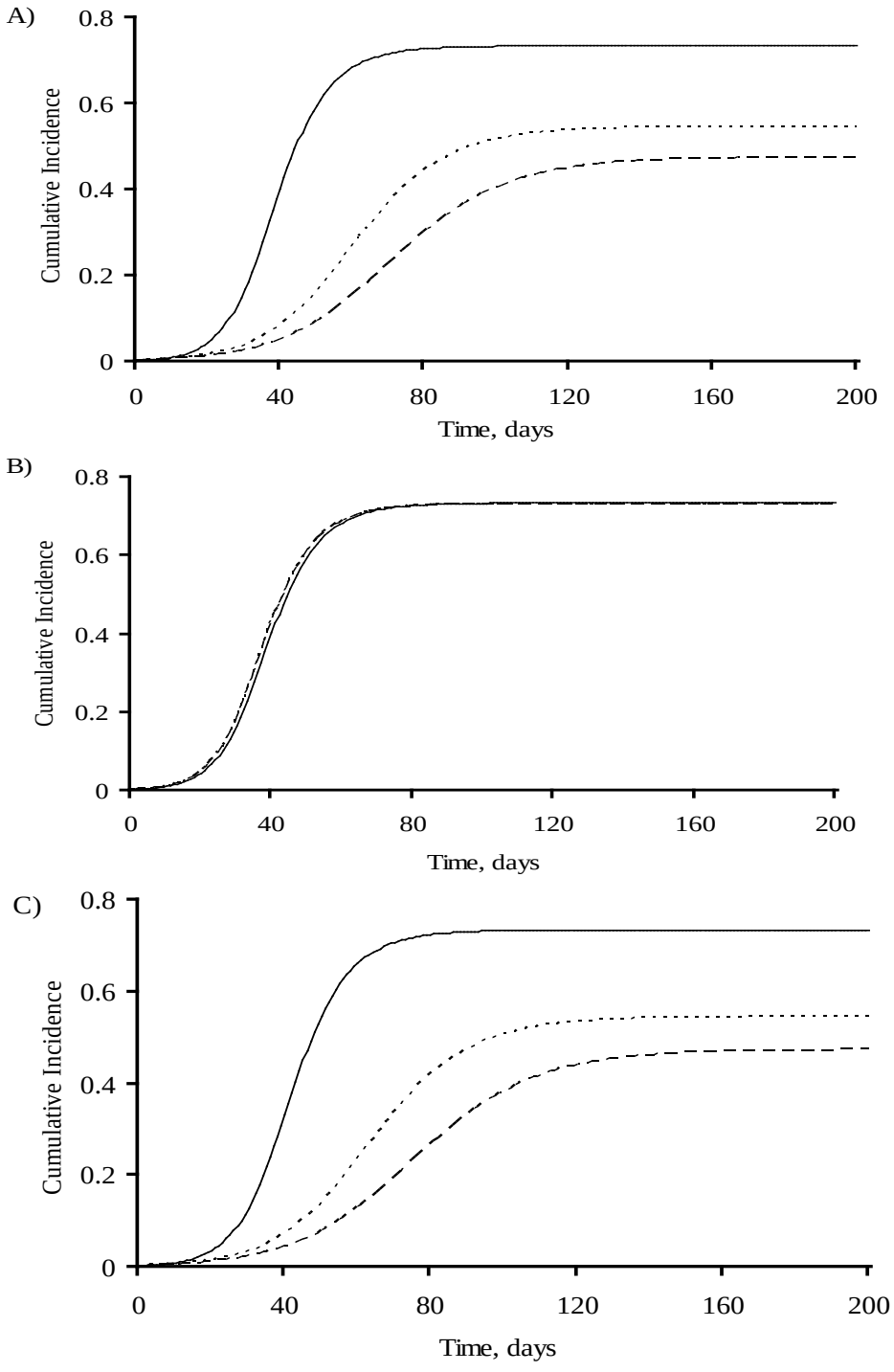

Figure 2.4 Probability of an outbreak for different initial environmental contamination levels using the EITS stochastic model and the frequently touched fomite scenario. Simulations use the parameter sets for the frequently touched fomite scenario shown in Table 2. Initial conditions are $I_0 = 0$, $E_0 = (1, 10, 26, 262, 2{,}622, 26{,}220, 52{,}440, 131{,}100, 262{,}200, 2{,}622{,}000)$.

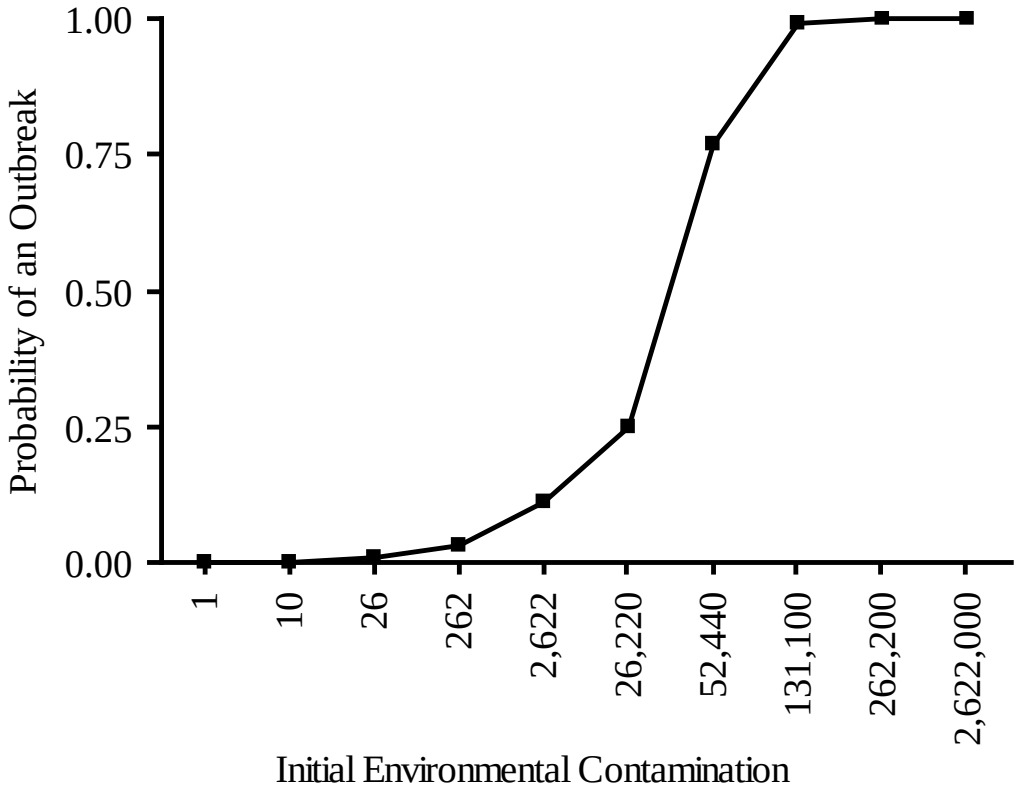

Figure 2.5 Probability of an outbreak for different levels of contamination excreted per person. R_0 are 4.0, 2.5, 1.8, and 1.3 for these four curves from top to bottom. For each curve the infectivity is decreased proportionally with the contamination ratio so that R_0 remains constant. Simulations use the parameter sets for the frequently touched fomite scenario shown in Table 2 ($\gamma = 0.2$, $\mu = 2.88$, $\rho = 0.2972$ for all simulations). For $R_0 = 1.8$, $[\pi, \alpha] = [1.810, 0.2]$, [0.362, 1], [0.072, 5.2], [6.9e-3, 52.4], [6.9e-4, 524.4], [6.9e-5, 5,244]; for other R_0 curves infectivity is increased or decreased proportionally and $[\pi, \alpha]$ is varied analogously. The initial condition is $I_0 = 1$, $E_0 = 0$.

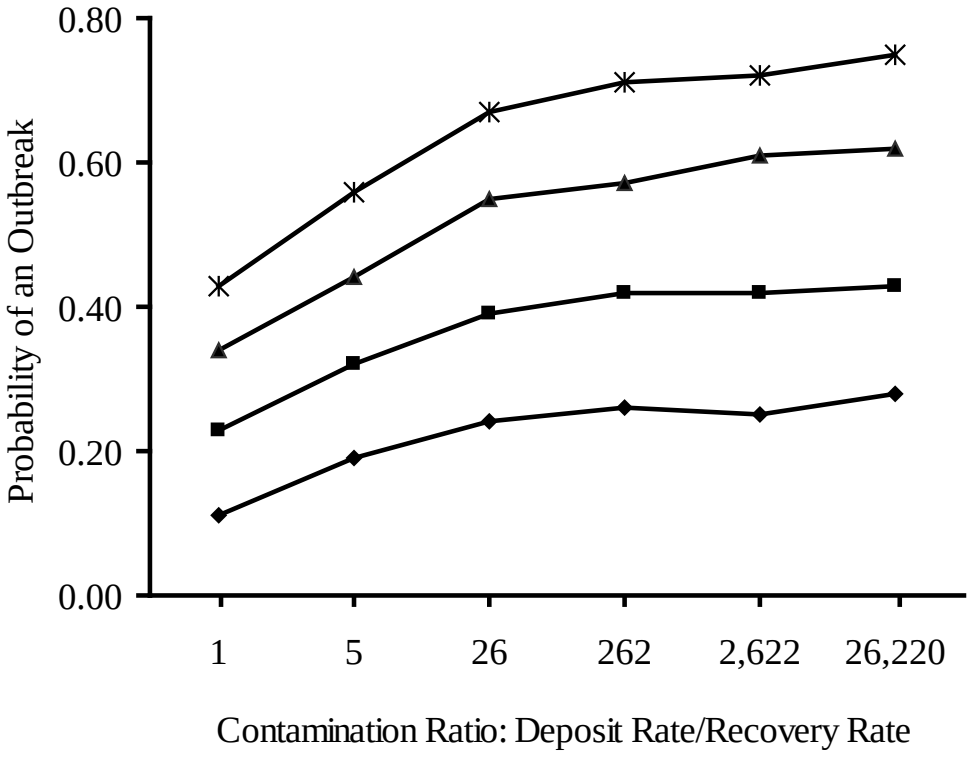

APPENDIX

I. Derivation of R_0 for the EITS deterministic compartmental model

To derive R0, we first evaluate the steady state conditions of the second and third equation from Equation 1 in the main text. We do this by setting rates of *I* and *E* to zero:

$$\frac{dI}{dt} = S\rho\pi E - \gamma I = 0 \qquad \text{(A1)}$$

$$\frac{dE}{dt} = \alpha I - E((S + I + R)\rho + \mu) = 0 \qquad \text{(A2)}$$

Solving equation A1 we get:

$$I = S\rho\pi E / \gamma \qquad \text{(A3)}$$

Substituting A3 into A2 we get:

$$\alpha \frac{S\rho\pi E}{\gamma} - E(\rho(S + I + R) + \mu) = 0 \qquad \text{(A4)}$$

Simplifying A4 we get;

$$\alpha \frac{\rho S}{\rho(S + I + R) + \mu} \pi \frac{1}{\gamma} = 1 \qquad \text{(A5)}$$

In a completely susceptible population, S approximates total population size, N, where N = S + I + R. Substituting N for S and S + I + R, we get:

$$R0 = \alpha * \frac{\rho N}{\rho N + \mu} * \pi * \frac{1}{\gamma} \qquad \text{(A6)}$$

II. Parameterization of the EITS Models

The following table is reproduced from the main text, but includes references for each parameter value.

Table 2.4 Model parameters and references for each parameter value.

		Parameter Estimates			
Parameter		**Air**	**Frequently Touched Fomite**	**Infrequently Touched Fomite**	**Notes**
Recovery rate (1/day)	γ	0.2	0.2	0.2	Based on empirical probability distribution (1, 2).
Infectivity	π	0.0517	6.93E-5	6.93E-5	Based on exponential dose response model. Route of transmission: air = inhalation (3, 4); Fomite = membrane (4, 5, 6)
Elimination rate (1/day)	μ	8.64	2.88	2.88	Loss in air comes from die-off (7) and loss on fomites reflects loss on non-porous surface (8).
Deposit rate (1/day)	α	693	5,244	1,040,177	Contamination based on cough and sneezing rates. Deposition based on size distribution from coughing where particles < 20 μm are assumed to not deposit onto surfaces (4, 9, 10, 11, 12, 13, 14, 15).
Pickup (1/day)	ρ	8.765E-5	0.2972	1.445E-5	Based on breathing rates (12, 13) and touching rates (14, 15, 16, 17). Exposure duration is assumed to be 8 hr/day

The details of how we obtained values for each parameter shown in the above table are provided below.

A. Recovery rate:

Recovery rate is calculated by taking the inverse of the contagious period. Data on contagious period range from 3 to 7 days (1, 2). For our simulation studies we use 5 days.

B. Infectivity:

Using TCID50 data (the amount of virus that infects 50% of cells in tissue culture) from the literature, we convert TCID50 to units of HID50 (the amount of virus particles that infects 50% of human) by a conversion factor of 20. The conversion factor is based on expert consultations, and our conclusions and inferences are independent to this conversion factor. Using the HID50 we obtain infectivity estimates based on the Exponential Dose-Response equation.

For the air scenario, we obtain a TCID50 estimate of 0.671, the virus dose delivered to respiratory epithelium that cause half of human infected, from the literature (3, 4), which converts to HID50 = 13.42. The risk of infection caused by a single virus particle using the exponential dose-response model is therefore 0.0517.

For fomite scenarios, we obtain a TCID50 of 500 from the literature (4, 5, 6), which converts to HID50 = 10000. The risk of infection caused by a single virus particle using the exponential dose-response model is therefore 0.0000693.

C. Elimination rate:

These parameter estimates come from the literature. Elimination rate for air consists of die-off in the environment. The die off rate in air is set at 0.36/hour (7); thus the daily elimination rate for air is 0.36*24 = 8.64 / day.

We constrain the elimination rate for fomites to die-off on non-porous surfaces. The die-off on non-porous is set at 0.12/hour (8), which converts to 0.12*24 = 2.88 / day for both frequently and infrequently touched fomites.

D. Deposit rate:

Based on the availability and quality of data on shedding particles, we assume that influenza virus particles are shed only via coughing and sneezing; we ignore speaking as a relevant transmission mode. We obtain daily deposit rates from shedding event rates (coughing and sneezing), the total fluid volume per shedding event, the droplet particle size distribution, viral titer in nasal washings, among other expert judgments regarding TCID50 to virion conversion factors, and proportions of particles settling to frequently, infrequently and never touched fomites.

1. Shedding event rate per person per day. Based on cough frequency data from pneumonia patients (14), the cough rate is estimated to be 360 /day (4). Using rhinovirus experimental data (15), the sneezing is estimated to be 11/day (4). The cough and sneezing frequency are not influenza specific and probably higher than influenza.
2. The mean total fluid volume per cough is estimated to be 0.044 mL (9, 10) using a study with fairly high quality standards. Using a second study, with lower quality standards which looked at both sneeze and cough particle distributions (13), we internally compare the cough and sneeze volumes and found that sneezes were 39.33 times greater in volume than coughs. However, we do not use this study directly to compute the actual sneeze volume; rather, we multiply the prior cough volume estimate of 0.044 mL by

39.33 to get a total sneeze volume of 1.757 mL.

3. We use the particle size distribution of coughs (9) and sneezes (13) to determine the proportion of the total shedding volume that remains in the air. We use a pre-evaporative particle diameter cut point of 20 μm to determine which particles will settle out immediately and which particles will remain aerosolized. The aerosol volume from one cough is estimated to be 0.00000006 mL (9, 10, 11). Using a similar approach as used to calculate the total sneeze volume, we estimate the aerosolized sneeze volume by internally comparing the volume of particles with pre-evaporative diameters less than 20 μm of sneezes compared to coughs; we observe that the volume of the small particles is 250 times greater in sneezes than in coughs. Then we use the prior aerosolized cough volume of 0.00000006 mL and multiply this by 250 to get an aerosolized sneeze volume of 0.000015 mL.
4. We use data on the virus titer of nasal washings (12) to estimate the viral concentration of all pre-evaporative volumes of material being shed. The virus titer is estimated at 185685 TCID50/mL.
5. We use a conversion factor of 20 to go from TCID50 units to potentially infective virus particles.
6. Based on expert adjustment, 0.004015% and 0.7965% of droplet particles greater than or equal to 20 μm are assumed to deposit on frequently touched fomites, infrequently touched fomites, respectively, and the remainders are assumed to deposit on never touched area.

Based on the above, we calculate the daily deposit rate for air, frequently, and infrequently touched fomites using the three following formulae:

total number of virus to air per day=

viral titer * viral particle conversion factor * [(volume(coughToAir) * coughsPerDay) + (volume(sneezeToAir) * sneezesPerDay))]

185685*20*[0.00000006*360 + 0.000015*11] = 693

total number of virus to frequently touched fomites per day=

viral titer * viral particle conversion factor * [(volume(coughToFreqFom) * coughsPerDay) + (volume(sneezetoFreqFom)*sneezesPerDay)] =

185685*20*[0.00000177*360 + 0.0000705*11] = 5244

total number of virus to infrequently touched fomites per day =

viral titer * viral particle conversion factor * [(volume(coughToInfreqFom) * coughsPerDay) + (volume(sneezetoInfreqFom)*sneezesPerDay)]

185685*20*[0.00035*360 + 0.014*11] = 1040177

E. Pickup rate:

The pick up rate is based on the following 11 factors:

1. Breathing rate, estimated at 14 breath / minute (16).
2. Tidal volume, estimated at 0.5 liter / breathe (16).

3. Deposition fraction in the respiratory tract to lung, estimated at 0.6. The majority of the virus particles breathed in is in the particle diameter range of 3-10 micro-meters, and this particle range has a fairly small range of deposition (17). By only excluding the anterior nasal passage we estimate the deposition fraction in the remaining respiratory tract to be 60%. This may be conservatively large.

4. Surface-hand touch rate, based on expert adjustment and conceptual scenarios, estimated at 20 time / hour for frequently touched fomites and 1 time / hour for infrequently touched fomites.

5. Fingertip surface area, based on expert adjustment, estimated to be 2 cm^2.

6. Surface-to-hand transfer efficiency, estimated at 0.3. This is an average of porous and non-porous surface values [non-porous surface = 0.5 (18), porous surface = 0.1 (19)].

7. Self inoculation rate, estimated at 15.7 contacts / hour (20).

8. Self-inoculation transfer efficiency from fingertip to mouth, eyes, or nose, estimated at 35% transfer efficiency (21).

9. Die off rate on hand, estimated at 55.3 / hour (8).

10. Exposure duration to environment, assumed to be 8 hour/day.

11. Environment volume is scenario based. For air we use 23000000 L; for frequently touched surface we use 25 cm^2; and for infrequently touched surface we use 25700 cm^2.

Based on these above values, the pickup rate for air is calculated as:

(14 breath/minute)*(0.5 liter/23000000 liter)*0.6*(8 hour/day)*(60 minute/hour) =

0.00008765 /day

For frequently touched surface, the pickup rate is calculated as:

(20 /hour)*(2 cm^2 / 25 cm^2)*0.3*(15.7/(15.7+55.3))*0.35*(8 hour/day) = 0.2972 /day

For infrequently touched surface, the pickup rate is calculated as:

(1 /hour)*(2 cm^2 / 25700 cm^2)*0.3*(15.7/(15.7+55.3))*0.35*(8 hour/day) = 0.00001445

/day

III. References for Model Parameterization:

1) Longini IM, Jr., Halloran ME, Nizam A, et al. Containing pandemic influenza with antiviral agents. *Am J Epidemiol.* 2004;159:623-633.

2) Elveback LR, Fox JP, Ackerman E, et al. An influenza simulation model for immunization studies. *Am J Epidemiol.* 1976;103:152-165.

3) Alford RH, Kasel JA, Gerone PJ, et al. Human influenza resulting from aerosol inhalation. *Proc Soc Exp Biol Med*. 1966;122(3):800-804.

4) Atkinson MP, Wein LM. Quantifying the routes of transmission for pandemic influenza. *Bull Math Biol*. 2008;70(3): 820-867.

5) Couch RB, Douglas RG Jr., Fedson DS, et al. Correlated studies of a recombinant influenza-virus vaccine. 3. Protection against experimental influenza in man. *J Infect Dis*. 1971;124(5):473-480.

6) Hayden FG, Treanor JJ, Betts BF, et al. Safety and efficacy of the neuraminidase inhibitor GG167 in experimental human influenza. *JAMA*. 1996;275:295–299.

7) Hemmes J.H., Winkler K.C., and Kool S.M. Virus survival as a seasonal factor in influenza and polimyelitis. *Nature*. 1960;188: 430-431.

8) Bean B, Moore BM, Sterner B, et al. Survival of influenza viruses on environmental surfaces. *J Infect Dis*. 1982;146(1):47-51.

9) Loudon RG., Roberts RM. Droplet expulsion from the respiratory tract. *Am. Rev. Resp. Dis.* 95:435–442 (1967).

10) Nicas M, Nazaroff WW, and Hubbard A. Toward understanding the risk of secondary airborne infection: emission of respirable pathogens. *J Occup Environ Hyg*. 2005;2(3):143-154.

11) Nicas M, Sun G. An integrated model of infection risk in a health-care environment. *Risk Anal*. 2006;26(4):1085-1096.

12) Murphy BR, Chalhub EG, Nusinoff SR, et al. Temperature-sensitive mutants of influenza virus. 3. Further characterization of the ts-1(e) influenza A recombinant(H3N2) virus in man. *J Infect Dis.* 1973;128:479-487.

13) Duguid JP. The size and duration of air-carriage of respiratory droplets and droplet-nuclei. *J hyg*. 1946;4:471-480.

14) Loudon RG, Brown LC. Cough frequency in patients with respiratory disease. *Am. Rev. Resp. Dis.* 1967;96:1137–1143.

15) Dick EC, Jennings LC, Mink KA, et al. Aerosol transmission of rhinovirus colds. *J. Infect. Dis*. 1987;156:442–448.

16) Guyton AC, Hall JE. Textbook of medical physiology (tenth edition). *W.B. Saunders Company*; 2000.

17) ICRP Publication 66: Human respiratory tract model for radiological protection. *Ann. ICRP*. *International Commission on Radiological Protection*. 1994; P.36-54 and 231-299.

18) Rheinbaben F, Schunemann S, Gross T, et al. Transmission of viruses via contact in a household setting: experiments using bacteriophage straight phiX174 as a model virus. *J Hosp Infect*. 2000;46(1):61-66.

19) Sattar SA, Springthorpe S, Mani S, et al. Transfer of bacteria from fabrics to hands and other fabrics: development and application of a quantitative method using Staphylococcus aureus as a model. *J Appl Microbiol*. 2001;90(6):962-970.

20) Nicas M., Best D. A study quantifying the hand-to-face contact rate and its potential application to predicting respiratory tract infection. *J Occup Environ Hyg*. 2008;5(6): 347-352.

21) Rusin P, Maxwell S, and Gerba C. Comparative surface-to-hand and fingertip-to-mouth transfer efficiency of gram-positive bacteria, gram-negative bacteria, and phage. *J Appl Microbiol*. 2002;93(4):585-592.

REFERENCES

1. Anderson RM, May RM. *Infectious Diseases of Humans Dynamics and Control.* Oxford University Press; 1992.

2. Diekmann O, Heesterbeek JAP. *Mathematical Epidemiology of Infectious Diseases.* John Wiley & Sons. Inc.; 2000.

3. Mossong J, Hens N, Jit M, et al. Social contacts and mixing patterns relevant to the spread of infectious diseases. *Plos Med*. 2008;5(3):e74.

4. Eubank S, Guclu H, Kumar VSA, et al. Modelling disease outbreaks in realistic urban social networks. *Nature.* 2004;429:180-184.

5. Del Valle SY, Hyman JM, Hethcote HW, et al. Mixing patterns between age groups in social networks. *Soc Networks*. 2007;29(4):539-554.

6. Noakes CJ, Beggs CB, Sleigh PA, et al. Modelling the transmission of airborne infections in enclosed spaces. *Epidemiol Infect*. 2006;134:1082-1091.

7. Eisenberg JNS, Seto EYW, Olivieri AW, et al. Quantifying water pathogen risk in an epidemiological framework. *Risk Anal*. 1996;16(4):549-563.

8. Eisenberg JNS, Brookhart MA, Rice G, et al. Disease transmission models for public health decision making: analysis of epidemic and endemic conditions caused by waterborne pathogens. *Environ Health Perspect.* 2002;110(8):783-790.

9. Eisenberg JNS, Lei XD, Hubbard AH, et al. The role of disease transmission and conferred immunity in outbreaks: analysis of the 1993 cryptosporidium outbreak in Milwaukee, Wisconsin. *Am J of Epidemiol.* 2005;161(1):62-72.

10. Soller JA, Olivieri AW, Crook J, et al. Risk-based approach to evaluate the public health benefit of additional wastewater treatment. *Environ Sci Technol.* 2003;37(9):1882-1891.

11. Soller JA. Use of microbial risk assessment to inform the national estimate of acute gastrointestinal illness attributable to microbes in drinking water. *J Water Heath*. 2006;4(suppl2):165-186.

12. Eisenberg JNS, Scott JC, Porco T. Integrating disease control strategies: balancing water sanitation and hygiene interventions to reduce diarrheal disease. *Am J Public Health*. 2007;97(5):846-852.

13. Atkinson MP, Wein LM. Quantifying the routes of transmission for pandemic influenza. *Bull Math Biol*. 2008;70(3):820-867.

14. Dingle JH, Badger GF, Jordan WS. *Illness in the home*. Cleveland, OH: The Press of Western Reserve University; 1964.

15. Fox JP, Hall CE. *Viruses in Families*. Littleton, Massachusetts: PSG Publishing Company, Inc; 1980.

16. Longini IM, Koopman JS, Monto AS, et al. Estimating household and community transmission parameters for influenza. *Am J Epidemiol*. 1982;115:736-757.

17. Becker N. An estimation procedure for household disease data. *Biometrika*. 1979;66(2):271-277.

18. Wallinga J, Edmunds WJ, Kretzschmar M. Perspective: human contact patterns and the spread of airborne infectious diseases. *Trends Microbiol*. 1999;7:372-377.

19. Wallinga J, Teunis P, Kretzschmar M. Using data on social contacts to estimate age-specific transmission parameters for respiratory-spread infectious agents. *Am J Epidemiol*. 2006;164(10):936-944.

20. Macey R, Oster G, Zahnley T. Berkeley Madonna User's Guide, Version 8.0. (http://www.berkeleymadonna.com). Accessed January 31, 2009.

21. Gillespie DT. Exact stochastic simulations of coupled chemical reactions. *J Phys Chem*. 1977;81(25):2340-2361.

22. Elveback LR, Fox JP, Ackerman E, et al. An influenza simulation model for immunization studies. *Am J Epidemiol*. 1976;103:152-165.

23. Longini IM, Jr., Halloran ME, Nizam A, et al. Containing pandemic influenza with antiviral agents. *Am J Epidemiol*. 2004;159:623-633.

24. Alford RH, Kasel JA, Gerone PJ, et al. Human influenza resulting from aerosol inhalation. *Proc Soc Exp Biol Med*. 1966;122(3):800-804.

25. Couch RB, R.G. Douglas RGJ, Fedson DS, et al. Correlated studies of a recombinant influenza-virus vaccine. 3. Protection against experimental influenza in man. *J Infect Dis*. 1971;124(5):473-480.

26. Hayden FG, Treanor JJ, Betts RF, et al. Safety and efficacy of the neuraminidase inhibitor GG167 in experimental human influenza. *JAMA*. 1996;275:295–299.

27. Hemmes J.H., Winkler K.C., and Kool S.M. Virus survival as a seasonal factor in influenza and polimyelitis. *Nature.* 1960;188:430-431.

28. Bean B, Moore BM, Sterner B, et al. Survival of influenza viruses on environmental surfaces. *J Infect Dis.* 1982;146(1):47-51.

29. Loudon RG, Roberts RM. Droplet expulsion from the respiratory tract. *Am. Rev. Resp. Dis*. 1967;95:435–442.

30. Nicas M, Nazaroff WW, Hubbard A. Toward understanding the risk of secondary airborne infection: emission of respirable pathogens. *J Occup Environ Hyg*. 2005;2(3):143-154.

31. Nicas M, Sun G. An integrated model of infection risk in a health-care environment. *Risk Anal.* 2006;26(4):1085-1096.

32. Murphy BR, Chalhub EG, Nusinoff SR, et al. Temperature-sensitive mutants of influenza virus. 3. Further characterization of the ts-1(e) influenza A recombinant(H3N2) virus in man. *J Infect Dis.* 1973;128:479-487.

33. Duguid JP. The size and duration of air-carriage of respiratory droplets and droplet-nuclei. *J Hyg.* 1946;44:471-479.

34. Loudon RG, Brown LC. Cough frequency in patients with respiratory disease. *Am. Rev. Resp. Dis*. 1967;96(6):1137–1143.

35. Dick EC, Jennings LC, Mink KA, et al. Aerosol transmission of rhinovirus colds. *J. Infect. Dis.* 1987;156(3):442–448.

36. Guyton AC, Hall JE. *Textbook of medical physiology (tenth edition).* W.B. Saunders Company; 2000.

37. ICRP Publication 66: Human respiratory tract model for radiological protection. International Commission on Radiological Protection. *Ann. ICRP*. 1994; P.36-54 and 231-299.

38. Rheinbaben F, Schunemann S, Gross T, et al. Transmission of viruses via contact in a household setting: experiments using bacteriophage straight phiX174 as a model virus. *J Hosp Infect*. 2000;46(1):61-66.

39. Sattar SA, Springthorpe S, Mani S, et al. Transfer of bacteria from fabrics to hands and other fabrics: development and application of a quantitative method using Staphylococcus aureus as a model. *J Appl Microbiol*. 2001;90(6):962-970.

40. Nicas M, Best D. A study quantifying the hand-to-face contact rate and its potential application to predicting respiratory tract infection. *J Occup Environ Hyg*. 2008;5(6):347-352.

41. Rusin P, Maxwell S, Gerba C. Comparative surface-to-hand and fingertip-to-mouth

transfer efficiency of gram-positive bacteria, gram-negative bacteria, and phage. *J Appl Microbiol*. 2002;93(4):585-592.

42. Kermack WO, McKendrick AG. A contribution to the mathematical theory of epidemics. *Proc Roy Soc Lond*. 1927;A(115):700-721.

43. Swerdlow DL, Malenga G, Begkoyian G, et al. Epidemic cholera among refugees in Malawi: treatment and transmission. *Epidemiol Infect*. 1997;118:207-214.

44. Hutin YJF, Sabin KM, Hutwagner LC, et al. Multiple modes of hepatitis A virus transmission among methamphetamine users. *Am J Epidemiol*. 2000;152(2):186-192.

45. Yoder JS, Beach MJ. Cryptosporidiosis surveillance--United States, 2003-2005. *MMWR*. 2007(September 7);56(SS07):1-10.

CHAPTER 3

THE TEMPORAL DYNAMICS OF INFLUENZA TRANSMISSION MODES DURING OUTBREAKS

INTRODUCTION

Influenza is associated with pandemics and annual epidemics, and causes significant burden on morbidity and mortality globally [1,2]. The global spread of a new swine influenza H1N1 strain in 2009 and ongoing spread of H5N1 avian influenza strains reveal the importance of next influenza pandemic preparedness. Various intervention recommendations such as vaccination, antiviral prophylaxis, school closure, social distancing, and border closure have been suggested for influenza pandemic preparedness in previous studies [3-9]. When one assesses some non-pharmaceutical interventions, such as mask using, hand washing and surface decontamination, disease transmission mode(s) should be considered.

Multiple transmission modes have been identified for influenza in previous studies [8,10-13]. Through coughing and sneezing, influenza infectious individuals shed contagious virus particles at wide range of diameter size. Based on virus particle size and environment characteristics, influenza transmission modes can be classified to four ways: (1) respiratory transmission, inhalation of respirable virus particles (<10 μm diameter) in air; (2) inspiratory transmission, inhalation of inspirable virus particles (10 < and < 100 μm) in air; (3) fomite mediated transmission, fingers (from contact with contaminated

fomites) with large virus particle (>100 μm) touching one's eye, nose, mouth; (4) droplet spray transmission, large virus particle (>100 μm) depositing directly to nearby person's mucous membranes [15-17].

Both respirable air and large droplet transmission mode have been suggested to be the unique dominant transmission mode [8,10-13]. Based on a theoretical transmission model, Spicknall et al found that all respiratory, droplet, and fomite mediated transmission modes can be dominant in specific scenarios [14]. However, these inferences arose from analyses constrained to simulated cumulative data collected at the end of outbreaks, and the potential temporal dynamics of the relative importance of different transmission modes were ignored. Human heterogeneities, especially super spreaders, have proved to be important in SARS, influenza and other infections [20, 21, 22]. However, in Spicknall's model, human individuals were assumed to be homogenous [14]. Further, in Spicknall's model, new cases are replaced by susceptible individuals instantaneously whenever new infections take place [14]. In this way, the Basic Reproductive Number (R_0) can be directly observed, however, the infections caused by second generation cases were ignored and the final fraction of infected (FFI) measurement was not available

To better understand the potential temporal dynamics of multiple influenza transmission modes during outbreaks, we extended Spicknall's model to a more detailed environmentally mediated influenza agent-based model by incorporating super spreaders. This model simulates influenza outbreak inside an abstract venue such as business building, dormitory or house, and reports FFI measurement. We observed the temporal dynamics of the relative importance of influenza transmission modes over the course of

outbreaks. Then we explicitly elucidate that virus particle dissemination and persistence are the underlying mechanisms affecting this temporal dynamics.

Our work was not meant to mimic realistic influenza outbreaks or to provide estimates of risk for public health policy decisions. The primary aim is to introduce new concepts regarding previously unrecognized temporal dynamic phenomena that change the relative importance of different transmission modes during outbreaks. Our work extends and contributes to recent efforts of understanding the relative importance of different influenza transmission modes [8, 14, 18, 23-25].

2. MATERIALS AND METHODS

2.1. The Environmentally Mediated Transmission Model

Our stochastic individual based model simulates environmentally mediated influenza infection transmission through respirable, inspirable, fomite mediate and droplet spray modes in an abstract venue. The model components include discrete individuals, pathogens, and raster environment units.

Individuals are susceptible, infectious, or recovered based on their infection status. Individuals are assumed to be complete immune after being infected. Individuals have a "hand" entity which mediates touching of environmental surfaces processes. Individuals move in venue independent of the distance and direction between the current location and target location. Susceptible individuals can get infection by breathing virus particles in air or by touching their eye, nose, and mouth with contaminated fingers. Transmission mode specific exponential dose-response relationship was used to determine the risk of infection. Some individuals are super spreaders who shed more

viral particles than others after being infected.

Infectious individuals excrete contagious viral particles over the course of infection. Influenza viral particles can stay in the air, on human's hand, or on surfaces, and eventually die out. Respirable virus particles are smallest and disseminate immediately to all air loci after shedding, and then stay suspended in air for long time. Inspirable viral particle are medium size and only disperse in current cell, and usually quickly settle down to surfaces. Large viral particles commonly immediately settle down to surfaces or directly upon nearby individuals' conjunctiva, mouth, or nasal mucosa through air. Respirable viral particle can reach the alveolar region in the lower respiratory tract, but the other transmission modes primarily only infect the upper respiratory tract [14,18,19].

Air and surface environment are presented by raster cells. Pathogens are assumed to be evenly distributed inside environment loci. Infectious individuals can contaminate the environment cells, and all individuals can pick up pathogens from surface or air loci via hand touching and breathing.

For greater model detail refer to the Appendix A.

2.2. Model Parameterization

Table 3.1 summarizes the primary parameter values used in the model simulations. Model parameters were primarily determined from empirical literature as well as expert judgment. Parameters relevant to human behavior and venue characteristics are tentatively specified in a reasonably large range of values. Based on parameter ranges suggested by Ispicknall et al [14], we chose four different parameter

value sets which lead to different transmission mode dominant scenarios: respiratory, droplet spray, fomite mediated, or no single transmission mode dominant case.

The majority of model parameter values are the same in these four scenarios, such as recovery rate and breathing rate, but a few model parameters were parameterized differently. Host density is high in droplet dominant scenario and low in respiratory dominant scenario. Lower HID50 for alveolar region is low in the respiratory mode dominant scenario. Upper HID50 for the upper respiratory region is low in the droplet spray and fomite mediated dominant scenarios. Movement rate is high in fomite mediated and no single mode dominant scenarios, and is low in respirable mode scenarios. Surface touching and self-inoculation rates are high in the fomite mediated mode dominant scenario and low in the respiratory and droplet transmission mode dominant scenario. Viral death rate in air is low in respiratory transmission mode dominant scenario, and viral death rate on surfaces is low in fomite mediated and no single mode dominant scenarios. The movement, surface touching and self-inoculation rates directly affect the viral particle dissemination in environment. The viral inactivation rates influence the viral particle persistence in environment. We varied these parameters to explore how they influence the environmental dissemination and persistence of virus particles and how they influence the temporal dynamics of influenza transmission modes in section 3.3.

2.3. The Implementation and Simulation of the Model

The model is implemented by applying Gillespie algorithm. This is an event-driven algorithm such that a single event occurs at each step of model simulations on a

continuous time scale. There are total 23 types of discrete events involving shedding pathogens, individual movement among different venue locations, surface touching, self-inoculation, breathing, and infection progression in the model. The likelihoods and the weights of all types of events were calculated to determine which event will occur and when the event will occur.

1000 independent simulation trials were conducted for each parameter set. All individuals were initially susceptible except a single index case. The model simulations directly report daily cumulative infection by transmission modes. Then cumulative infection and the relative importance of different influenza transmission modes were calculated. The relative importance of a transmission mode refers to the proportion of infections attributable to this mode among all infections.

The model was programmed using standard Java libraries. All statistical analysis was implemented in R package 2.10.

3. RESULTS

We examine the temporal dynamics of the relative importance of different influenza transmission modes over the course of outbreaks in four basic modeling scenarios. We then illustrate the underlying causes affecting this temporal dynamics. Finally, we explore the impacts of some model parameters on this temporal dynamics.

3.1. The Temporal Dynamics of Influenza Transmission Modes during Outbreaks

Based on parameter values in table 3.1, typical influenza outbreaks can be simulated. The outbreaks peaked at around the second week (13-17 days), and ended

between four and five weeks later for all four scenarios. This is consistent with the duration of the influenza outbreaks observed in previous outbreak investigations [26, 27]. The FFI was approximately 0.68 (95% CI: 0.61-0.75), a relatively high value but comparable to the common theoretical R_0 of 1.7. This might be partially due to the unrealistic complete susceptibility at the onset of outbreak.

As shown in Figure 3.1, the environmentally mediated model simulations laed to the respiratory, droplet spray, fomite mediated, or no single transmission mode dominant outbreak scenarios. The inspiratory transmission mode is negligible in all scenarios since inspirable viral particles quickly settle down to surfaces and enter fomite mediated transmission process. In respiratory, droplet spray or fomite mediated mode dominant scenarios, the final relative importance of the dominant transmission mode was around 60%, and the other two non-dominant transmission modes were not negligible. In no single dominant transmission mode scenario, all three transmission modes were similarly important.

As shown in Figures 3.1.a, the temporal variation of the relative importance of different influenza transmission modes over the course of outbreaks can be observed in all four scenarios. The relative importance commonly increases for respiratory and fomite mediated modes, and decreases for the droplet spray mode, when these transmission modes are not negligible. In the droplet spray, fomite mediated and no single transmission mode dominant scenarios (Figures 3.1.b), the relative importance of influenza transmission modes over the course of outbreaks vary slightly, and the dominant transmission mode is unique over the course of outbreaks.

However, in the respiratory transmission mode dominant scenario, the temporal

variation of the relative importance of influenza transmission modes over the course of outbreaks is much greater (figure 3.1.b). The absolute infection transmissions through all transmission modes gradually increase, but the respiratory mode transmission rises more to take over non-respiratory modes over the course of outbreaks (Figure 3.1.a). The non-respiratory transmission modes are more important during early outbreaks, but the respiratory mode becomes dominant later. On average, it takes around 10.0 days for respiratory transmissions to rise above non-respiratory transmissions. More than 95% of the rise of the relative importance of the respiratory transmission mode takes place before the average outbreak peak day 16. The trade off of the relative importance is primarily between the respiratory and droplet spray modes, and the fomite mediated mode is relatively constant. To avoid possible confounding effect on this temporal variation by averaging epidemics with different sizes and timings, we examined each single result from 1000 repeated model simulations. We found that this temporal increase of the relative importance of the respiratory transmission mode occurs among more than 95% epidemic simulations ($P<0.001$, H_0: No temporal rise of the relative importance of the respiratory mode over the course of epidemics.), although the time period between the simulation beginning and the moment when the respiratory mode rises above non-respiratory modes does vary (Mean =10.0, SD=3.6). Further, we found that in 62% of simulations the first transmission was from a non-respiratory mode.

Environmental viral distribution in these four scenarios is slightly different due to the different model parameter values. In the respiratory mode dominant scenario, total, maximum and average viral amount in air and on surface loci present a unimodal pattern and peak around day 20, and then gradually decreases. The contaminated air locus

percent has a similar unimodal pattern but peaks (50%) around day 15. The contaminated surface locus percent peaks (80%) around day 10, and then stays at a similar level longer. The reason for this is that the majority (>99%) of viruses go to surfaces after shedding, and the viral die off on surfaces is relatively low [14]. In fomite mediated and no-single transmission mode dominant scenarios, environmental virus dissemination presents similar patterns. In the droplet spray mode dominant scenario, the environmental virus distribution patterns are similar, but the peak time is relatively early around day 15, and more air and surface loci are contaminated during the peak period primarily due to the high population density.

3.2. Causes of Temporal Dynamics in Influenza Transmission Modes: Dissemination and Persistence Processes

Virus dissemination and persistence were found to be the primary underlying causes for the temporal dynamics of the relative importance of different influenza transmission modes.

Different influenza transmission modes need different level of timing and physical requirements for virus being picked up by susceptible individuals. The droplet spray mode needs the tightest requirements where the shedder and susceptibles must be co-located at the moment of shedding. The respiratory mode needs the least requirement because respirable virus particles disseminate to everywhere and virus die off rate in air is lowest. The fomite mediated mode needs intermediate requirements since susceptible individuals can move to surface contaminated loci recently inhabited by a shedder.

Virus dissemination influences the physical requirement. The effect of

dissemination on the timing of respiratory transmissions can be shown by decreasing the airborne dissemination. As shown in Figure 3.2.a which presents only the respiratory dominant scenario, we see that when we decrease the respirable virus dissemination range keeping all other parameters unchanged, the rise in the relative importance of respiratory mode as the epidemic progresses markedly decreases. Further, as shown in Figure 3.2.b, we see that dissemination does not much affect the total number of transmissions from respiratory infection. The underlying reason is that the virus dissemination effect partially depends on the viral particle amount. At the beginning of outbreaks, the single index case only sheds small amount of virus particles. Thus virus particles through respirable and droplet spray modes have similar chance to reach susceptible individuals. In the late stage of outbreaks, infectious individuals shed more viruses simultaneously and susceptible individuals decrease. Viral particles through droplet spray mode could continuously spray to the same co-located individuals who might be already infected. Thus the large virus particles through droplet mode can be "wasted" in the late stage of outbreaks. On the other hand, respirable virus particles always disseminate to all loci and reach more susceptible individuals, which strengthen the respiratory mode relative importance.

Virus particles persist in air or on surfaces until being picked up by co-located individuals or dying. Virus persistence is related to the timing requirement and could increases the chance of being picked up by co-located individuals. The effect of persistence can be shown by the theoretical calculation of the cumulative infection risk caused by different transmission modes (Figure 3.3.a). The detailed calculation processes refer to appendix B. The cumulative effect on infection risk is greatest for the respiratory

mode, is slight for the fomite mediated transmission mode, and is zero for the droplet spray mode. The effect of persistence is partially depends on the die off rate on hands, on surfaces and in air. Unrealistically eliminating the persistence process in the model can also present the effect of persistence. In this case, all transmission modes will take place instantaneously after shedding events occur. As shown in Figure 3.3.b, the temporal variation of the relative importance of different influenza transmission modes decreases without environmental persistence effect in the respiratory mode dominant scenario.

3.3. The Impact of Some Model Parameters on the Temporal Dynamics of the Different Influenza Transmission Modes over the Outbreaks

The absolute temporal variation level of the different influenza transmission modes over the course of outbreaks is influenced by some mode parameters relevant to virus particle dissemination and persistence.

We examined the impact of these model parameters (human movement, surface touching, die off rate in air and on surfaces) on the temporal dynamics of different influenza transmission modes. Since the temporal variation level of different influenza transmission modes is much greater in the respiratory transmission mode dominant scenario, we only present the results from the respiratory transmission mode dominant scenario here.

3.3.(a). The Impact of Host Movement Rate on the Temporal Dynamics of Different Influenza Transmission Modes over the Outbreaks

The effects of host movement on the temporal dynamics of different influenza transmission modes were explored. As shown in Figure 3.4.a, when host movement rate

decreases from 0.033 to 0.02 per minute in the respiratory mode dominant scenario, the cumulative infections over the course of outbreaks greatly decrease for the fomite mediated and droplet modes (>32.0%), but only slightly decreases for respiratory mode (5.0%). The FFI for all transmission modes slightly decreases by 7.4%. Correspondingly, as shown in Figure 3.4.b, the final relative importance decreases for fomite mediated and droplet modes but increases for respiratory mode. The temporal variation of different influenza transmission modes slightly decreases over the course of outbreaks.

The reason for these different impacts of host movement rate on respiratory and non-respiratory modes is that host movement only directly influences droplet and fomite mediated transmission modes, but not the respiratory mode. Host movement is the only way to bring susceptible individuals to co-locate with viral particles on surfaces and to co-locate with infectious people. Low host movement could decrease the number of susceptible individuals in cells with pathogens on surface by 1) bringing less susceptible individuals into cell with pathogens, 2) less movement of infectious individuals to contaminate other cells, and 3) decreasing virus dissemination to new cell surfaces via surface touching. With low movement rate, the large virus particles via droplet mode reach few co-located individuals, and might repeatedly spray to the same co-located people. However, host movement does not directly affect the co-location between the respirable viral particles and susceptible people, because the respirable viral particles can randomly disseminate to any loci after shedding.

The virus distribution on surfaces and in air is also altered by the decreased host movement rate. As shown in Figures 3.4.c and 3.4.d, the maximum value of total virus

number on surfaces decrease by 20% due to lower epidemic level, but the maximum value of contaminated surface locus count decreases by 40%. Correspondingly, the average virus count on a single contaminated surface locus increases greatly. Due to the low movement rate, few people come in touch and "clean" the contaminated surfaces and shedders shed to less surface loci, so the viruses on surface are more localized and lead to highly contaminated surfaces. On the other hand, low host movement rate does not directly influence instant and complete dissemination of the respirable virus dissemination in air, but it does lower the total air contamination level due to lower FFI. Therefore the total number of viruses in air, the number of contaminated air loci, and the average number of viruses in a contaminated air locus all decrease slightly.

3.3.(b). The Impact of the Surface Touching Rate on the Temporal Dynamics of the Relative Importance of Different Influenza Transmission Modes

We explored the effects of surface touching on the temporal dynamics of the different influenza transmission modes. As shown in Figure 3.5.a, when the surface touching rate increases from 0.2 to 0.6 per minute, the total FFI by all transmission modes increases by 45.0%. The fomite mediated mode specific FFI greatly increases by 3.5 times, but respiratory and droplet mode specific FFI slightly decreases by 20.0% and 10.0% respectively. Correspondingly, as shown in Figure 3.5.b, the relative importance greatly increases for the fomite mediated mode, but decreases for respiratory and droplet modes. The trade off of the relative importance is primarily between the cases with the extreme dissemination (air Vs. droplet), but the intermediate dissemination mode (fomite mediated) is more constant. By increasing the surface touching rate, the model

simulations change from a respiratory dominant scenario to an equal respiratory and fomite mediated mode dominant scenario by displacing respiratory and droplet transmissions with fomite mediated transmissions.

As shown in Figure 3.5.c, due to the higher infection transmission, the daily total viruses on surfaces and in air increase more than 2 times, and peak at a similar time. The contaminated air locus count greatly increases because of more respirable viral particles dissemination in air and low die off in air. The contaminated surface locus count only increases slightly since the majority of the surface loci have been contaminated even in the basic scenario with small surface touching case.

The reason for these results is that the increase of surface touching rate directly strengthens absolute infection transmission and the relative importance through the fomite mediated mode. On the contrary, the increased surface touching rate indirectly mitigates the infection transmission and the relative importance through respiratory and droplet modes due to competition among different transmission modes for susceptible persons on which to cause infection.

3.3.(c). The Impact of the Virus Die Off Rate in Air and Respiratory Mode Specific Shedding Rate on the Temporal Dynamics of the Different Influenza Transmission Modes

The respirable viral particle persistence partially depends on the viral die off rate in air and host breathing rate. To understand the impact of the respirable viral particle persistence process on the temporal dynamics of the different influenza transmission modes, we explored the simulations where both the virus die off rate in air and the respirable specific shedding rate increase.

As shown in Figure 3.6a, when both the viral die off rate in air and the respirable specific shedding rate increase by 3 times in the respiratory mode dominant scenario, the cumulative infection transmission over the course of epidemics slightly increase for all transmission modes. The total FFI through all transmission modes increases by 7.5%. Correspondingly, the temporal variation of the relative importance of different influenza transmission modes barely changes over the course of epidemics, but the absolute level of the temporal variation decreases (Figure 3.6.b). The viral distribution pattern varies greatly as shown in Figures 3.6.c and 3.6.d. Both the total virus particle counts in air and on surfaces peak at the similar time as that in basic scenario, but the peak value increases by 90% and 30% in air and on surfaces respectively. The peak value of contaminated air locus count increase 55% due to the increased respiratory specific shedding rate. The maximum number of contaminated surface loci barely changes.

The underlying reason for these results is that this change in model parameter mitigates the respirable virus particles persistence effects. When both die off rate in air and respirable deposit rate increase, the respirable virus particle amount shed from infectious people increase but their life span in air decrease. The total chance of expose to respirable virus particles for all susceptible people is similar theoretically, but the persistence effect of respirable virus particles decreases.

3.3.(d). The Impact of Super Shedders on the Temporal Dynamics of the Relative Importance of Different Influenza Transmission Modes

The heterogeneity of host shedding capacity affects the relative importance of different transmission modes [14]. We examined how super shedders alter the temporal

dynamics of the relative importance of different influenza transmission modes.

Super shedders refer to those who shed more virus particles than non-super shedders when they are infectious. The total virus shedding capacity for the host population was assumed to be the same when there are or there are no super shedders. To achieve this, the model assumes that a super shedder will shed X times more viruses than a non-super shedder during their infectious period, Y fraction of total population are super shedders, and virus amount shed from per shedding event is D when there is no super shedder. Then when there are super shedders in the model, the virus amount per shedding event will be computed by D/(1-Y+Y*X) for non-super shedders, and X*D/(1-Y+Y*X) for super shedders. This was verified by the similar total virus particle amount shed by infectious people from simulations with and without super shedders in our model.

As shown in Figure 3.7.a, in the respiratory mode dominant scenario, when 5% of the population are super shedders and super shedders shed 1000 times more viruses than non-super shedders, the chance of epidemics decrease greatly by almost 95%, since the single index case is usually a non-super shedder from random assignment and epidemics have less chance to take off. The cumulative infection decreases for all transmission modes over the course of epidemics. The average FFI greatly decreases by 50%. The epidemics take off and reach peak level much earlier, and die out quickly in two weeks, because the epidemics are primarily caused by super shedder index cases, and the most infectious individuals are super shedders and the secondary cases are directly generated by infectious super shedder individuals. When non-super shedders are infectious, they excrete much less virus particles and have low capacity to continue infection

transmission. Correspondingly, as shown in Figure 3.7.b, the final relative importance of influenza transmission modes barely changes, but the level of the temporal variation of the relative importance of influenza transmission modes decreases greatly. The changes in the temporal pattern of the relative importance of different transmission modes originate from the large number of viral particles at the beginning of epidemics, which is similar phenomenon as in the late stage of epidemics in the basic scenario. With super shedders, there is less accumulation from multiple infected individuals over the short time of epidemics. Comparing to no-super shedder scenario, more viral particles through droplet mode directly spray to few susceptible individuals. The surface contamination is much more localized on few surfaces, and the viral particles on surfaces can be repeatedly picked up by few co-located individuals and shedders themselves. Therefore, large size viral particles through droplet and fomite mediated modes are wasted. The respirable viral particles reach more susceptible individuals by dissemination process.

4. DISCUSSION

Commonly, infection transmission processes have been formulated as a simple probability, and the detailed physical contact processes were ignored in epidemic models [28,29]. Recent studies have shown that the environment significantly mediates influenza transmissions from one person to another [14, 20, 30]. Previous works normally ignored the temporal variation of different transmission modes over the course of outbreaks.

In this work, analysis of an environmentally mediated agent based model has shown that the relative importance of different influenza transmission modes does vary

greatly over the course of outbreaks. Specially, even in scenarios where respiratory transmission mode is ultimately dominant, non-respiratory transmission modes contribute to more to the overall transmission at the beginning of the epidemics. It takes about 10.0 days for respiratory transmissions to rise above non-respiratory transmissions.

Virus particles dissemination and persistence are found to be the underlying causes for these temporal dynamics of different transmission modes. A clear evidence is that decreasing dissemination and persistence of virus particles mitigates the temporal variation level of the relative importance of different influenza transmission modes. The environmental dissemination and persistence are directly relevant to the chance of co-location between susceptible individuals and virus particles. The environmental dissemination and persistence effects originate from the different model assumptions between small respirable virus particles through respiratory transmission mode and large particles through droplet spray and fomite mediated transmission modes. First, large virus particles through the droplet spray mode directly spray to co-located individuals instantaneously at the moment of shedding. Small respirable virus particles through respiratory mode and large virus particles through fomite mediated mode experience an intermediate environmental stage before exposure to susceptible individuals. Second, during the intermediate environmental stage, small respirable virus particles reach human individuals much faster by instantaneous dissemination in air, while large particles reach individuals slowly through human movement. Third, viruses survive greatest in air, medium on surface, and least on human hands. So the cumulative effect on infection risk is greater for the respiratory mode, is slight for the fomite mediated transmission mode, and is zero for the droplet spray mode. The zero dissemination and persistence of droplet

spread assumptions in our model might be slightly different from what we expect in reality where a droplet might reach susceptible people but take some time to be transferred from the place it arrives on the body to mucosal surfaces. But the dissemination and persistence of the droplet spray mode is reasonably much less than other modes in reality, and our inference directions should not be biased by these assumptions.

Further, varying some virus particle dissemination and persistence relevant mode parameters (host movement, surface touching, die off rate in air and respiratory shedding rate) alter the temporal dynamics of influenza transmission modes, which also support the causal hypothesis. Super spreaders have been confirmed as one of the most important factors for the SARS epidemic in Hong Kong and also occur for many other pathogens [20,30]. The super shedders mitigate temporal dynamics of the relative importance of different influenza transmission modes over the course of outbreaks, although the final relative importance of different transmission modes barely changes. The changes in temporal dynamics of different transmission modes caused by superspreader originate from the increased viral particles at the beginning of epidemics, which agrees to the explanation of the virus particles dissemination effect.

Although our results inform environmentally mediated transmission temporal dynamics via all transmission modes across time, this work alone does not allow policy makers to make specific intervention decisions in the real world. Changing of dominant transmission mode over the course of outbreaks observed here does not mean that one should simply exclude intervention strategies that primarily focus on late dominant transmission mode in the early stage of epidemics, since changing prevention emphasis

and strategies during the short course of an epidemic could be impractical and counterproductive in reality. However, the temporal dynamics of different influenza transmission modes still are of great public health significance, because it reminds us that it is unwise to simply exclude some interventions which specifically target less important transmission modes at the end of epidemics. This work is to convince people to pay attention to the previously un-recognized temporal dynamics of different transmission modes over the course of influenza epidemics, and to the potentially new direction of influenza researches.

We have intentionally avoided some realistic complexities in order to make the mechanism clear behind what we have discovered clear. For example, the model describes an unrealistic theoretical, homogeneous indoor environment. All individuals stay for all time in a single venue while in fact individuals could move from one venue to another. Realistic relaxation of this assumption could decrease the infection transmission equally through all transmission modes, but the model inference direction should be similar. The host movement in this model is random teleport and uniform for all individuals, which is different from the reality. The exponential dose response relation in this model is time independent, which might significantly differ from time dependent dose response [31]. But the model inferences made for a theoretical venue should be not biased by these assumptions. Some model parameters were determined from limited sources or expert opinion,[14], it would be useful to have future studies examining parameters such as influenza viral particle size distribution, host environment contact pattern, transfer efficiency.

This work in addition to some previous studies provide framework for

understanding the influenza epidemic impacts based on not only the final morbidity, but also the temporal dynamics. These initial steps will hopefully allow us to eventually better understand transmission mode relative importance and provide better intervention suggestions on time.

Table 3.1 Parameter values used to generate different transmission mode dominant scenarios

Parameter Description	Unit	Final dominant transmission mode				Reference
		Respirable	Droplet spray	Fomite mediated	No single dominant mode	
number of infectious seeds	Person	1	1	1	1	study design dependent
Host density	people / m^2	0.33	5.60	1.40	0.8	[14] Ispickna 2010
Inactivation rate—air	Min^{-1}	0.002	0.0024	0.004	0.0036	[32] Hemmes 1960
Inactivation rate—surfaces	Min^{-1}	0.006	0.006	0.0002	0.001	[33] Bean 1982
Inactivation rate—hands	Min^{-1}	0.75	0.74	0.74	0.9	[33] Bean 1982
Rate of changing location	Min^{-1}	0.033	0.05	0.1	0.1	[14] Ispickna 2010
Lower HID50	$TCID_{50}$	0.15	0.5	0.5	0.25	[34] Alford 1966; [14] ispicknall 2010
Upper HID50	$TCID_{50}$	500	250	250	380	[35] Couch 1971; [14] ispicknall 2010
Proportion of respirable virus among all viral particles		4.5E-6	1.4E-6	1.4E-6	1.4E-6	[36] Nicas 2005 [37] Loudon 1967
Proportion of inspirable virus among all virus particles		0.0095	0.0095	0.0095	0.0095	[36] Nicas 2005 [37] Loudon 1967
Rate of self inoculation	Min^{-1}	0.1	0.1	0.3	0.26	[38] Handley 1973 [39] Nicas 2008
Rate of surface touching	Min^{-1}	0.2	0.2	2.0	0.7	[14] ispicknall 2010
Rate of breathing	Min^{-1}	16	16	16	12	[14] ispicknall 2010
Transfer efficiency (surface to hand to surface)		0.3	0.3	0.6	0.5	[40] Sattar 2001 [14] ispicknall 2010
Recovery rate for infectious individuals	Min^{-1}	0.0007	0.0007	0.0007	0.0007	[36] Nicas 2005
Shedding volume	mL	0.044	0.044	0.044	0.044	[36] Nicas 2005 [37] London 1967

NOTE: HID_{50} = quantity of virus required to cause infection in 50% of humans.

Figure 3.1.a. the average daily cumulative infection through different transmission modes in four different transmission mode dominant scenarios (A.respiratory; B.droplet spray; C.fomite meditated; D.no-single transmission mode).

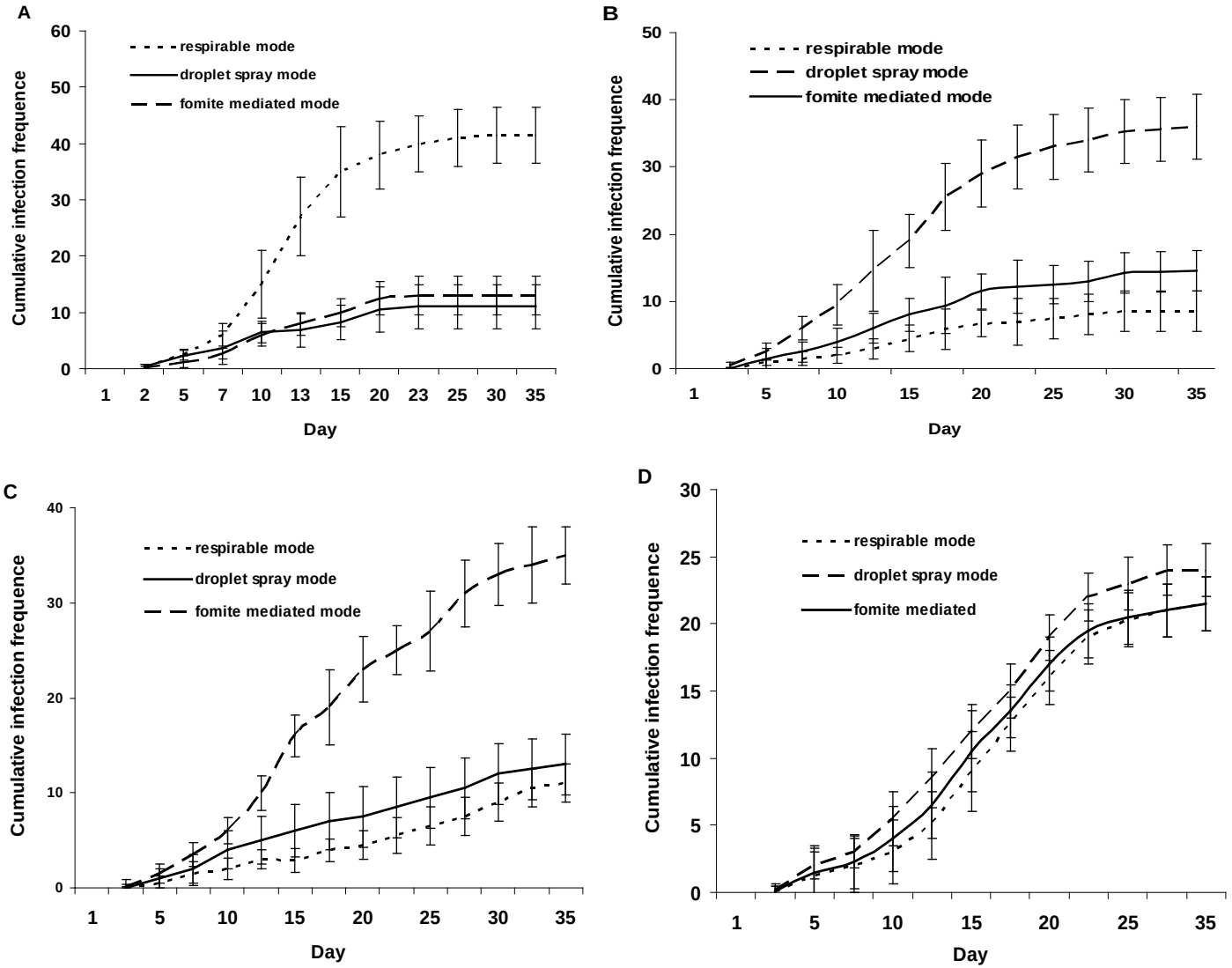

Figure 3.1.b The average daily relative importance of different influenza transmission modes in four different mode dominance scenarios (A.respiratory; B.droplet spray; C.fomite meditated; D.no-single transmission mode).

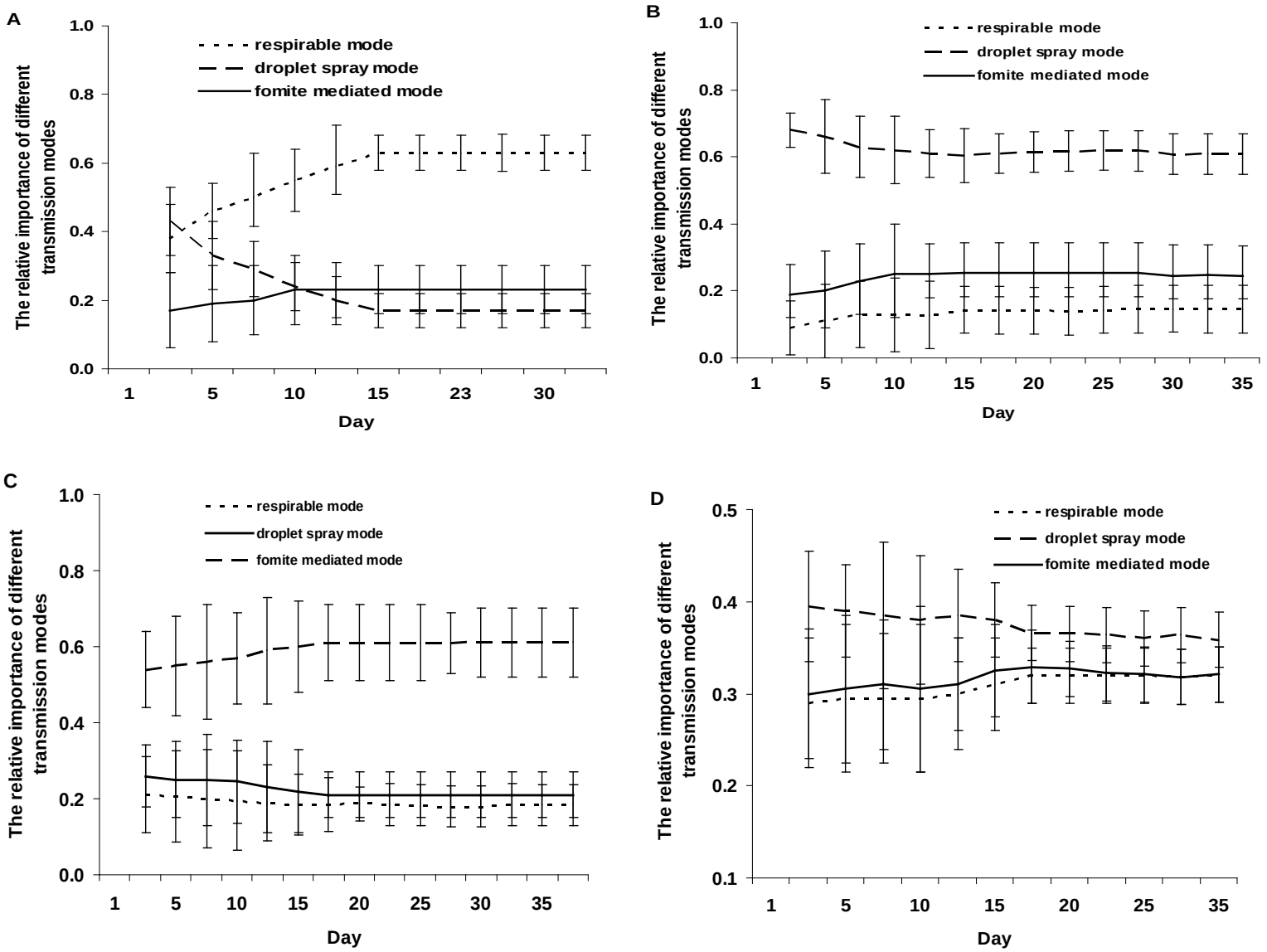

Figure 3.2.a The impact of respirable viral particle dissemination process on the temporal dynamics of the relative importance of the respiratory transmission mode. (High dissemination: disseminate to all loci. Medium dissemination: disseminate to 8 neighboring loci. No dissemination: disseminate to only the current occupied locus.)

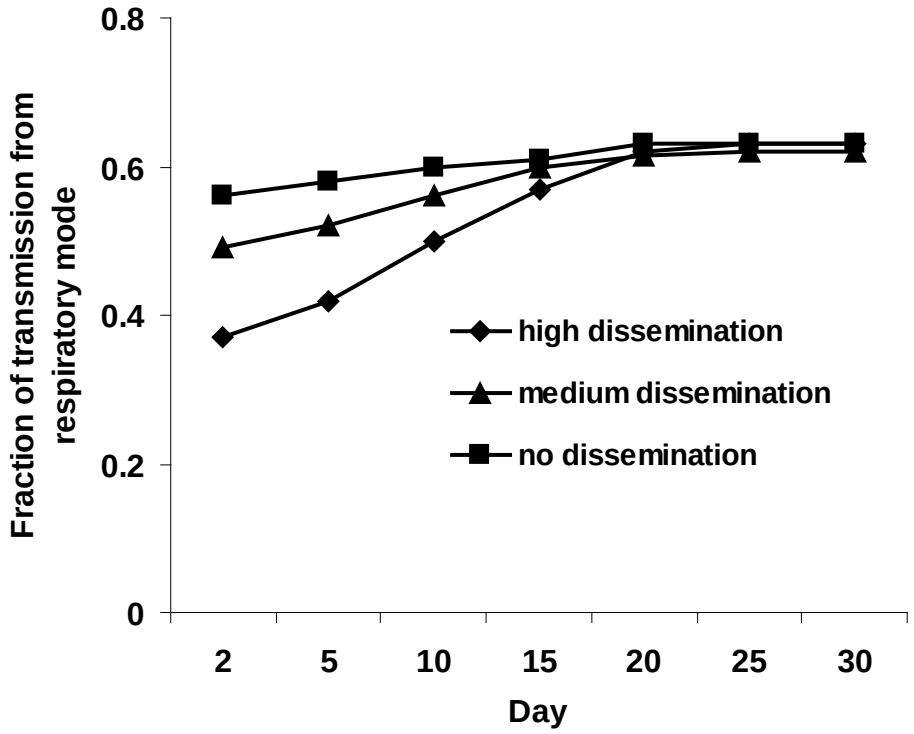

Figure 3.2.b. The average daily cumulative infection frequence by varying respirable virus particle dissemination range in the respiratory transmission mode dominant scenario. (global dissemination: disseminate to all loci. local dissemination: disseminate to current shedder occupied locus).

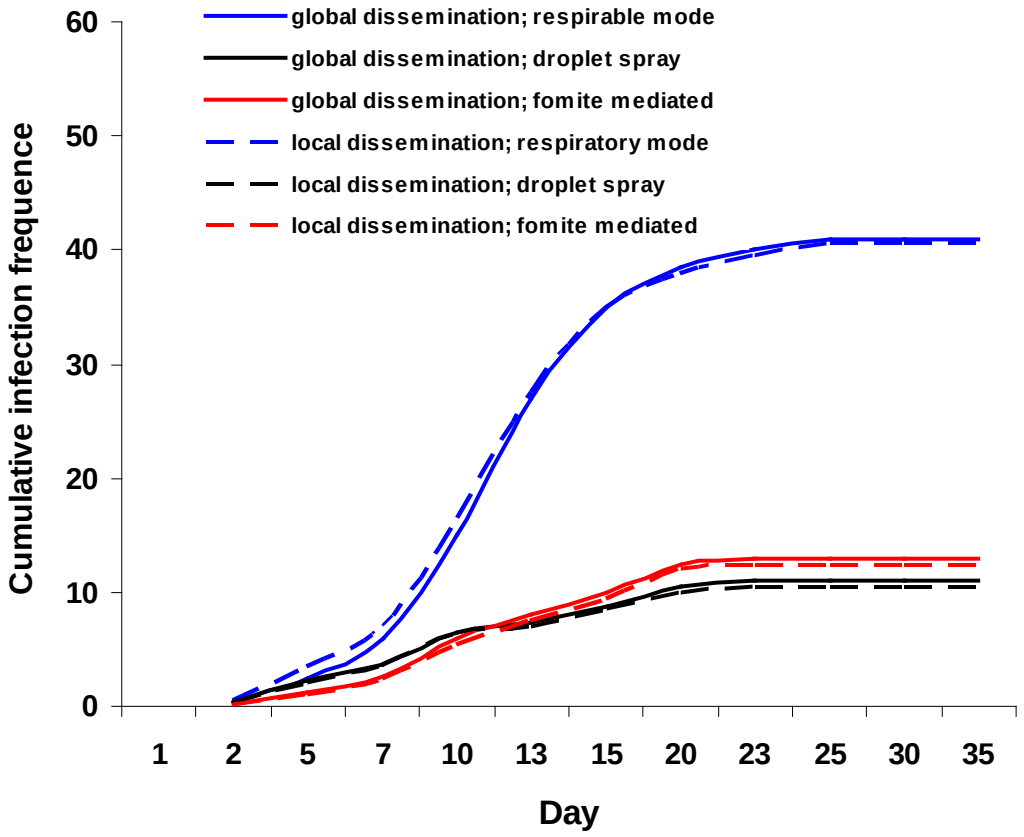

Figure 3.3.a. Theoretical calculation of average secondary case generated by an index case through different influenza transmission modes in the respiratory transmission mode dominant scenario.

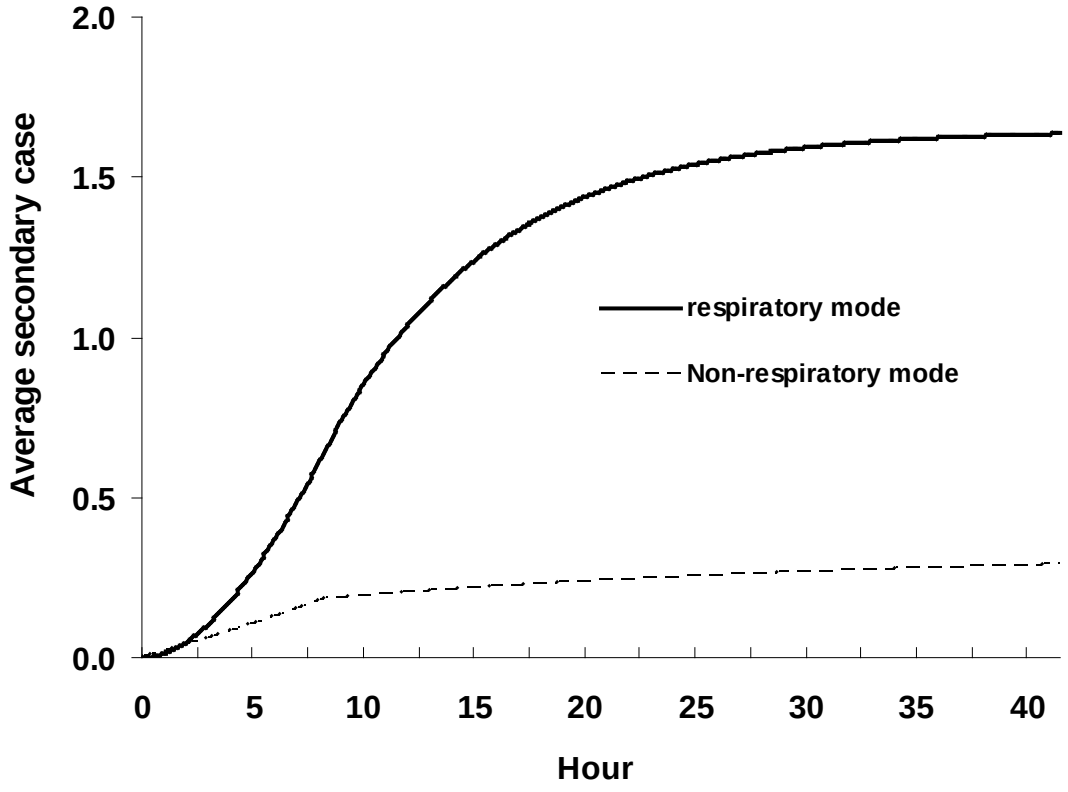

Figure 3.3.b. The relative impact of persistence of respirable virus particles on the temporal dynamics of the relative importance of the respiratory transmission mode.

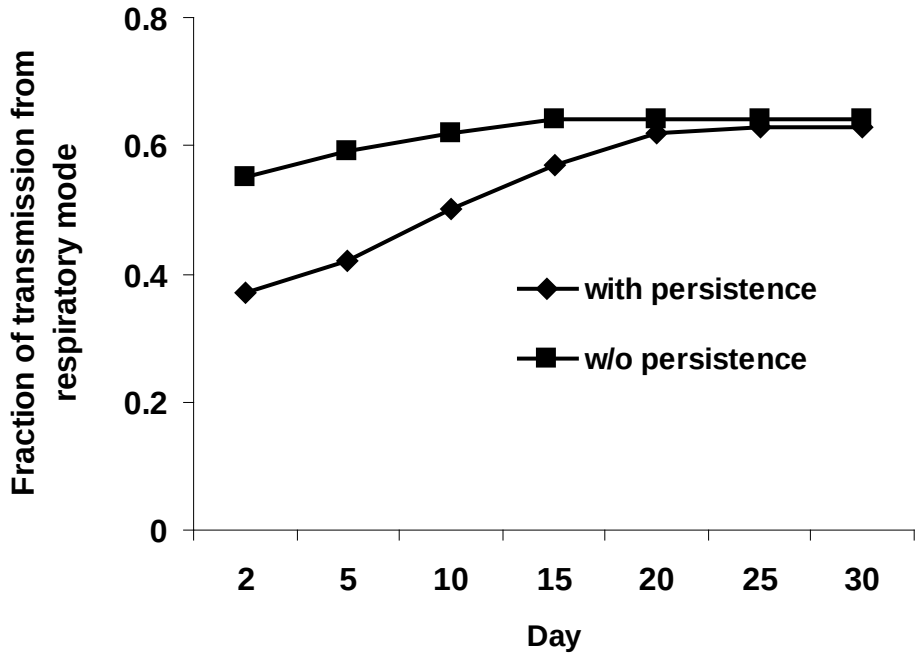

Figure 3.4.a. the average daily cumulative infection by different transmission modes and host movement rate in the respiratory transmission mode dominant scenario.

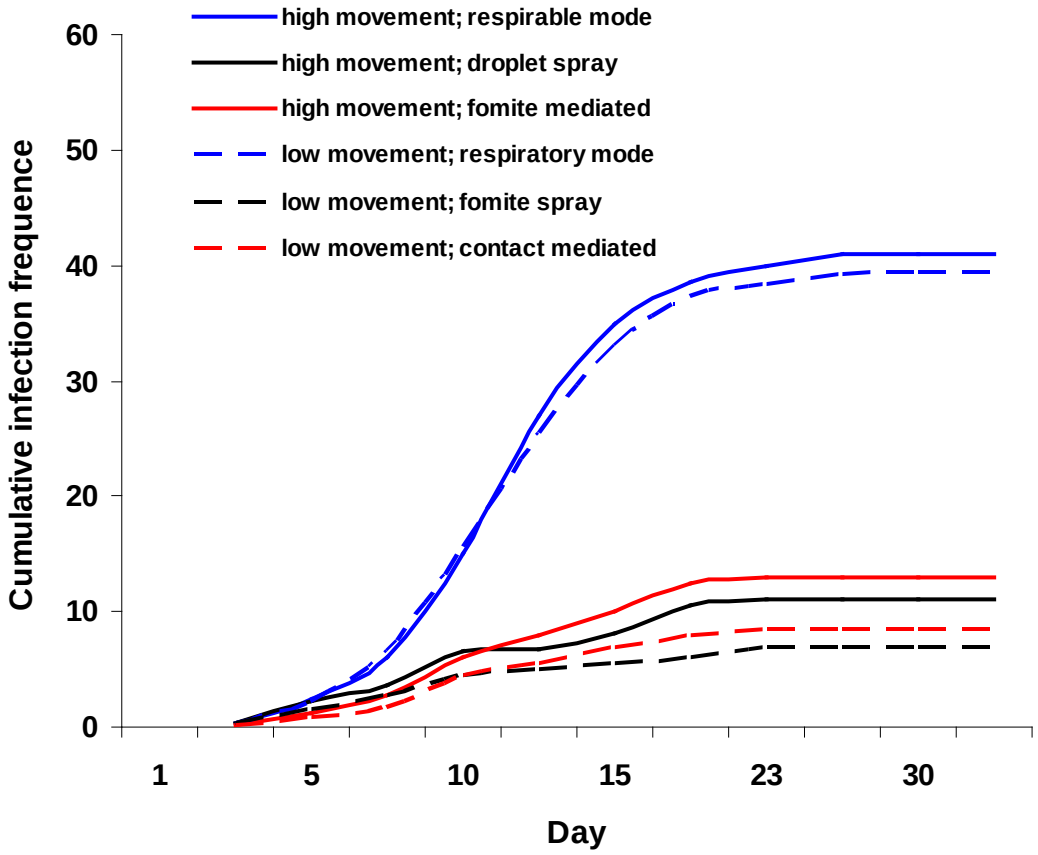

Figure 3.4.b. The relative importance of different influenza transmission modes by varying host movement rate in the respiratory transmission mode dominant scenario.

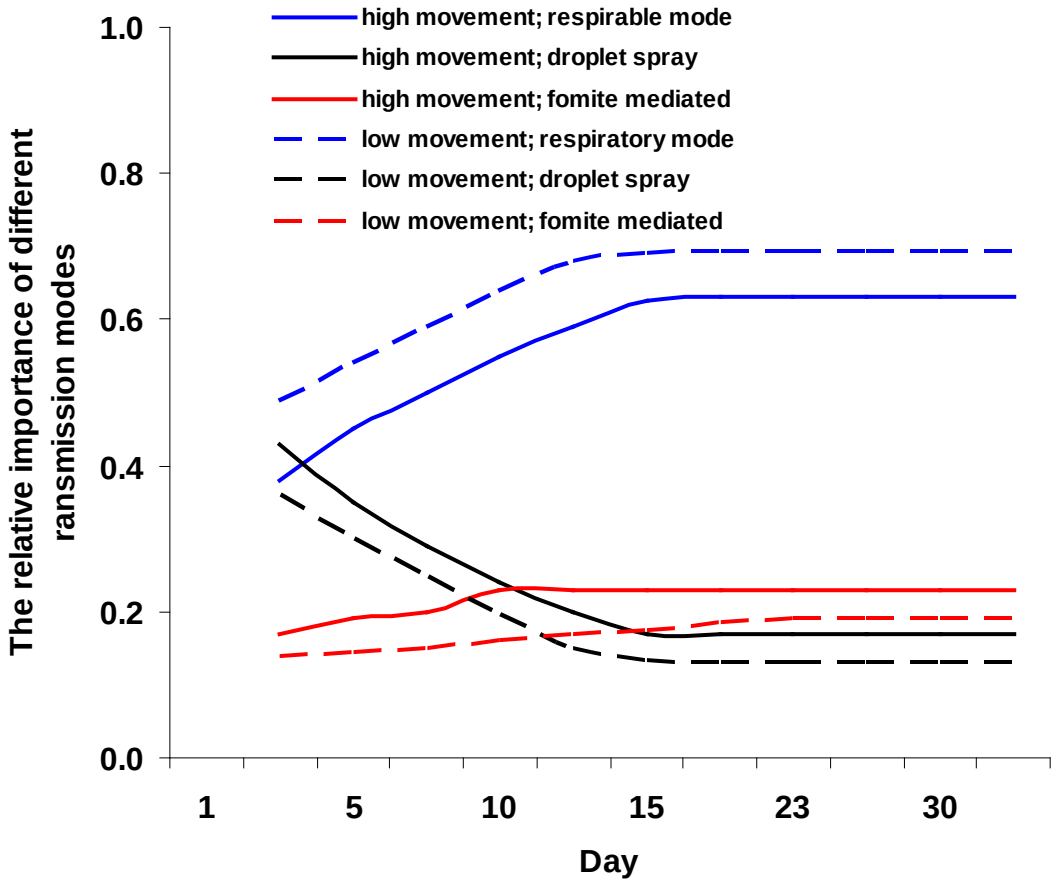

Figure 3.4.c. The environmental dissemination of influenza viral particles (total viral particle number in air and on surfaces) by varying host movement rates in the respiratory transmission mode dominant scenario. (note: the unit for total viral particle number on surface is 10^6 count.)

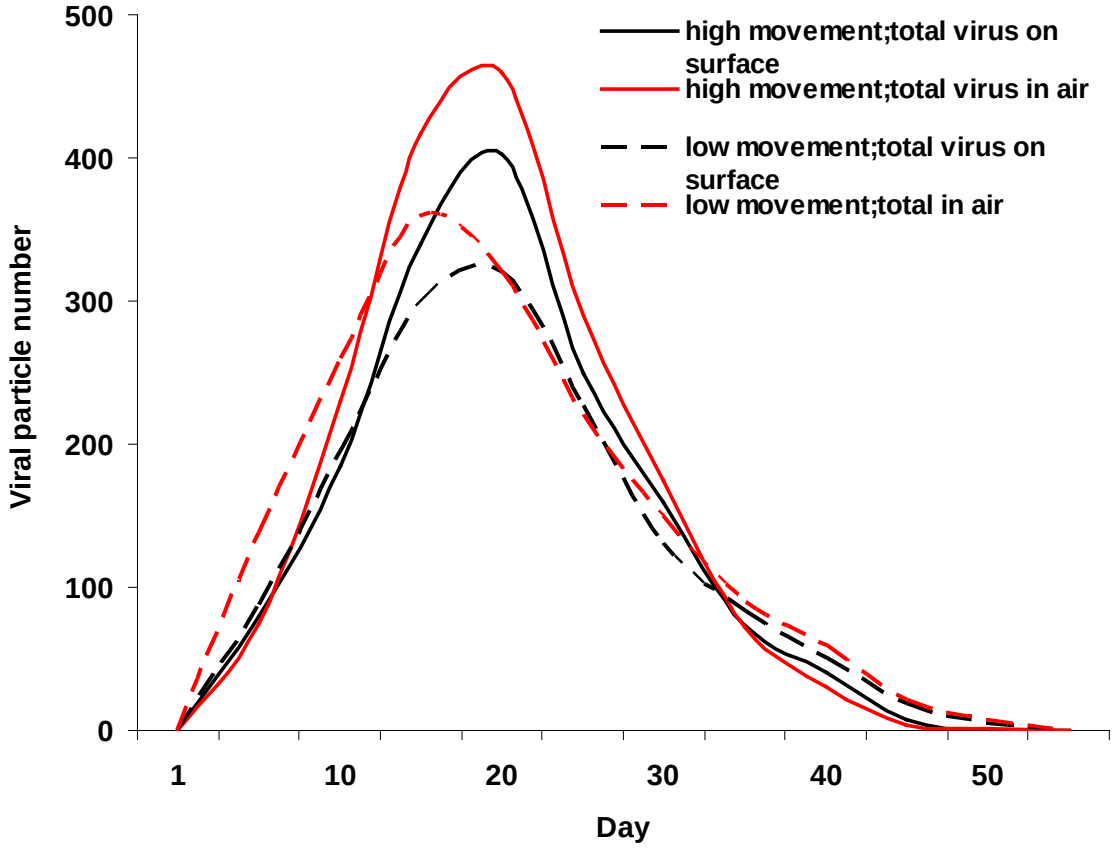

Figure 3.4.d. the influenza virus contaminated air and surface locus by varying host movement rates in the respiratory transmission mode dominant scenario.

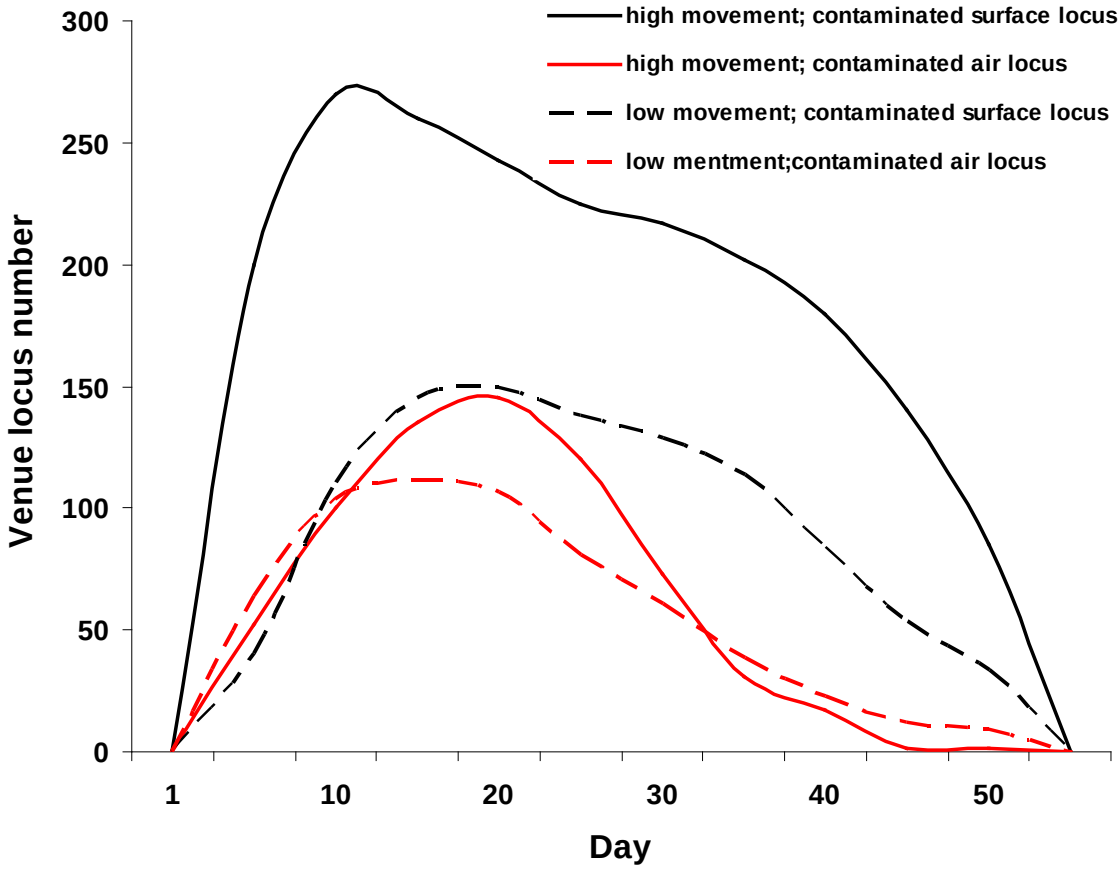

Figure 3.5.a. The average daily cumulative infection by transmission mode and surface touching rate in the respiratory transmission mode dominant scenario.

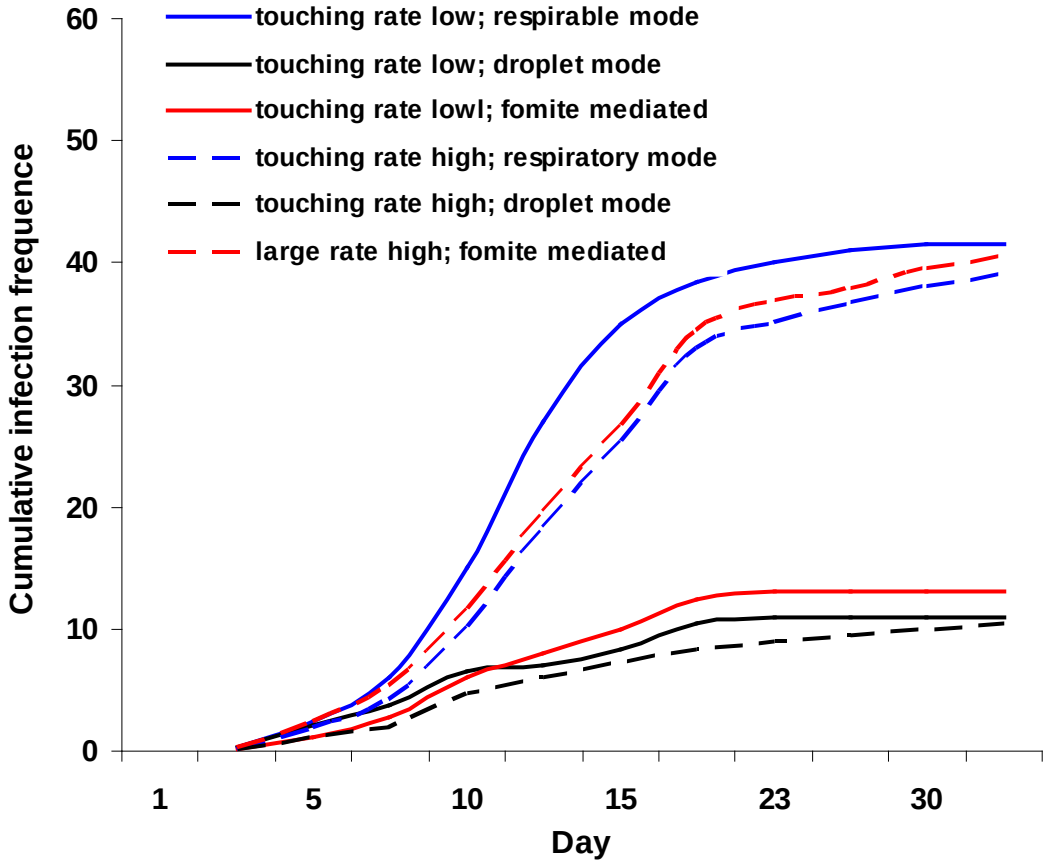

Figure 3.5.b. the relative importance of different influenza transmission modes by varying host surface touching rate in the respiratory transmission mode dominant scenarios.

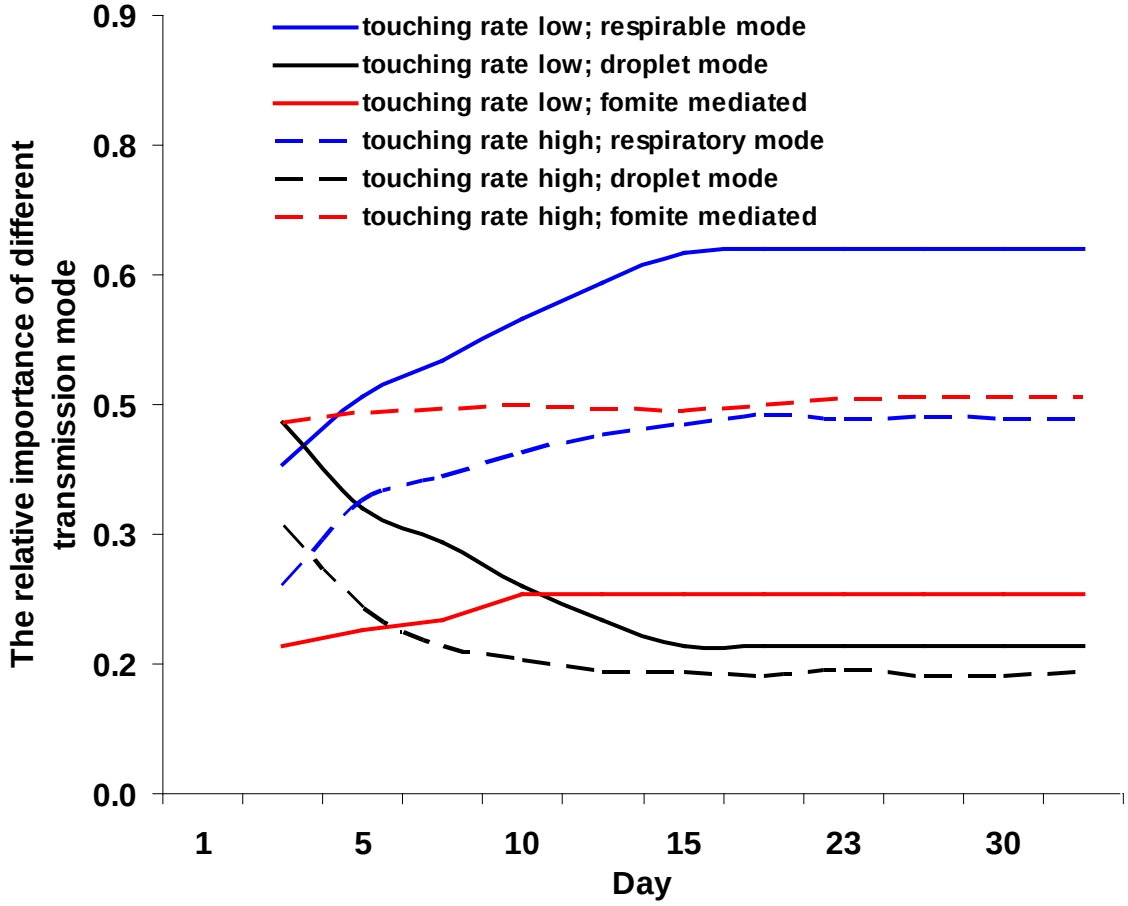

Figure 3.5.c. the environmental dissemination of influenza viral particles (total viral particle number in air and on surfaces) by varying surface touching rate in the respiratory transmission mode dominant scenario. (note: the unit for total viral particle number on surface is 10^6 count.)

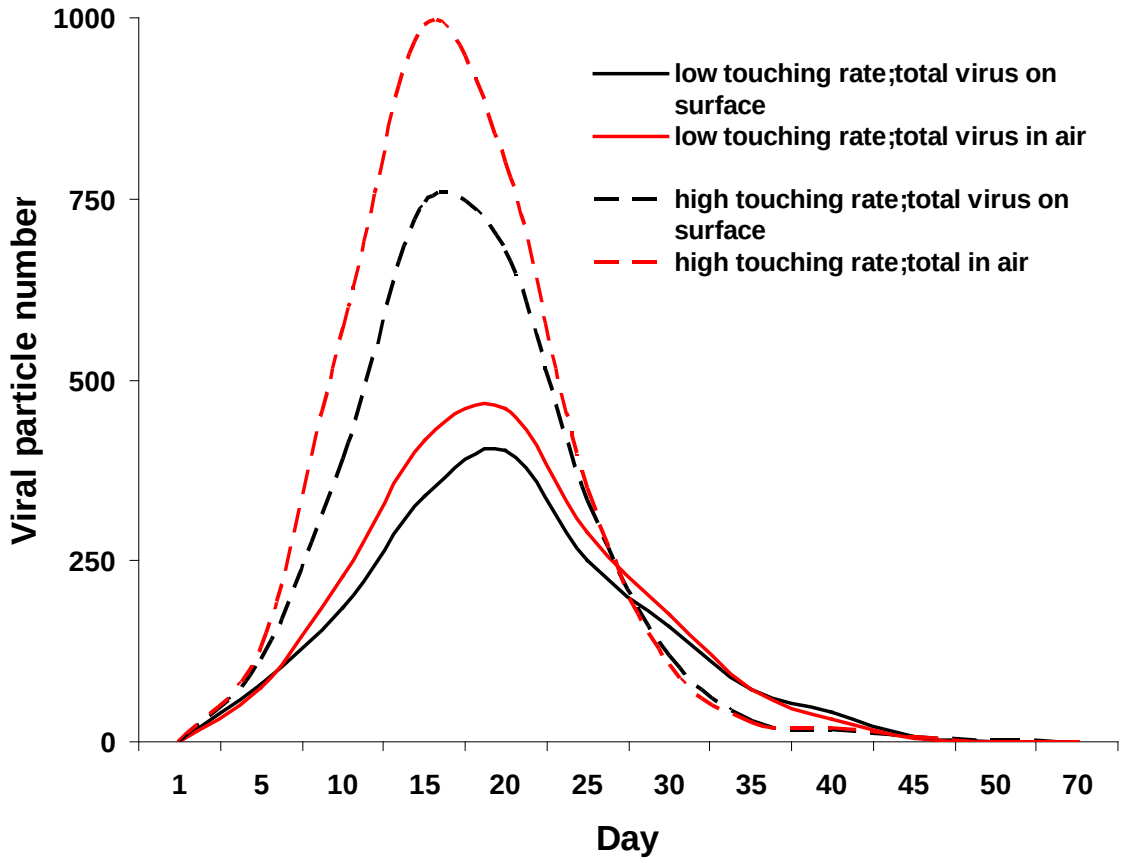

Figure 3.5.d. the contaminated air and surface locus count by varying surface touching rate in the respiratory transmission mode dominant scenario.

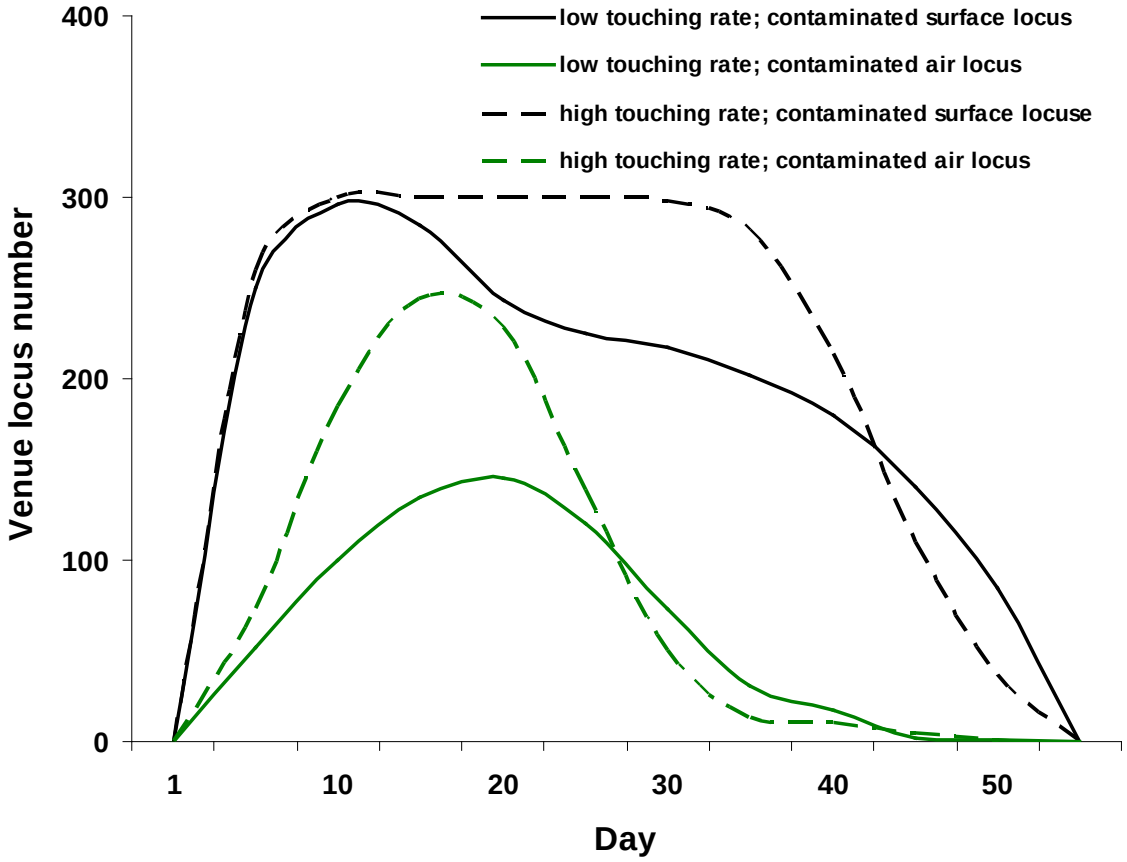

Figure 3.6.a. The average cumulative infection over the course of epidemics by varying virus die off rate in air and respirable virus shedding rate in respiratory transmission mode dominant scenario.

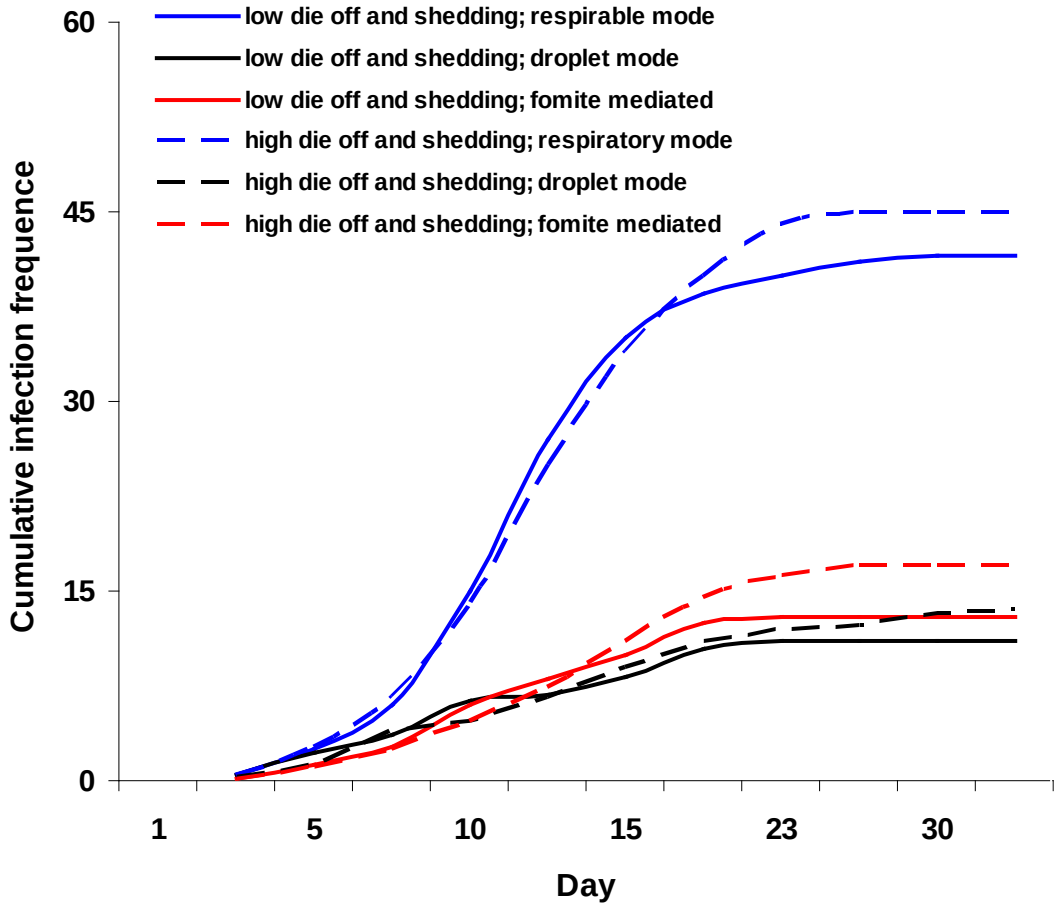

Figure 3.6.b. The relative importance of different influenza transmission modes by varying virus die off rate in air and respirable virus shedding rate in the respiratory transmission mode dominant scenarios.

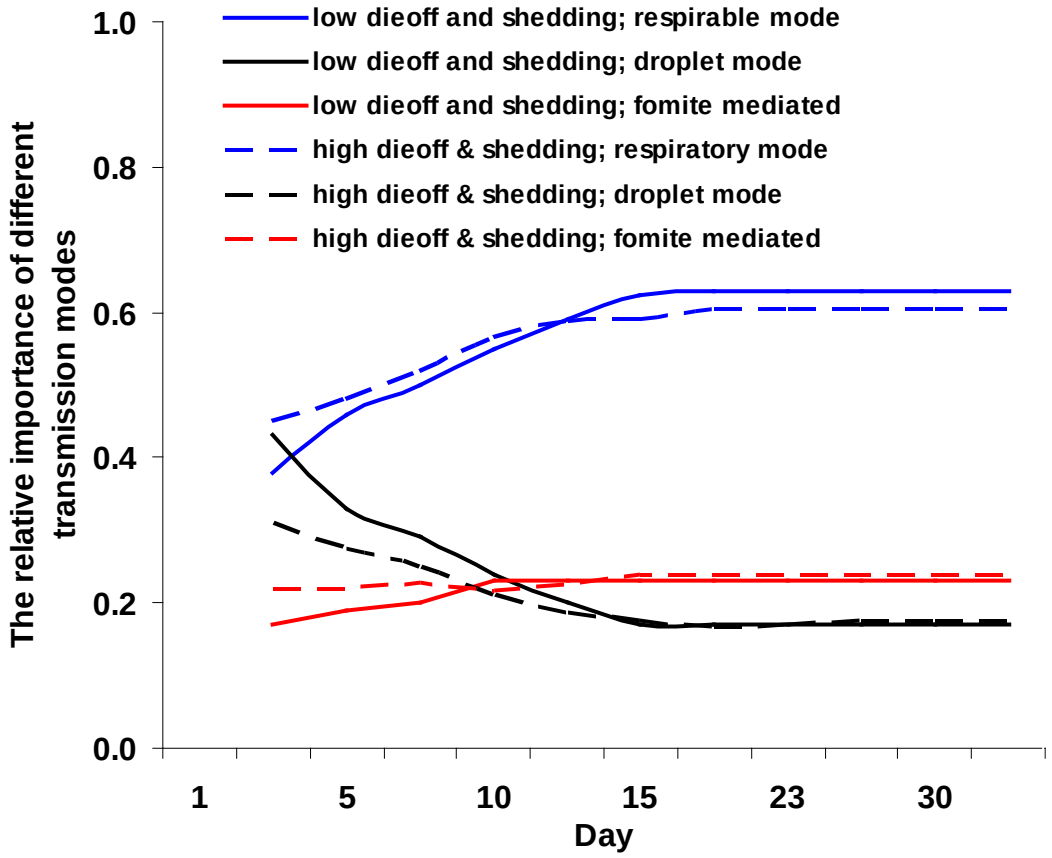

Figure 3.6.c. The environmental distribution of influenza viral particles (total viral particle number in air and on surfaces) by varying virus die off rate in air and respirable virus shedding rate in the respiratory transmission mode dominant scenario. (note: the unit for total viral particle number on surface is 10^6 count.)

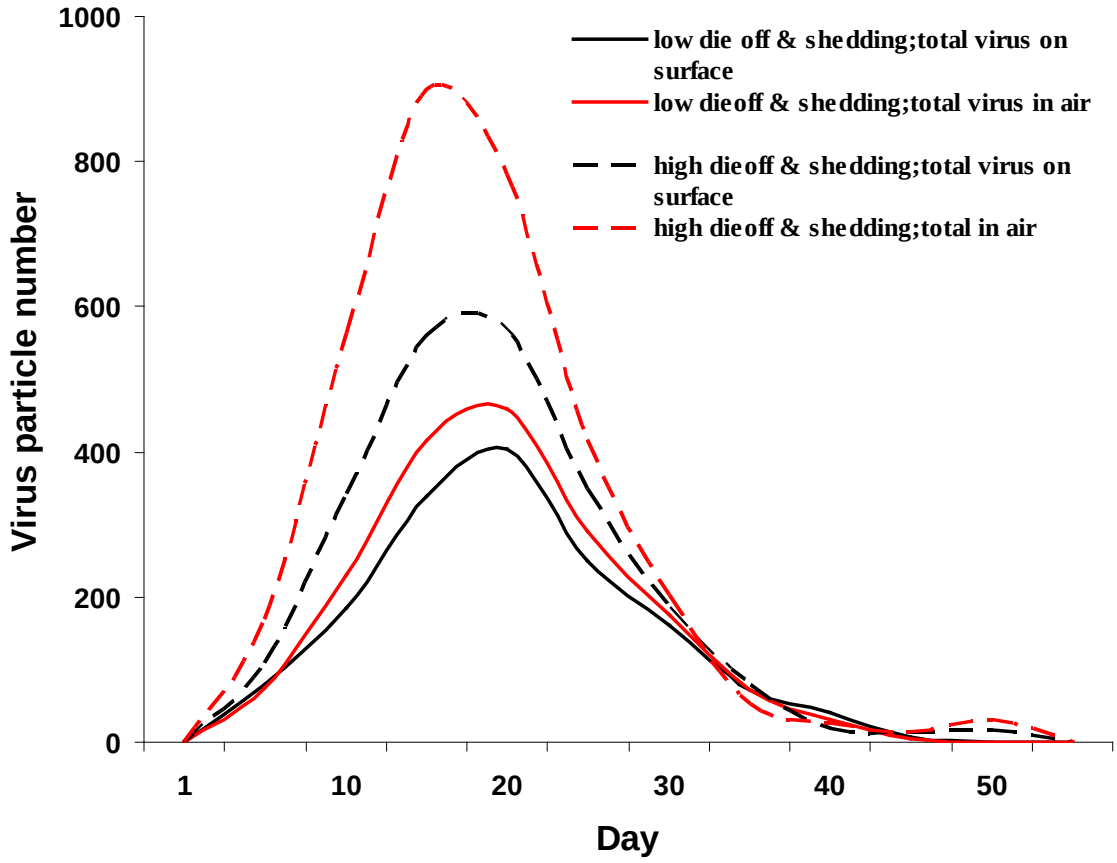

Figure 3.6.d. the contaminated air or surface locus count by varying virus die off rate in air and respirable virus shedding rate in the respiratory transmission mode dominant scenario.

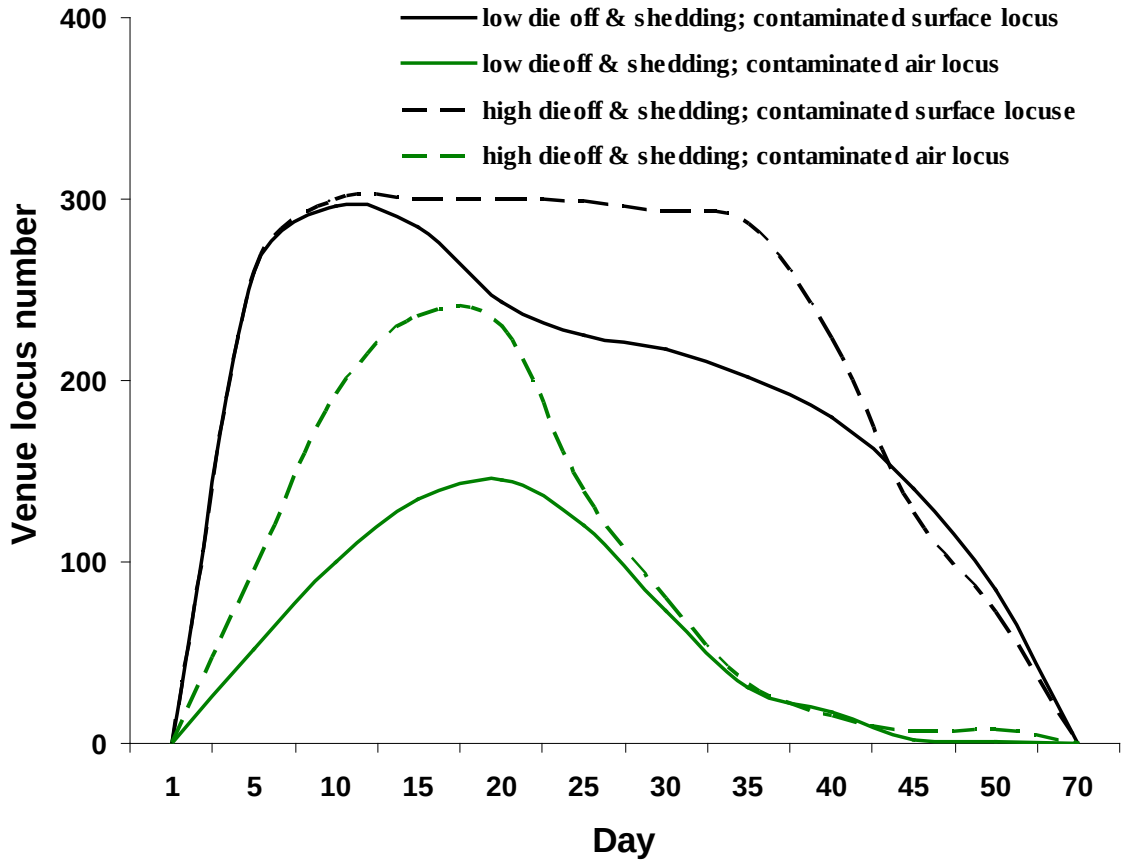

Figure 3.7.a. The average cumulative infection with 5% super shedders who shed 1000 times more viruses than non-super shedders in host population in the respiratory transmission mode dominant scenario.

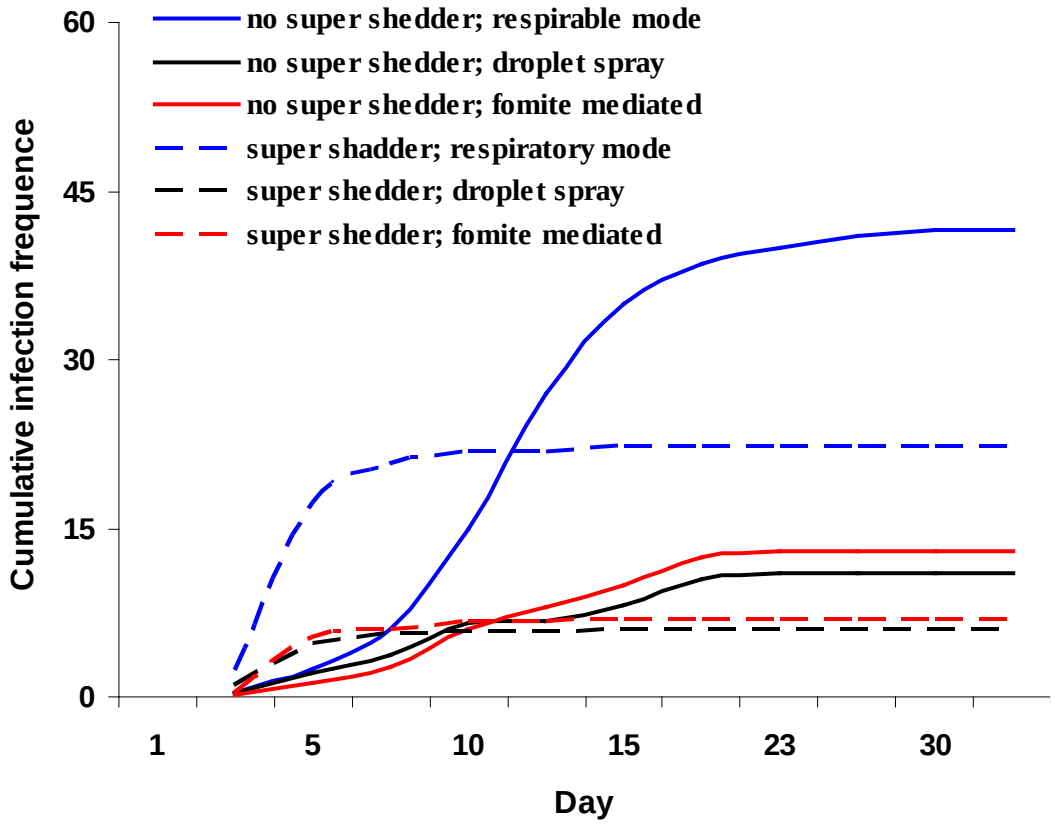

Figure 3.7.b. The relative importance of different influenza transmission modes with 5% super shedder who shed 1000 times more viruses than non-super shedders in the population in the respiratory transmission mode dominant scenarios.

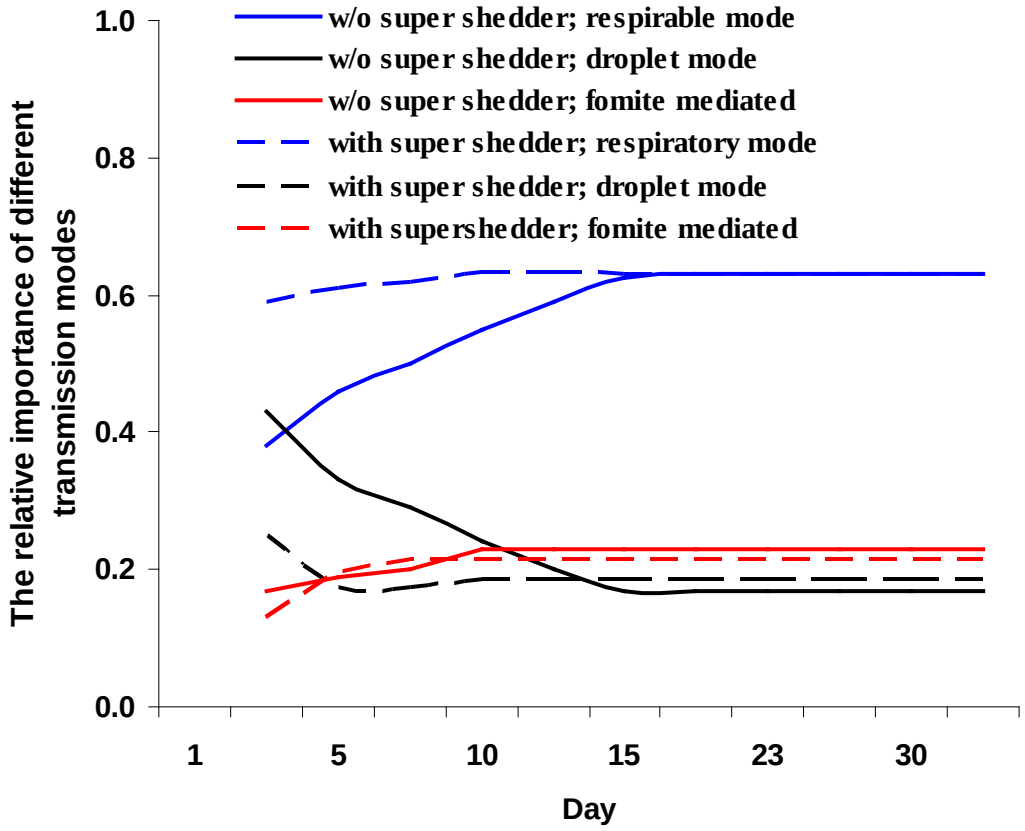

APPENDIX A

The Detailed Environmentally Mediated Transmission Model

This is a stochastic individual based model that simulates environmentally mediated influenza infection transmission. The model components include discrete individuals, pathogens, and raster environment units.

The Pathogens and the Human Individuals

Influenza viral particles are assumed to be uniformly identical entities, excreted by infected individuals. Influenza viral particles can persist in the air, on a person's hand, or on surfaces, and eventually die out in these locations based on different die off rates. Inspirable particles can settle onto surfaces from air and enter fomite mediated transmission mode. Virus particles in air can be removed by air exchanging too.

The Human Individuals

Human individuals in this model are uniform with regard to influenza infection status. All individuals are either susceptible, infectious, or recovered based on their infection and immunity status. Individuals have a "hand" entity which mediates touching of environmental surfaces processes. Individuals are heterogeneous regarding infectivity when considering super spreaders in the model. Super spreaders are individuals who shed more viral particles than non-super spreaders. Susceptible individuals become infectious by either breathing viral particles or by touching their eye, nose, and mouth with contaminated hands. After being infected, the individuals become complete immune.

The Venue Environment

In this model, two types of environment settings, air and surfaces, are presented by raster cells. The size of environmental cells is set as 2*2*3 meter. All environmental cells are similar with regard to how people contact air or surfaces. Pathogens are assumed to be evenly distributed inside surface and air cells. Infectious individuals can contaminate the environment cell surface where they are currently located. Individuals can pick up a fraction of pathogens from a surface or air cell via hand touching and breathing. Individuals are assumed to stay in the venue all the time.

The Microbial Dose-response Relationship

An exponential dose-response model was used to calculate the risk associated with a given virus dose. When we calculate the risk after individuals pick up pathogens from environment, risk from previously picked up pathogens are independent of the risks from newly picked up pathogens. The respiratory and inspiratory transmission mode specific HID_{50} is same with a mean of 0.67 $TCID_{50}$ units of virus particles. The fomite mediated and droplet spray mode specific HID_{50} values are the same with means of 500 $TCID_{50}$ units of virus particles [14].

The Discrete Events in the Model

The model was implemented by using Gillespie algorithm, a time to event-based modeling simulation process. At each simulation step, a single event is chosen and performed based on the likelihood of all events. There are 23 types of events in this model involving shedding pathogens, individual movement, surface touching, self-

inoculation, breathing, and infection progression.

Human Individual Breathing: Individuals breathe in certain volume of air through breathing event based on breathing rate parameter. If there are pathogens in the air, we determine the quantity of viruses being inspired by considering the volume of air inspired ($Vol_{inspire}$) and the total air volume in current air locus (Vol_{cell}). Then we determine the pathogen number that deposits in the alveoli regions to potentially cause infection based on a deposition efficacy parameter. Those inspired pathogens which do not deposit in the alveoli are instantaneously exhaled back to air with no loss in viral viability. The chance of being breathed in for virus particles in air depends on the density of virus particles in the current air locus (Vair), and the fraction of inhaled virus deposited to alveoli ($t_{airDposit}$). The amount of respirable virus particles transferred to the alveolar region:

$P_{toLung} = V_{air} * (Vol_{inspire} / Vol_{cell}) * t_{airDeposit}$

Human Self-inoculation: Individuals with pathogens on their hands may touch their own eyes, nose or mouth based on model parameter of self-inoculation rate. Some proportion of the pathogens on hands will be transferred to the target mucous membranes. The amount of virus particles on hand being inoculated ($V_{inoculate}$) is determined by the amount of virus particles on hands ($V_{fingertip}$), the transfer efficiency (likelihood) from hand to mouth/nose/eye ($t_{handToMouth}$), and to target mucus membranes ($t_{mouthToMucus}$). This inoculated virus quantity is:

$V_{inoculate} = V_{fingertip} * t_{handToMouth} * t_{fingerToMouth.}$

Shedding Events: Infectious individuals shed pathogens over the course of infection

through discrete shedding events, analogous to coughs or sneezes. The likelihood of shedding event is determined by shedding rate parameter. Each shedding event excretes some volume of mucous material. This mucous has a viral concentration which varies by day of infection. Therefore, the total virus amount from a single shedding event varies by day of infection. The overall pathogen output starts low after being infected, rises to a peak on the third day of infection, and then tails off until day eight, when it is back to the low levels of the first day. Some fraction of the excreted viruses is in respirable particles, and is assumed to disperse immediately to all environment air cells and stay aerosolized in air after shedding. Some fraction of the excreted viruses is in inspirable particles, and is assumed to only stay in current cell and could settle down. The remaining either spray to nearby individuals' eyes, mouth and nose through droplet spray mode, or settles down to fomite surfaces in the shedder's current location to enter fomite mediated mode.

Virus inactivation: the loss of viability of the viruses in the model is assumed to be a simple first order process. The likelihood of virus inactivation events are based on different die off rates in the air, on hands, or on fomite surfaces. In addition, air exchange process can eliminate viruses from the air, and has same consequences as virus inactivation in air.

Surface touching: individuals touch environment cell surfaces where they are currently located. When a surface touching event occurs, viruses can be transferred from the surface to human fingertips or vice versa. Once there has been pathogen transfer, we assume that the pathogens are evenly distributed over the surface in the given cell. Viral amount on a surface locus ($A_{surface}$) and fingertips ($A_{fingertip}$), the surface area of the

fingertips ($P_{Surface)}$, the surface area of the environment cell surfaces ($P_{Surface}$), and the transfer efficiency ($t_{surfaceToFingertip}$) were used to determine the actual quantity of pathogens transferred as below.

The amount of pathogens transferred to the hand is:

$P_{toHand} = P_{Surface} * t_{surfaceToFingertip} * A_{fingertip} / A_{surface}$

The amount of pathogens transferred to the surface is:

$P_{toSurface} = P_{fingertip} * t_{fingertipToSurface}$

Infection progression: influenza infectious period lasts eight days after the onset of infection. To implement infection progression from day one of infection to day two and so forth, we use an exponential distribution between each day. By this way, the model generates a distribution of infection duration and total virus excretion that corresponds to model assumptions and previous observations.

Movement events: in the model, individuals can change location by teleporting. The likelihood of individual movement is based on the model parameter of movement rate. When a movement event occurs, individuals change current location to target location independent of the distance and direction between the current location and target location. The time spent in transit was assumed to be negligible. Based on reasonable parameter range suggested by Ispicknall et al, a spatial flow from one raster cell to another cell does not change the model simulation results, thus this unrealistic model assumption will not change our inference in this modeling contex [14].

APPENDIX B

This is the theoretical calculation of the cumulative infection risk via different modes caused by an index case repeatedly shedding events implemented in R code simulations. To simplify the calculation and presents easily, we ignore the host movement due to relative high movement rate in the mode. When the host movement is slow, this calculation needs to be slightly modified to address the host movement issue, but the comparison among different transmission modes is similar.

For the respiratory transmission mode:

(1) N, Viral amount to respiratory mode from one shedding event, assuming that one TCID50 includes 100 respirable viral particles:

Shedding virus amount from a single shedding event (TCID50 unit) : 0.4*10^5

The fraction of viruses to respiratory mode: 4.5*10^-6

viral particle number per TCID50 unit: 100

N = 0.4*10^5 * 4.5*10^-6 * 100 = 16

(2) $cumuB_i$, the cumulative chance of being breathed in by a co-located individual for a respirable virus particle after i-th breathing events during T minutes since shedding:

Breathing event frequency during T time, i: i <= T*16

The chance of being removed for respirable virus particles between two continuous breathing events: 0.002/16 = 0.000125

The chance of being breathed in for respirable virus particles by a single breathing events: 0.000042

B_i: The chance of being breathed in by a co-located individual for a respirable virus particle at i-th breathing event,

B_1: 0.000125

B_i: cumprod (1-B_1, 1-B_2, …, 1-B_{i-1}) * (1-0.000125)^(i-1) * 0.000042

So the cumuBi: cumsum(B_1, B_2, …., B_i)

(3) R_i, the cumulative infection risk caused by respirable virus particles after i-th

breathing events during T minutes since a single shedding event:
Breathing event frequency during T time, i: i <= T*16
The chance of being co-located with a susceptible host for a respirable virus particle: 0.33
The chance of causing infection by one respirable virus particle after being breathed in: 0.027
R_i = N*cumuB_i*0.027*0.33 = 0.143*cumuB_i where B is determined by time period since shedding in (2)

(4) cumuR_i, the cumulative infection risk caused by respirable virus particles after i-th breathing events during T minutes after multiple shedding events:
cumuR_i = cumsum(R_1, R_2, …, R_i)

For droplet spray mode:
(1) N, Viral amount to droplet mode from one shedding event, assuming that one TCID50 includes 100 respirable viral particles:
Shedding virus amount from a single shedding event (TCID50 unit): 0.4*10^5
The fraction of viruses to respiratory mode: 3.75*10^-4
viral particle number per TCID50 unit: 100
N = 0.4*10^5 * 3.75*10^-4 * 100 = 1500

(2) R, the infection risk through droplet mode for a co-located susceptible individual after one shedding event, based on exponential dose-response function:
The transfer efficacy from mouth to upper respiratory track membrane: 0.2
The chance of being co-located with a susceptible host for a respirable virus particle: 0.33
R = 0.33*0.2* (1-exp(-((-log(0.5)/50000) *N))) = 0.0041

(4) cumuR, the cumulative infection risk caused by droplet mode T minutes since introducing the index case:
The shedding event frequency during T minutes, j: j <= T/5
cumuR = cumsum(R)

For fomite mediated transmission mode:

(1) N, Viral amount to the surface from one shedding event, assuming that one TCID50 includes 100 respirable viral particles:

Shedding virus amount from a single shedding event (TCID50 unit) : 0.4*10^5

The fraction of viruses to respiratory mode: 0.9996

The viral particle number per TCID50 unit: 100

N = 0.4*10^5 * 0.9996 * 100 = 4000000

(2) $cumuB_i$, the cumulative chance of reaching co-located individual upper respiratory track for surface virus particles after i-th surface touching events during T minutes since shedding:

Surface touching event frequency during T time, i: i <= T/5

The chance of dying for virus particles between two continuous surface touching events, due to high death rate on surfaces and on hands: 0.92

The chance of being picked up and transferring to upper respiratory track membrane from surfaces by a single hand surface touching event: 0.000000005

Bi: The chance of reaching upper respiratory track membrane for virus particle at i-th surface touching event,

B_1: 0.000000005

cumprod ($1-B_1$, $1-B_2$, …., $1-B_{i-1}$) * $(1-0.92)^{i-1}$ * 0.000000005

$cumuB_i$: cumsum(B_1, B_2, …., B_i)

(3) R_i, the cumulative infection risk caused by surface virus particles after i-th surface touching events during T minutes since a single shedding event:

Surface touching event frequency during T time, i: i <= T/5

The chance of being co-located with a susceptible host for a respirable virus particle: 0.33

HID50 for fomite mediated mode: 500 TICID50

Cumulative virus particles amount reaching upper respiratory track membrane after i surface touching event, n : $N*cumuB_i$

$R_i = (1-\exp(-((-\log(0.5)/50000) *N*cumuB_i))) * 0.33 = 0.143*cumuB_i$

(4) $cumuR_i$, the cumulative infection risk caused by virus particles on surfaces after i-th surface touching events during T minutes after multiple shedding events:

$cumuR_i = cumsum(R_1, R_2, \ldots, R_i)$

REFERENCES

1. Brammer TL, Murray EL, Fukuda K, Hall HE, Klimov A, Cox NJ. Surveillance for influenza--United States, 1997-98, 1998-99, and 1999-00 seasons. MMWR *Surveill Summ.*. 2002 Oct 25;51(7):1-10.

2. Fleming DM, Zambon M, Bartelds AI, de Jong JC. The duration and magnitude of influenza epidemics: A study of surveillance data from sentinel general practices in England, Wales and The Netherlands. *Eur J Epidemiol* 1999;15:467–473.

3. Ferguson NM, Cummings DAT, Cauchemez S, Fraser C, Riley S, et al. Strategies for containing an emerging influenza pandemic in Southeast Asia. *Nature* 2005 ;437: 209-214. doi:10.1038/nature04017

4. Ferguson NM, Cummings DAT, Fraser C, Cajka JC, Cooley PC, et al. Strategies for mitigating an influenza pandemic. *Nature* 2006;442:448-452. doi:10.1038/nature04795

5. Eubank S, Guclu H, Kumar VSA, Marathe MV, Srinivasan A, et al. Modelling disease outbreaks in realistic urban social networks. *Nature* 2004;429:180-184. doi:10.1038/nature02541

6. Germann TC, Kadau K, Longini IM, Macken CA. Mitigation strategies for pandemic influenza in the United States. *Proc. Natl. Acad. Sci.* 2006;103:5935-5940. doi:10.1073/pnas.0601266103

7. Glass RJ, Glass LM, Beyeler WE, Min HJ Targeted social distancing design for pandemic influenza. *Emerging Infect. Dis* 2006;12:1671-1681.

8. Atkinson M, Wein L. Quantifying the routes of transmission for pandemic influenza. *Bull Math Biol.* 2008;70:820-867. doi:10.1007/s11538-007-9281-2.

9. Wein LM, Michael P. Atkinson. Assessing Infection Control Measures for Pandemic Influenza. *Risk Anal* 2009;29:949-962. doi:10.1111/j.1539-6924.2009.01232.x

10. Samira Mubareka, Anice C. Lowen, John Steel, et al. Transmission of influenza virus via aerosols and fomites in the guinea pig model. *J Infect Dis.* 2009; 199:858–65.

11. Brankston G, Gitterman L, Hirji Z, Lemieux C, Gardam M Transmission of influenza A in human beings. *Lancet Infect Dis.* 2007;7: 257-265. doi:10.1016/S1473-3099(07)70029-4

12. Carolyn Buxton Bridges, Matthew J. Kuehnert, and Caroline B. Hall. Transmission of Influenza: Implications for Control in Health Care Settings. *Clin Infect Dis* 2003; 37:1094–1101.

13. Garner JS. Guideline for isolation precautions in hospitals. The Hospital Infection Control Practices Advisory Committee. *Infect Control Hosp Epidemiol.* 1996;17:53–80.

14. Spicknall IH, Koopman JS, Nicas M, Pujol JM, Li S, et al.. Informing Optimal Environmental Influenza Interventions: How the Host, Agent, and Environment Alter Dominant Routes of Transmission. *PLoS Comput Biol* 2010;6(10): e1000969. doi:10.1371/journal.pcbi.1000969

15. Kilbourne ED. Influenza. New York: Plenum Medical Book Co. 1987.

16. Weber TP, Stilianakis NI. Inactivation of influenza A viruses in the environment and modes of transmission: a critical review. *J. Infect* 2008;57: 361-373. doi:10.1016/j.jinf.2008.08.013

17. Cannell JJ, Zasloff M, Garland CF, Scragg R, Giovannucci E. On the epidemiology of influenza. *Virol. J* 2008;5: 29. doi:10.1186/1743-422X-5-29

18. Nicas M, Rachael M. Jones. Relative Contributions of Four Exposure Pathways to Influenza Infection Risk. *Risk Anal.* http://dx.doi.org/10.1111/j.1539-6924.2009.01253.x. Accessed 3 Aug 2009.

19. Raymond Tellier. Review of aerosol transmission of influenza a virus. *Emerg Infect Dis.* 2006;Vol. 12, No. 11.

20. Alison P. Galvani and Robert M. May. Epidemiology: Dimensions of superspreading. *Nature* 2005;438, 293-295. doi:10.1038/438293a.

21. Li S, Eisenberg JNS, Spicknall IH, Koopman JS. Dynamics and Control of Infections Transmitted From Person to Person Through the Environment. *Am. J. Epidemiol.* 2009;170: 257-265. doi:10.1093/aje/kwp116

22. Richard I. Joh, HaoWang, Howard Weiss, Joshua S. Weitz. Dynamics of Indirectly Transmitted Infectious Diseases with Immunological Threshold. *Bull Math Biol.* 2009;71: 845–862. DOI 10.1007/s11538-008-9384-4.

23. Lee RV. Transmission of influenza A in human beings. *Lancet Infect Dis* 2007;7: 760-761; author reply 761-763. doi:10.1016/S1473-3099(07)70270-0

24. Tang JW, Li Y. Transmission of influenza A in human beings. *Lancet Infect Dis* 2007;7: 758; author reply 761-763. doi:10.1016/S1473-3099(07)70268-2

25. Lemieux C, Brankston G, Gitterman L, Hirji Z, Gardam M. Questioning aerosol transmission of influenza. *Emerging Infect. Dis* 2007;13: 173-174; author reply 174-175.

26. Marc A. Strassburg, Sander Greenland, Frank J. Sorvillo, Loren E. Lieb and Laurel A. Habel. Influenza in the elderly: report of an outbreak and a review of vaccine effectiveness reports. *Vaccine.* 1986;Vol.4:1:38-44.

27. Reiko Saito, Danjuan Li, Chieko Shimomura et al.. An Off-Seasonal Amantadine-Resistant H3N2 Influenza Outbreak in Japan. *Tohoku J Exp Med.* 2006;Vol. 210:1:21-27.

28. Anderson RM, May RM. Infectious Diseases of Humans: Dynamics and Control. New York, NY: Oxford University Press; 1992.

29. Diekmann O, Heesterbeek JAP. Mathematical Epidemiology of Infectious Diseases: Model Building, Analysis and Interpretation. New York, NY: John Wiley & Sons, Inc; 2000.

30. J. O. Lloyd-Smith, S. J. Schreiber, P. E. Kopp, and W. M. Getz. Superspreading and the effect of individual variation on disease emergence. *Nature* 2005;438, 355-359. doi:10.1038/nature04153

31. Bryan T. Mayer, James S. Koopman, Edward L. Ionides, Josep M. Pujol, and Joseph N. S. Eisenberg. A dynamic dose–response model to account for exposure patterns in risk assessment: a case study in inhalation anthrax. *J R Soc Interface*. 2010.0:rsif.2010.0491v1-rsif20100491; doi:10.1098/rsif.2010.0491

32. Hemmes JH, Winkler KC, Kool SM. Virus survival as a seasonal factor in influenza and polimyelitis. *Nature* 1960;188: 430-431.

33. Bean B, Moore BM, Sterner B, Peterson LR, Gerding DN, et al. Survival of influenza viruses on environmental surfaces. *J Infect Dis.* 1982;146: 47-51.

34. Alford RH, Kasel JA, Gerone PJ, Knight V. Human influenza resulting from aerosol inhalation. *Proc. Soc. Exp. Biol. Med* 1966;122: 800-804.

35. Couch RB, Douglas RG, Fedson DS, Kasel JA. Correlated studies of a recombinant influenza-virus vaccine. 3. Protection against experimental influenza in man. *J. Infect. Dis* 1971;124: 473-480.

36. Nicas M, Nazaroff WW, Hubbard A. Toward understanding the risk of secondary airborne infection: emission of respirable pathogens. *J Occup Environ Hyg* 2005;2:143-154. doi:10.1080/15459620590918466

37. Loudon RG, Roberts RM. Droplet expulsion from the respiratory tract. *Am. Rev. Respir. Dis* 1967;95: 435-442.

38. Hendley JO, Wenzel RP, Gwaltney JM. Transmission of rhinovirus colds by self-inoculation. *N. Engl. J. Med* 1973;288: 1361-1364.

39. Nicas M, Best D. A study quantifying the hand-to-face contact rate and its potential application to predicting respiratory tract infection. *J Occup Environ Hyg* 2008;5: 347-352. doi:10.1080/15459620802003896.

40. Sattar S, S. Springthorpe, S. Mani, M. Gallant, R. C. Nair, et al. Transfer of bacteria from fabrics to hands and other fabrics: development and application of a quantitative method using Staphylococcus aureus as a model. *J Appl Microbiol* 2001;90: 962-970. doi:10.1046/j.1365-2672.2001.01347.x

CHAPTER 4

TEMPORAL PATTERNS OF INFLUENZA AND RELATIONSHIPS WITH WEATHER VARIABLES IN HONG KONG, CHINA, 1998-2008

INTRODUCTION

Influenza poses a serious public health threat through both occasional global pandemics and typically yearly epidemics, at least in temperate regions. Annual influenza epidemics are responsible for significant morbidity, mortality, and economic burden on human populations globally. In the United States, influenza is estimated to cause more than 114,000 hospitalizations, and 20,000 deaths annually (1). In European countries, influenza also has similar substantial heath impacts (2,3). Influenza sentinel surveillance systems have been functioning for decades in temperate regions such as North America, Europe and Australia. Influenza seasonality in those regions is relatively well-identified, with annual epidemics occurring in winter months for both the northern and southern hemispheres (1-5). However, in most tropical and sub-tropical countries, influenza surveillance systems have only recently been developed or remain non-existent. Influenza temporal patterns and impacts in these tropical and/or impoverished regions are still poor defined and are not studied enough (5-7).

Southern China, including Hong Kong and Guangdong adjacent regions, has long been referred to as one of the possible global influenza epidemic centers based on influenza

virus transmission among birds, pigs and humans (8). Two of the three recorded influenza pandemics in human history, the "Asian Flu" caused by an H2N2 strain in 1957-58 and the "Hong Kong Flu" caused by an H3N2 strain in 1968-69, emerged from or were first detected in Hong Kong and adjacent regions in China (9). A significant fraction of WHO-confirmed new influenza virus strains were first identified in China (10,11). The first human H5N1 avian influenza case was identified in Hong Kong in 1997 (12). Recent antigenic and genetic analyses have also shown that East Asia/South-East Asia might be an important breeding ground for novel influenza strains that then travel globally to other regions (13). Hong Kong enhanced and extended its existing influenza sentinel surveillance system after the first human H5N1 outbreak in 1997 (14). Since then, Hong Kong has been an important contributor to the WHO global influenza surveillance network (15). Therefore, understanding the seasonal pattern and potential determinants of influenza in Hong Kong is important from both local and global perspectives.

Previous studies on influenza have reported various factors that might be associated with influenza seasonal variation, such as virus antigenic shift and drift, human living in overcrowded settings, contact patterns among people, some environmental factors such as temperature, relative humidity (RH), and the El Nino Southern Oscillation (ENSO) (16-18). Awareness of relationships between seasonal influenza and local weather variables reaches back to early twentieth century in the United States (19). The associations between weather and human influenza transmission are highly complex, with some evidence suggesting that upper respiratory infection epidemics, including those due to influenza, might be associated with rapid change in

temperature and sudden cold weather (20). Rainfall has been associated with subtype B influenza in Singapore and relative humidity may also be linked to influenza transmission in Germany and Japan (21-23). A laboratory study on guinea pigs showed that absolute humidity (AH) is more significantly associated with influenza virus survivability and transmissibility than with temperature and relative humidity (RH) (24,25). The association between AH and influenza-related mortality has been also demonstrated in different regions of the USA recently (26).

Despite these and other studies, the role of local weather variables and the underlying mechanisms by which weather variability affects influenza seasonal variation still remain poorly understood, especially in the tropical and sub-tropical regions. Possible reasons for this problem include potential confounders such as environmental factors, human social behavior, and influenza clinical classification (27). These confounders are difficult to be controlled in analyses when seeking causal relationships between weather factors and influenza patterns. Hypothesized mechanisms include that weather might alter patterns of human social activity, human-to-human contact, human immunity relevant to Vitamin D absorption, virus survival in the environment, as well as virus transmissibility and coexistence with other pathogens (28-31). Further investigations are needed to explore whether the relation between weather variables and influenza exists in various population groups across broader geographic regions, especially in tropical/subtropical countries.

In addition to local weather variables, several recent studies have also linked influenza seasonal variability to global climate indices which represent multiple climatic phenomena across large geographic scales, such as atmosphere, precipitation, sea surface

temperature (SST) and "teleconnections". Teleconnection refers to climate anomalies from geographically distant regions being related to each other. Some important teleconnections in the northern hemisphere include El Niño Southern Oscillation (ENSO), Pacific/North American pattern (PNA), West Pacific (WP) and Pacific Decadal Oscillation (PDO). Viboud et al. examined the influence of global climate on influenza activities during 1979-2000 in France, demonstrating associations between the Multivariable ENSO Index (MEI) and influenza-related mortality and influenza-like illness (ILI) (16). Greene et al. examined both local weather and global climatic indices in relation to pneumonia and influenza (P&I) mortality in different climate regions in the United States, and found that temperature and West Pacific teleconnection were weakly associated with P&I mortality in some climate regions (32).

Probably the most important teleconnection is ENSO, which involves two related climatic phenomena: the oceanic components of El Niño and atmospheric patterns termed the Southern Oscillation. El Niño refers to higher than normal SST over the central and eastern equatorial Pacific Ocean, an anomaly that usually recurs every few years, lasting 12 months or so. Conversely, La Niña involves lower than normal SST in this ocean region. ENSO significantly affects global and local year-to-year climate variability. In Hong Kong, ENSO brings more rainfall in winter and spring, fewer tropical cyclones before June (33). These ENSO characteristics can be measured by a weighted average of the main ENSO features, namely MEI, which includes SST, sea-level pressure, surface air temperature, total cloudiness fraction, the east-west and north-south components of the surface wind over the tropical Pacific (33).

Another teleconnetion relevant to Hong Kong is the pacific/North American (PNA) pattern which presents low-frequency variability in the Northern Hemisphere extratropics. The PNA is related to the East Asian jet stream. The positive phase in PNA is related to an enhanced East Asian jet stream; on the other hand, the negative phase in PNA is associated with a westward retraction of that jet stream toward eastern Asia (34). The PNA is associated with temperature variation in Hong Kong (35) and is strongly influenced by ENSO (36).

The West Pacific (WP) teleconnection presents a primary mode of low frequency variability over the North Pacific region all year long. In winter and spring, WP includes a north-south dipole of anomalies, one centering over the Kamchatka Peninsula and the other over parts of southeastern Asia including Hong Kong and the western subtropical North Pacific. The strong phases of WP pattern indicate variations in the Pacific jet stream and are associated with unusual temperature and precipitation in the North Pacific region (37).

The Pacific Decadal Oscillation (PDO) is defined by a shift in the SST pattern of the North Pacific Ocean, occurring on a 20- to 30-year cycle. The positive phase PDO represents negative anomalies of northwest Pacific SST (38,39).

Our study was designed to evaluate whether local weather and global climate indices might help predict influenza disease dynamics in the sub-tropical region of Hong Kong. We analyzed temporal patterns of influenza using surveillance data from the city of Hong Kong, and considered the role of viral strain type/subtypes in identifying associations. Our goal was to better understand how weather and climate variability might affect influenza transmission in the east/southeast Asian, tropic/sub-tropic region,

perhaps leading to better “early warning” of future epidemics, thereby strengthening influenza prevention not only in local regions but also in other tropical/subtropical regions.

MATERIALS AND METHODS

Study Area

Located in the Southeastern China Pacific coast region (22.3^{o}N, 114.2^{o}E, Figure 4.1), Hong Kong is a high-density metropolitan area with 6.8 million residents within a 1,104 square kilometer area.

Hong Kong has a typically sub-tropical climate with temperate weather for nearly half the year. January and February are the coldest months of the year, with low temperatures reaching 10 ^{o}C. March and April are pleasant spring months with occasional spells of high humidity and reduced visibility. May to September are hot and humid months with occasional showers and thunderstorms. Afternoon temperatures are often higher than 30 ^{o}C, with night temperatures near 26 ^{o}C. Due to tropical cyclones, strong winds and heavy rain are common during these summer months when more than 80% of annual rainfall (range from 130 to 300 cm.) occurs. October to December has pleasant breezes, sunshine and comfortable temperatures. Snow and tornadoes are rare in Hong Kong (40).

Influenza Surveillance Systems in Hong Kong

The influenza surveillance system in Hong Kong consists of 62 public-sector sentinel general outpatient clinics (GOPC) and 50 private-sector sentinel general

practitioners (GP). This influenza surveillance network collects and reports the weekly number of outpatient visits for all causes, and those for ILI (defined as high fever ≥38 ºC plus cough or sore throat). The surveillance network, primarily GOPC, also submits specimens from ILI patients to the Public Health Laboratory Services Branch (PHLSB) for influenza virus testing (15).

Influenza Morbidity Data Sources and Definitions

Influenza morbidity is measured by both the weekly proportion of outpatient visits with a diagnosis of ILI (ILI proportion), and weekly proportion of samples from ILI patients that test positive for influenza virus. The Hong Kong Department of Health (DOH) publishes online weekly and monthly proportion of ILI among all patients who seek treatments through GOPCs and GPs. The weekly total number of specimens tested and those found positive for influenza virus were provided by Hong Kong's PHLSB. This weekly influenza virus positive proportion (VPP) was calculated overall, and by type/subtype. In our study, the ILI proportion and VPP data from 1998 through 2008 were analyzed.

Relative Index of Weekly Influenza Transmissibility Based on ILI and VPP

A relative measurement of weekly influenza incidence, $\boldsymbol{I_t}$, can be estimated by ILI proportion multiplied by VPP during each specific week (41). A modification of the ratio between each current week's incidence $\boldsymbol{I_t}$, to the previous week's incidence $\boldsymbol{I_{t-1}}$, $\mathbf{(I_t/I_{t-1})^{u/7}}$, can be considered as a relative indicator of weekly influenza transmissibility, where **u** is the influenza serial interval (the time between successive cases in a chain of transmission

and can be estimated by the time interval between infection and subsequent transmission) and equals to ~3 days (41). The potential associations between weather variables and the influenza transmissibility index were explored in this study.

Summarized Index of Influenza Morbidity Impact during Annual Epidemic Period

To understand the annual influenza epidemic season variations from multiple perspectives, we calculated several summarized indices for each influenza epidemic period. These indices included the onset date of epidemics, the duration of epidemics, the maximum VPP and ILI proportion, and the cumulative VPP and ILI proportion level during the epidemic.

The onset of each epidemic period was determined by both dynamic linear modeling and CUSUM approaches based on weekly ILI proportion and VPP data (25). The dynamic linear modeling is a time series technique. This approach defines an epidemic "alert" when the current week observed data is greater than the forecasted ILI based on previous nine weeks' data. The CUSUM method defines the epidemic onset date by using a running average and running variation for previous seven weeks' data. Epidemics were defined whenever at least two consecutive weeks have equal or greater VPP or ILI proportion than that at epidemic onset period. The length of each epidemic was the period of weeks with equal or higher influenza levels after the epidemic onset. The maximum levels of epidemic were the highest VPP and ILI proportion among the epidemic period. The influenza morbidity impact was presented by the sum of all ILI cases or virus positive counts during the epidemic period.

Weather Data Sources and Transformations

Both local weather variables and global climatic indices data were collected. Daily local weather variable data from 1998 through 2008 were provided by meteorologists from the Hong Kong Observatory (HKO), including mean absolute humidity (kg/m^3), mean relative humidity (%), maximum, mean and minimum air temperature (^oC), mean dew point temperature (^oC), global solar radiation (MJ/m^2), total daily rainfall (mm), prevailing wind direction (degree), mean wind speed (km/h), mean cloud cover (%), reduced visibility (hour number), and total bright sunshine (hour number). Measures were averaged from several weather station records in Hong Kong.

Daily "normal" was calculated for all variables and each day from January 1 through December 31 by averaging all daily values for each specific date from 1998 to 2008. Then, anomalies for each day and for all variables were calculated by subtracting that day's normal from the observed daily data. Weekly crude and anomaly values were calculated from daily data by simple averaging of seven days in a specific week.

Global Climatic Indices

Monthly global climatic indices for ENSO and other teleconnection patterns, including MEI, PNA, WP, and PDO, were downloaded online for the period 1998-2008 (42).

Correlation Analysis among ILI Proportion, Influenza VPP, Transmissibility Index and Weather Variables

Lagged and non-lagged correlations between weekly influenza measurements (VPP, ILI proportion and transmissibility index) and weather variables were analyzed. Both Pearson's correlation and Spearman Rank correlation were applied to evaluate linear only and linear/polynomial correlations between two variables respectively. Partial Correlations were also calculated to address the inherent collinearity among weather variables (e.g. in Hong Kong summers tend to be hot and humid while winters are usually cold and windy). In this way, relationships between influenza and a specific weather variable were analyzed by controlling for cross-correlation among different weather variables.

To address lagged effects more efficiently, cross-correlation maps were used to present and visualize various time-lags of weather associations with influenza. The cross-correlation map approach proposed by Curriero et al. (43) was modified and then applied to analyze associations between weekly ILI proportion, VPP and weather variables. First, lagged correlation/partial correlation coefficients, $corr(Y_i, f(X_{i-a,\, i-b}))$, between a weekly influenza measurement Y_i and a lagged climate variable X_i was computed by applying Pearson or Spearman correlation. The lagged effect was characterized by a, b with $a \geqq b$. a should be at least larger or equal to 17 days, based on the possible lagged weather effect on influenza in previous study (21). The function $f(.)$ is a summary function of climate variables. In our study, we set this summary function as the average, maximum and minimum weekly weather variables. Second, the correlation values were plotted on time interval lags space (lag a and b) to generate cross-correlation maps. The highest and lowest correlation coefficients for each climate variable and time lag were output, indicating the largest potential influence of a climate variable for

different lagging intervals. Multiple cross-correlation maps were generated for both VPP and ILI proportion. This cross-correlation map can present results for multiple time-lag correlations simultaneously, an advantage over the traditional correlation test for one single time lag.

Statistical Analyses of Epidemic Onsets and Daily Weather Variables Anomaly

To test statistical significance of associations between weather anomalies and epidemic onset dates, bootstrapping test approaches were applied to daily anomalous climatic variables prior to epidemic onset date. The null hypothesis in this bootstrapping test was that daily anomalous values for a specific weather variable preceding the epidemic onset date have mean zero. We randomly sampled daily anomalous values in 4-week blocks before the epidemic onsets for 10,000 times. An average sample value for each of these 10,000 samples was calculated to create a distribution of these sampled average values. Statistical significance was assessed by determining the location of the observed value of average climatic variable values in the distribution of 10,000 sampled average values.

Statistical Analyses of Epidemic Summarized Indices and Global Climatic Indices

The partial correlations between the summarized epidemic indices (epidemic period length, cumulative VPP and ILI proportion) and global climatic variables were computed. The lagged effects of global climate variables on influenza activity were assessed by using global climatic data 0-3 months prior to the epidemic onset month.

The lagged interval showing the most significant association with influenza activity was identified.

For climatic indices that produced a larger Spearman Correlation coefficient than Pearson's Correlation coefficient, the associations may not be deemed linear, so quadratic terms were explored.

ARIMA Time Series Analyses of Weekly Virus and Local Weather Variables

Autoregressive Integrated Moving Average (ARIMA) modeling was applied to explore the association between weekly influenza VPP and local climatic variables. ARIMA models enable us to study relationships between multiple time series data adjusted for autocorrelation of the time series data. Multiple time series analysis can explore the time dependence of the relationship between influenza and weather variables. Autoregression coefficients R^2 and log-likelihood were reported from these analyses. Model validity was checked by comparing Akaike Information Criterion (AIC) and log likelihood.

All statistical tests were 2-tailed, and statistically significant P-values were <0.05. The statistical software R (version 2.10) was used for all analyses.

RESULTS

Two annual transmission peaks were found in 9 of 11 study years, usually occurring during February through April and again in "early summer" (June-July). We hypothesized that a new emerging predominant subtype strain might be associated with the second epidemic peak. In addition, the relationships between influenza morbidity measurements and meteorological variables were examined. We found that the adjusted

association between AH and influenza VPP was the strongest among all meteorological variables. We also found significantly negative AH anomaly two weeks prior to the onset of influenza epidemics.

Descriptive Statistics

The patterns of weekly ILI proportion and VPP for the entire studying period (Figure 4.2) and by week in a year (Figure 4.3) showed complex patterns. From the GOPC surveillance, the average weekly ILI proportion was 5.34 (range 1.0 to 19.7) per 1,000 patient visits. From GP surveillance, the average weekly ILI proportion was 46.85 (range 22.9 to 123.0) per 1,000 patient visits (data not show). Monthly ILI proportion data are summarized in Table 4.1. In most years, a first higher peak appeared in February to April, and a second lower peak appears in June to August

A median of 1,857 specimens (range 665- 5613) were collected each week for influenza etiology testing, primarily from sentinel hospitals. There is influenza virus transmission year round. The average weekly influenza VPP was 13.0%, ranging from 0.3% to 51.9%. Multiple subtypes of influenza virus strains were simultaneously co-circulating (Table 4.2). Among the 11 years of the study period, H3N2 was the single predominant strain in seven years; H3N2/H1N1 or H3N2/B predominated during three years; and H1N1/B was most often isolated in 1 year. Subtype H3N2 dominant years had relatively higher morbidity levels than non-H3N2 dominant years.

The annual pattern of weekly influenza VPP was slightly different from weekly ILI proportion pattern. Weekly VPP seasonal swings were much more distinct than weekly ILI proportion. In general, influenza VPP outside of the epidemic period was

much lower and even close to zero. A larger first peak in late winter/early spring occurred every year. A smaller second peak in summer was usually observed, and was more apparent in the VPP pattern than in ILI data (Figure 4.3). In 9 of 11 years, a clear bimodal pattern of VPP was evident, with the other 2 years showing a single wide "plateau" epidemic peak.

Influenza Epidemic Onsets and Temporal Patterns Based on Influenza Morbidity

Onset of each epidemic period was defined by linear dynamic modeling and CUSUM approaches based on weekly ILI proportion and VPP. The general results from these two methods were similar, but the onsets were sometimes slightly different. During 1998 through 2008, ILI-base analysis produced 23 epidemic periods, while there were only 20 epidemic periods based on VPP data as shown in Figure 4.6. When comparing the epidemic onsets based on both ILI proportion and VPP, we found that the epidemic onsets based on VPP data commonly began 1-2 weeks earlier and the epidemic periods were longer than that based on ILI data. After an epidemic took off, the VPP and ILI proportion quickly rose to a maximum within 3-5 weeks. Then ILI proportion and VPP declined to a lower non-epidemic baseline level after a few weeks to three months (but extended to 7 months in 2002). This influenza temporal pattern is different from that seen in temperate climate regions by the usual timing of onset (late winter/early spring), the shorter duration of intense transmission, and a typical second, smaller, summer transmission period.

We further explored the virus subtype classification information, and found that the second "summer" epidemic peak was associated with a new dominant subtype strain

appearance from 1998 to 2008 except the year of 2004. Subtype H3N2 was dominant throughout 2004, but influenza VPP was significantly low between the first and second epidemic peak. A possible new H3N2 subtype strain might have been involved with the second epidemic peak, but we were not able to determine this from the available subtype data.

Local Weather Variable Data

The local weather in Hong Kong is typical sub-tropical. Most weather variables displayed a unimodal pattern over the year as shown in Figure 4.4. Daily temperature averages ranged from 12.6 to 32.4 ^{o}C with the average annual temperature being 23.6 ^{o}C. January and February generally were the coldest months of the year, and June through September the hottest. Similar to daily temperature, daily rainfall and relative humidity (RH) also reached a peak in summer. Daily rainfall displayed the greatest variation in summer months. Absolute humidity (AH) was lower in December and January, but slowly increased to peak levels in August. Daily cloud amount only varied slightly during the year, peaking in spring and early summer. Daily 60-minute wind speed was relatively stable throughout the year.

Global Climatic Indices, 1998-2008

Global climatic indices varied somewhat by monthly average as shown in Figure 4.5. Monthly MEI and PNA were, on average, similar throughout each year. Monthly WP displayed two peaks in February and September. PDO reached a low level in

October. Over the 11 years of study, MEI and PDO varied at low frequency and displayed great variation. WP and PNA varied at high frequency and less regularly.

Weekly Local Weather Association with ILI Proportion and Influenza VPP

A strong correlation between weekly ILI proportion and influenza VPP was found (r^2=0.64, P<0.001), suggesting that the two show similar patterns. However, the associations between local weather variables and these two influenza indicators were different.

Some weather variables are temporally correlated with each other. In Hong Kong, there were strong correlations among all pairs of daily variables including maximum, average and minimum temperature, dew point temperature, AH and radiation (all $R^2 \geq 0.6$, P<0.001). There were weaker, but statistically significant correlations, among temperature, AH, RH, solar radiation, cloud amount, and rainfall (data not shown). To adjust for these intercorrelations, partial correlations among weather variables and influenza VPP, ILI proportion were analyzed along with crude correlation estimates. All correlations were calculated by using both Pearson and Spearman approaches, and the results were similar.

The non-lagged relations between weekly weather variables and influenza were explored first as shown in Table 4.3. Weekly mean wind velocity, cloud amount, and rainfall were significantly correlated with current week ILI proportion. Statistically significant but weaker correlations between the weekly absolute humidity, radiation, dew point, mean temperature and current week ILI proportion were also found. On the other hand, only current week dew point, rainfall, and relative humidity were significantly

correlated with the influenza VPP. Adjusted correlations were generally smaller than crude correlations except for the case of wind speed.

Lagged correlations between weather variables and influenza are shown in Tables 4.4 and 4.5, and Figures 4.7 and 4.8. AH roughly 7 weeks prior was positively correlated (R^2 = 0.32~0.34) with both ILI proportion and influenza VPP. The association was consistent in both GOPC and GP surveillance settings, and for all virus strains or for H3N2 stains only. After adjusted for other weather variables, AH was the most significant weather variable, but the association became negative. The reversed adjusted relationship might be caused by correlation between temperatures and AH measures. Preceding RH (0-2 weeks lagged) was also significantly correlated with both ILI proportion and VPP after adjusting for other weather variables, but the association was much weaker that of AH.

Preceding precipitation (prior 7-12 weeks), solar radiation (1-14 weeks), and mean sea level pressure (10-14 weeks) were significantly correlated with both ILI proportion and VPP for both GOPC and GP surveillance settings and all virus strains classification (Tables 4.4 and 4.5). The associations were still among the strongest significant ones after adjusting for other weather variables.

Four temperature variables, preceding (3-12 week) average, maximum, minimum, and dew point temperature, were all significantly correlated with both ILI proportion and VPP at similar degree (R^2 = 0.30~0.50, P<0.01). However, after adjusting for other weather variables, the correlation between preceding minimum temperature and both ILI proportion and VPP was still consistent and strong; the correlation between preceding average temperature and ILI proportion and VPP still remained but was decreased; the

correlations between preceding maximum temperature, dew point temperature and influenza disappeared.

Preceding wind (0-13 week) and cloud amount (0-14 week) were correlated with both ILI proportion and VPP at low level comparing to other weather variables. After adjusting for other variables, the association between preceding cloud amount and influenza decreased. However, the association between preceding wind and influenza slightly increased for VPP or significantly increased for ILI proportion.

Weekly Local Weather Variable Associations with the Influenza Transmissibility Index

The associations between non-lagged weekly local weather variables and influenza transmissibility index are slighter comparing to that based on ILI proportion or VPP. Non-lagged temperature measurements (maximum, mean and minimum) and AH were similarly related to influenza transmissibility index (R^2 = -0.21~-0.22, P<0.01). Statistically significant but weaker correlations between non-lagged weekly wind speed, radiation and influenza transmissibility index were also found (R^2 = -0.13, P<0.05).

Lagged correlations between weekly weather variables and influenza transmissibility index decrease compared to non-lagged ones. Only preceding AH (prior 4-7 weeks) was still slightly associated with influenza transmissibility (R^2 = -0.10, P<0.05). Similarly, all adjusted partial correlations between weekly weather variable and influenza transmissibility index decrease comparing to crude ones. Only adjusted minimum temperature was still slightly associated with influenza transmissibility (R^2 = -0.11, P<0.05).

Weekly Local Weather Anomaly Association with ILI Proportion and Influenza VPP

Cross-correlation map analyses demonstrated interesting patterns in anomalies of weekly weather variables and influenza morbidity (VPP and ILI proportion) compared to crude weather variables as shown in Tables 4.6-4.7 and Figures 4.9. Non-lagged weekly weather variable anomalies were not significantly correlated with influenza VPP or ILI proportion. However, adjusted lagged correlations between weather anomalies and influenza were stronger than non-lagged ones, and some were statistically significant. Compared to crude weather variable values, weather anomaly values for all variables were correlated with influenza morbidity in the same directions, but were much weaker. Preceding weekly AH, minimum temperature, solar radiation, and precipitation anomalies were consistently negatively significantly correlated with influenza VPP and ILI proportion based on different lag periods. Preceding weekly wind and sea level pressure anomalies were consistently positively correlated with weekly influenza VPP and ILI proportion. The remaining weather variables anomalies were weakly related to influenza morbidity, and the relationship direction changed in different surveillance settings or for different virus type classifications.

Weekly Local Weather Anomalies and the Influenza Transmissibility Index

To explore the potential relationship between local weather anomalies and influenza transmission index, correlation coefficients were developed. The correlations between weekly influenza transmissibility index and weather anomalies were generally

weaker than those based on crude weather variables. The most significant correlations were found between influenza transmissibility index and 1 week preceding anomalies of average and minimum temperature (R^2=-0.13, P<0.01). The second biggest and weaker correlation was found between influenza transmissibility index and 2 week preceding AH anomalies (R^2=-0.093, P≈0.052).

Daily Preceding Local Weather Anomalies and Epidemic Onsets

Influenza epidemic onsets were analyzed in relation to daily local weather variable anomalies during 30 days before and after each onset. Analysis of all daily weather variable anomalies showed associations but no statistical significance except for that of AH. A period of low AH (negative anomaly) was found around two weeks prior to the onset of VPP-defined epidemic onsets as shown in the Figure 4.10. This correlation between negative AH anomaly and epidemic onset was statistically significant by a bootstrapping method (P<0.01). These results were robust when we applied the CUSUM and MOVING AVERAGE approaches to define the onset of epidemics. We also detected an association of lower RH with epidemic onset that was not strong and significant as for AH.

Similar analyses based on epidemic onsets determined from ILI proportion data produced correlations with negative AH, negative Temperature, negative Dew Point, negative Solar Radiation, and positive RH, but the same bootstrapping tests failed to detect statistical significance for these correlations. The directions of association of solar radiation and RH with epidemic onset agree to long time believed epidemic conceptions, but are contrary to recent findings by Shaman et al. (26,27).

Monthly Global Climate Indices and Monthly VPP or ILI Proportion

As shown in the correlation matrix in Table 4.8, monthly influenza VPP was positively associated with preceding 1 month WP, average preceding 2 month WP, average preceding 2 month PNA, average preceding 3 month PNA, current month PDO, and preceding 1 month PDO. Since subtype strain H3N2 was predominant during the study period, we explored the correlation between H3N2 and global climate indices. Monthly H3N2 positive proportion was significantly positively correlated with the current month MEI, PNA and PDO, with preceding 1 month MEI and PDO, with average preceding 2 month MEIT, PDO, PNA, and with average preceding 3 month MEI, PDO, PNA. Monthly H3N2 VPP also was significantly correlated with current month and average preceding 1, 2 and 3 month SOI in negative direction. The monthly ILI proportion was significantly positively correlated with current monthly PNA and PDO, preceding 1 month WP and PNA, average preceding 2 month WP and PNA, and average preceding 3 month WP and PNA.

Global Climate Indices and Summarized Influenza Epidemic Periods

For each epidemic period, we identified the cumulative influenza VPP and ILI proportion, the maximum virus positive proportion and ILI proportion, and the duration of epidemic period. We averaged 1-3 month global climatic indices before epidemic onsets to explore the correlations with summarized epidemic impact. As shown in Table 4.9, significant positive correlations were found between average preceding 1, 2, 3 months PNA and cumulative virus positive proportion, as well as length of epidemic

period. ILI count in epidemic period was positively associated with average preceding 2 and 3 month PNA.

ARIMA Modeling of Influenza VPP and Local Weather Variables

To explore if weather variables could predict the influenza morbidity variation, ARIMA modeling was applied to weekly VPP and weekly local weather variables. Weekly influenza VPP was log-transformed to stabilize the variation of the time series. Since some weekly influenza VPP values are close to 0, we added a small constant to prevent the log-transformation outliers which could ruin the analysis before taking log-transformation. Then the AR order, MA order and degree of non-seasonal differencing of ARIMA model were determined based on Auto-Correlation Function (ACF) and Partial Auto-Correlation Function (PACF). No seasonal differencing was needed in this ARIMA effort due to weekly time resolution and non-seasonal differencing process. The AR order, MA order and degree of differencing were set as 0, 3, and 1 respectively. As shown in Table 4.10, the ARIMA(0,1,3) had the lowest Akaike Information Criterion (AIC) and was considered as a baseline model for our comparisons. Univariate models with single lagged weather variables, AH, average, maximum, minimum temperature, dew point temperature and rainfall, improve significantly comparing the baseline model ARIMA(0,1,3). Among multivariate models, ARIMA(0,1,3) with AH, minimum temperature, and rainfall performed the best and improve the univariate models. Multiple models were compared based on AIC, Log likelihood and X^2 test. The fitted and observed weekly influenza VPP of this model were plotted in Figure 4.11.

DISCUSSION

As in several previous studies (15, 47), besides the initial annual epidemics that usually occurred between February and April, we identified a second smaller or equal-sized summer epidemic in 9 of 11 years in a subtropical region based on relatively longer time and more reliable influenza data. The other 2 of 11 years displayed a single wide "plateau" epidemic pattern. We further explored the virus subtype classification information, and found that the second “summer” epidemic peak was associated with a new dominant subtype strain appearance from 1998 to 2008 except the year of 2004. Subtype H3N2 was dominant throughout 2004, but influenza VPP was significantly low between the first and second epidemic peak. A possible new H3N2 subtype strain might have been involved with the second epidemic peak, but we were not able to determine this from the available subtype data. Additional analysis on subtype immunogenecity or subtype genetic sequencing test might help confirm this possibility in the future. A new dominant influenza virus subtype and low level of host immunity to it might the primary driven forces for the second epidemic perk.

We examined the potential relationships between influenza morbidity (ILI proportion and VPP) and meteorological variables in a subtropical metropolitan region. We found that local weather variables were statistically significantly associated with the proportion of ILI cases that tested positive for influenza virus, and the proportion of ILI diagnosis in outpatients visiting Hong Kong influenza surveillance sites. We also found that relationships between influenza morbidity and time-lagged weather/climate variables were much stronger than non-lagged ones. Our results not only extend previously demonstrated influenza associations with weather variables such as temperature, relative humidity, dew point, solar radiation, and rainfall to a new region, but also identify newly

recognized correlations with absolute humidity. The association between AH and influenza VPP was strongest after adjusting for other weather variables in all settings. It was much stronger than those for relative humidity, temperature and solar radiation.

We also explored the associations between daily weather anomaly and epidemic onsets. Significant negative daily AH anomaly two weeks prior to the onset of VPP-defined influenza epidemics was found. Considering the difference of how to define epidemic onsets, this result is similar to previous findings from Shaman et al based on P&I mortality data in the US (26). However, at the weekly time scale, the AH anomaly was only slightly associated with a theoretical weekly influenza transmissibility index. This slight inconsistency might be due to the weekly averaging effect or an inappropriate transmissibility index. We were not able to detect significant correlations between epidemic onset and daily relative humidity, temperature and radiation as Shaman did (26). Overall, these results based on influenza morbidity data are consistent with recent new findings from laboratory guinea pig studies and influenza mortality analysis in U.S. (24-26).

Our study is the first that we are aware of to explore the relationship between AH and influenza based on weekly influenza morbidity data. Further, minimum temperature was consistently correlated with influenza morbidity, as was average temperature, but minimum temperature normally was much stronger. Results of the relationships between influenza morbidity and temperature, relative humidity, rainfall and solar radiation are in agreement with previous studies in different geographic/climatic regions such as Germany, USA and Japan (22-24).

The underlying mechanisms for these relationships are complex and remain unclear. From recent laboratory studies involving transmission in animal models, absolute humidity more significantly altered influenza virus survival and transmissibility in the environment than relative humidity or temperature (25). Increased temperature might lower influenza virus infectivity by altering hemagglutinin (HA) secondary structure and destabilizing HA's trimeric form (44). Temperature seems to alter aerosol transmission, but not that operating through contact (45). Rainfall might change the temperature, humidity and human social behavior, which could alter contact transmission. Also, decreased solar radiation seems to influence influenza risk by lowering human melatonin and vitamin D levels, thus reducing host resistance (25). While weather variables might have multiple effects on influenza that involve virus survival, transmission, human immunity, disease expression, human contact pattern, human social activity (18), most epidemiological studies, including ours, cannot distinguish the direct biological effects of individual weather variable from human behavioral changes associated with weather fluctuations.

In addition to local weather associations, global climatic indicators that operate over large geographic regions were also found to be associated with observed influenza patterns. A significant association between the preceding three month average global climate index of PNA and summarized influenza epidemic impact was found in our study. The PNA was positively related to the East Asian jet stream which brings cold weather over East Asia (37). The PNA was associated with local temperature variation in Hong Kong (38), possibly increasing extra-host survival of influenza virus, decreasing human immunity, and altering human social physical activity in public venues. Although other

global climate indices such as ENSO and NAO have been associated with influenza morbidity and human health in temperate regions of Europe and the USA (16, 46), we were unable to detect these associations in our subtropical setting. This could be due to the different influences of ENSO and NAO on Hong Kong's local weather, or to the relative small number of epidemic seasons in our data set. Our study is the first to examine global climate indices and influenza in subtropical East Asian regions. We did detect significant correlations between monthly influenza VPP and lagged global climate indices MEI, PNA, PDO, and WP.

Changes in weather variables before the second summer epidemic peak might also have influenced this second period of intense transmission. During late spring/early summer, increased temperature and relative humidity may have lead to lower influenza aerosol transmission, but not to decrease contact transmission (48). Increased rainfall probably increases contact transmission by altering human social activities (50). Absolute humidity generally increases later than relatively humidity and peaks in August and September, so the lower absolute humidity in late spring may strengthen influenza transmission.

In our study, both influenza VPP and ILI proportion were considered as influenza morbidity measurements. The relationships between weather variables and influenza VPP were in the same direction as that with ILI proportion, but were stronger with VPP. Similar to in temperate regions, a previous study from Hong Kong found that on average 10% of ILI cases were caused by influenza virus in residential care homes (49). The influenza temporal patterns based on influenza VPP and ILI proportion were also slight different as we applied dynamic linear modeling to identify influenza epidemics. Both

influenza VPP and ILI proportion are not true population level measurements of influenza morbidity. Their values are influenced by non-influenza respiratory pathogens. The ILI proportion is not a highly specific index of influenza activity, and also has sensitivity problems. On the other hand, influenza VPP is more sensitive, but involves usually less coverage of the target population. Overall, the relationships between influenza morbidity and weather variables based on influenza VPP are more sensitive and desirable. Even having these disadvantages, VPP and ILI proportion are still considered the most valid indicators of influenza morbidity based on existing influenza surveillance system globally (50). The results based on influenza VPP and ILI proportion reported here need to be assessed by using more valid data in future research.

Further, based on both influenza VPP and ILI proportion, Shaman et al suggested another relative influenza transmissibility index that might be proportional to AH (41). Although we did identify a significant association between weekly AH crude data and this influenza transmissibility index, the association becomes insignificant after adjusting for other weather variables. This transmissibility index might be not appropriate to use for long time period where biased noise is likely to be strong. In a short period, the noise is less likely to be biased as seen in previous work (41).

Soebiyanto et al. analyzed Hong Kong influenza weekly virus positive counts during 2004 - 2008 from the online source and reported an association with local weather variables temperature, relative humidity and rainfall (51). Influenza virus count data only represented the absolute reporting of positive tests, and did not consider the total sample size tested in a week. However, influenza virus count data are influenced by both the influenza incidence and the total specimen count collected for virus isolation. Data from

Hong Kong DOH which we analyzed showed that the weekly influenza specimen counts for virus isolation testing varied dramatically from 238 to 824 and sometime might be not collected proportionally to total potential ILI case population due to the laboratory capacity. The total specimen count was generally greater in the first half of a year. The influenza virus positive count could be a strongly biased measure of influenza morbidity comparing to influenza virus positive proportion. Further, positive virus count reported in one week sometimes includes samples that were collected in the previous week. Although Soebiyanto et al. also found associations between influenza and some local weather variables, the associations from out study based on influenza positive proportion are much greater and more reliable. Moreover, they failed to discover the importance of AH.

To help explore multiple associations and co-correlation, we modified and improved standard cross-correlation maps by computing and displaying partial Pearson and Spearman correlation coefficients. This approach helps to directly visualize adjusted correlation patterns. Another major analytic approach involved ARIMA modeling of weekly influenza VPP with local weather variables, significantly improving the model prediction. By applying ARIMA model, we could identify weather variables which were more likely to influence the changing rate of influenza activity.

Non-pharmaceutical prevention hygiene such as mask use and hand washing has increased in Hong Kong, especially after the H5N1 avian influenza outbreak in 1997, the SARS outbreak in 2003, and newly swine influenza strain H1N1 in last year (15). Also the effects of weather may have less impact in a high density metropolitan region like Hong Kong where people normally spend considerable time indoors. Thus, consistent

and reliable associations between climate variables and influenza are difficult to identify from multiple epidemiology studies, due to possible confounders (51). Despite these issues, our study was able to find strong climate associations.

Because the majority of years in our study period were dominated by the H3N2 subtype, we were not able to investigate the relationships between weather variables and different influenza virus strains. Although human immunity status, antiviral medication and vaccine use could affect the association between influenza morbidity and climate variables, data on these factors were not available for our study. Socioeconomic factors also could modify the association between weather and mortality (52). To better understand this association, future analyses that include immunity status, vaccine, and socioeconomic factors could provide a more complete understanding of associations. Many weather variables tend to strongly correlated to each other. Kalkstein et al. found significant relationships between synoptic weather variables and influenza-associated mortality (53). Synoptic factors might be an alternative consideration in future studies that examine multiple weather variables simultaneously.

In conclusion, this study is one of the first to demonstrate associations between influenza morbidity and local meteorological variables and in tropical/subtropical region. Significant associations between AH and influenza morbidity, as well as between PNA and influenza epidemic patterns, were identified for the first time using influenza surveillance data. Our results advance understanding of the complex associations between weather and influenza, even though additional studies are needed to explore the mechanisms underlying this relationship. Our new findings of these associations provide potential avenues for future studies, help develop possibilities for better early warning of

influenza, and strengthen our predictive capacity for temporal patterns of influenza transmission.

Table 4.1. Monthly average ILI proportion in GOPC and GP settings in Hong Kong, China, 1998-2008.

Month	ILI proportion (per 1000)	
	GOPC	GP
Jan	5.71	51.34
Feb	7.65	57.35
Mar	7.62	58.52
Apr	4.93	47.06
May	5.50	49.00
June	6.10	48.94
July	6.44	46.75
Aug	4.75	41.13
Sep	4.26	42.95
Oct	4.00	41.18
Nov	3.85	41.06
Dec	4.05	42.25

Table 4.2. Monthly average influenza virus isolation positive proportion in Hong Kong, China,1998-2008.

Month	Mean specimen size	H3N2 strain positive proportion	H1N1 positive proportion	B positive proportion
Jan	1930.23	9.07	2.97	3.51
Feb	2269.31	15.21	4.83	5.55
Mar	2971.62	13.45	3.56	5.98
Apr	2373.08	8.45	1.69	3.01
May	2454.92	8.77	3.18	1.67
June	2922.38	11.33	3.08	1.55
July	3529.38	14.00	3.35	1.65
Aug	3579.31	8.08	2.25	1.95
Sep	3485.85	3.52	0.82	1.61
Oct	2239.77	1.02	0.25	0.87
Nov	2210.92	0.44	0.27	0.65
Dec	2552.62	1.36	0.50	1.16

Table 4.3. Non-Lagged Pearson correlations between weekly weather variables and influenza VPP, ILI proportion in Hong Kong, 1998-2008.

Weather variables	Influenza VPP				ILI proportion			
	Pearson		Partial Pearson		Pearson		Partial Pearson	
	R^2	*P*	R^2	*P*	R^2	*P*	R^2	*P*
Max Temp	-0.2	0.0001	-0.08	0.11	-0.02	0.62	0.06	0.10
Avg Temp	-0.21	0.0001	-0.08	0.09	-0.04	0.32	-0.02	0.63
Min Temp	-0.22	0.0001	-0.17	0.0005	-0.06	0.14	-0.15	0.00001
Absolute Humid	-0.11	0.03	-0.18	0.0002	0.01	0.82	-0.13	0.0001
Relative Humid	0.31	0.0001	0.13	0.01	0.12	0.001	0.014	0.73
Radiation	-0.06	0.22	-0.12	0.01	-0.01	0.76	-0.02	0.68
Rainfall	-0.01	0.77	-0.05	0.29	-0.02	0.66	-0.04	0.29
Dew point	-0.11	0.02	0.07	0.15	-0.01	0.84	-0.07	0.09
Cloud amount	0.28	0.0001	0.095	0.053	0.13	0.0008	0.07	0.10

Table 4.4. Largest lagged correlation coefficient estimates and correlation test between weekly influenza VPP and local weather variables in Hong Kong, 1998-2008.

Weather Variables	Pearson			Partial Pearson			Spearman			Partial Spearman		
	lag	R^2	*P*	lag	R^2	*P*	lag	R^2	*P*	lag	R^2	*P*
						All influenza virus strain VPP						
Abs. Humidity	7-14	-0.5	***	7-12	0.34	***	10-14	-0.58	***	5-9	-0.13	***
Relative Humidity	0-1	0.29	***	6-12	-0.21	***	0-2	0.36	***	14-14	0.21	***
Avg. Temp	4-12	-0.5	***	14-14	0.1	*	9-13	-0.57	***	3-14	0.18	***
Min. Temp	5-11	-0.50	***	6-11	-0.20	***	9-13	-0.57	***	3-7	-0.15	***
Max. Temp	4-13	-0.51	***	9-13	-0.12	**	9-13	-0.58	***	3-14	-0.18	***
Dew Point Temp	6-13	-0.49	***	7-8	0.08	*	10-14	-0.58	***	7-12	-0.13	**
Radiation	1-14	-0.53	***	14-14	-0.12	***	4-14	-0.54	***	0	0.24	***
Rainfall	8-14	-0.47	***	7-12	-0.2	***	10-14	-0.54	***	11-11	-0.13	***
Cloud Amount	0-2	0.33	***	2-9	0.21	***	0-2	0.39	***	4-13	0.30	***
Wind speed	13-14	0.16	***	2-12	-0.17	***	13-14	0.18	***	4-12	-0.29	***
Sea level Pressure	10-14	0.55	***	14-14	0.24	***	11-14	0.60	***	14-14	0.24	***
						H3N2 subtype strain VPP						
Abs. Humidity	8-14	-0.35	***	7-12	0.14	***	13-14	-0.43	***	5-9	-0.11	*
Avg. Temp	7-11	-0.34	***	0-13	-0.14	***	11-13	-0.42	***	4-7	0.09	*
Min. Temp	7-11	-0.34	***	7-11	-0.13	**	10-14	-0.41	***	4-7	0.10	*
Max. Temp	5-14	-0.35	***	0-14	0.08	0.052	10-14	-0.42	***	5-12	-0.08	0.054
Dew Point Temp	6-14	-0.33	***	3-11	0.13	***	13-14	-0.43	***	11-12	-0.08	0.07
Relative Humidity	0-2	0.22	***	4-11	-0.18	***	0-2	0.26	***	14-14	0.16	***
Radiation	1-14	-0.39	***	0-14	-0.20	***	5-14	-0.37	***	0-0	0.13	**
Rainfall	8-14	-0.34	***	0-14	-0.23	***	8-14	-0.38	***	0-14	-0.09	*
Cloud Amount	0-2	0.25	***	4-9	0.11	*	0-2	0.29	***	4-13	0.29	***
Wind speed	13-14	0.14	***	0-1	0.14	***	13-14	0.19	***	3-12	-0.18	***
Sea level Pressure	10-14	0.41	***	13-14	0.22	***	11-14	0.46	***	10-14	0.21	***

***: $p<0.001$, **:$p<0.01$, *: $p<0.05$

Table 4.5. Lagged correlation coefficient estimates and correlation significance test between weekly ILI proportion and local weather variables in Hong Kong, 1998-2008.

Weather Variables	Pearson			Partial Pearson			Spearman			Spearman Partial		
	lag	R^2	*P*	lag	R^2	*P*	lag	R^2	*P*	lag	R^2	*P*
						ILI proportion in GOPC setting						
Abs. Humidity	9-14	-0.32	***	8-13	0.32	***	13-14	-0.35	***	0	-0.16	***
Avg. Temp	3-14	-0.33	***	13-14	0.16	***	10-14	-0.35	***	0-12	0.18	***
Min. Temp	3-14	-0.33	***	10-14	-0.32	***	10-15	-0.36	***	0-12	-0.24	***
Max. Temp	3-14	-0.33	***	4-5	0.14	***	10-14	-0.35	***	0-12	-0.06	***
Dew Point Temp	10-10	-0.32	***	14-14	-0.09	***	13-14	-0.36	***	10-14	-0.25	***
Relative Humidity	10-14	-0.19	***	8-12	-0.18	***	0- 4	0.22	***	2- 8	-0.19	***
Radiation	2-14	-0.43	***	2-6	-0.23	***	4-14	-0.40	***	4-14	-0.14	***
Rainfall	10-14	-0.29	***	10-13	-0.20	***	10-14	-0.34	***	11-14	-0.15	***
Cloud Amount	0-5	0.28	***	3-10	0.22	***	0-6	0.31	***	4-10	0.25	***
Wind speed	0-14	0.30	***	0-3	0.41	***	13-14	0.22	***	0-2	0.32	***
Sea level Pressure	10-14	0.34	***	1-6	0.18	***	13-14	0.36	***	13-13	0.14	***
						ILI proportion in GP setting						
Abs. Humidity	9-10	-0.40	***	8-12	0.16	***	9-11	-0.40	***	4-10	-0.12	***
Avg. Temp	3-11	-0.41	***	2-14	0.16	***	9-10	-0.41	***	1-14	0.20	***
Min. Temp	3-11	-0.41	***	10-14	-0.22	***	9-10	-0.42	***	10-14	-0.23	***
Max. Temp	2-13	-0.40	***	0-14	-0.13	***	3-14	-0.41	***	0-14	-0.13	***
Dew Point Temp	3-14	-0.41	***	2-14	-0.13	***	9-11	-0.40	***	2-14	-0.11	***
Relative Humidity	9-14	-0.29	***	10-12	-0.12	***	9-14	-0.22	***	5-9	-0.17	***
Radiation	1-14	-0.42	***	13-14	-0.18	***	3-14	-0.42	***	12-14	-0.21	***
Rainfall	8-14	-0.30	***	10-11	-0.11	***	9-14	-0.36	***	10-13	-0.15	***
Cloud Amount	10-14	-0.14	***	4-9	0.23	***	0-5	0.22	***	2-9	0.23	***
Wind speed	0-1	0.12	**	0-2	0.16	***	14-14	0.07	0.09	0-2	0.10	*
Sea level Pressure	8-11	0.38	***	14-14	0.09	*	9-11	0.39	***	3-4	-0.10	***

***: $p<0.001$, **:$p<0.01$, *: $p<0.05$

Table 4.6. Lagged correlation coefficient estimates and correlation test between weekly influenza VPP and local weather variable anomalies in Hong Kong, 1998-2008.

Weather Variables	Pearson			Partial Pearson			Spearman			Partial Spearman		
	lag	R^2	*P*	lag	R^2	*P*	lag	R^2	*P*	lag	R^2	*P*
						All influenza virus strain VPP						
Abs. Humidity	0-14	0.16	***	5-6	-0.10	*	11-14	0.09	*	1-12	-0.16	***
Avg. Temp	12-14	0.09	*	4-6	0.09	*	10-14	0.09	*	3-5	0.13	**
Min. Temp	12-14	0.10	*	3-8	-0.10	*	10-14	0.10	*	3-5	-0.14	***
Max. Temp	0-2	-0.06	0.19	0-14	0.04	0.40	10-14	0.06	0.14	0-6	-0.06	0.14
Dew Point Temp	5-14	0.15	***	5-5	-0.06	0.14	11-14	0.12	**	12-13	0.24	**
Relative Humidity	0-14	0.16	***	5-5	0.09	*	0-14	0.09	*	11-13	-0.08	0.06
Radiation	0-14	-0.23	***	0-3	-0.15	***	0-6	-0.14	***	1-5	-0.11	***
Rainfall	8-11	-0.04	0.32	0-14	-0.13	**	12-12	0.16	***	11-11	0.16	***
Cloud Amount	0-12	0.25	***	2-8	0.12	**	1-13	0.16	***	0-14	0.16	***
Wind speed	12-14	0.10	*	13-14	0.07	0.08	13-14	0.09	*	0-10	-0.12	**
Sea level Pressure	0-7	0.07	0.09	3-7	0.18	***	0-11	0.07	0.08	1-12	0.15	***
						H3N2 subtype strain VPP						
Abs. Humidity	0-14	0.21	***	2-14	-0.18	***	0-2	0.05	0.22	0-10	-0.22	***
Avg. Temp	0-14	0.18	***	0-13	-0.09	*	0-10	0.15	***	7-14	-0.10	*
Min. Temp	0-14	0.19	***	10-10	-0.06	0.14	0-14	0.16	***	7-14	0.11	**
Max. Temp	0-14	0.12	**	0-14	0.18	***	2-14	0.14	***	2-13	0.14	0.054
Dew Point Temp	0-14	0.22	***	0-12	0.11	**	12-14	0.06	0.16	2-13	0.16	0.07
Relative Humidity	7-14	0.13	**	12-14	0.10	*	3-8	-0.14	***	5-7	-0.09	***
Radiation	0-14	-0.20	***	0-14	-0.31	***	11-13	-0.10	***	4-7	-0.27	***
Rainfall	0-10	-0.12	**	0-14	-0.15	***	12-12	0.11	*	11-11	0.11	*
Cloud Amount	0-12	0.16	***	13-14	-0.12	**	3-8	-0.08	0.06	13-14	-0.11	**
Wind speed	0-14	0.13	**	0-1	0.11	*	13-14	0.13	**	13-14	0.14	***
Sea level Pressure	3-11	0.18	***	3-11	0.31	***	0-13	0.24	***	3-13	0.35	***

***: $p<0.001$, **:$p<0.01$, *: $p<0.05$

Table 4.7. Correlation coefficient estimates and correlation test between weekly ILI proportion and local weather variable anomalies in Hong Kong, 1998-2008.

Weather Variables	Pearson			Partial Pearson			Spearman			Partial Spearman		
	lag	R^2	*P*	lag	R^2	*P*	lag	R^2	*P*	lag	R^2	*P*
						ILI proportion in GOPC setting						
Abs. Humidity	5-14	0.20	***	4-5	-0.14	***	0-9	0.15	***	3-14	-0.19	***
Avg. Temp	6-14	0.12	**	6-14	0.16	***	0-0	0.10	*	3-13	0.17	***
Min. Temp	1-4	-0.13	**	10-14	-0.23	***	0-0	0.08	0.06	3-13	-0.24	***
Max. Temp	6-14	0.11	**	4-5	0.14	**	0-0	0.11	**	3-3	0.09	*
Dew Point	5-14	0.17	***	6-7	-0.12	**	0-9	0.12	**	1-1	-0.12	**
Relative Humidity	4-9	0.16	***	6-7	0.15	***	2-9	0.10	*	3-9	-0.10	*
Radiation	1-14	-0.32	***	2-5	-0.27	***	1-14	-0.22	***	1-5	-0.13	***
Rainfall	3-9	0.06	0.17	1-14	-0.13	**	9-9	0.12	**	0-2	-0.10	***
Cloud Amount	1-13	0.37	***	4-9	0.16	**	2-14	0.30	***	4-11	0.19	***
Wind speed	0-14	0.36	***	0-3	0.35	***	7-14	0.30	***	1-8	0.28	***
Sea level Pressure	5-14	-0.12	**	1-5	0.21	***	8-14	-0.14	***	1-6	0.15	***
						ILI proportion in GP setting						
Abs. Humidity	2-10	-0.09	*	5-7	-0.13	**	12-13	0.09	*	2-13	-0.16	***
Avg. Temp	2-5	-0.12	**	6-14	0.14	***	3-4	-0.09	*	2-14	0.14	***
Min. Temp	2-13	-0.14	***	1-14	-0.17	***	2-14	-0.13	**	2-12	-0.23	***
Max. Temp	2-5	-0.11	**	9-9	0.09	*	3-4	-0.07	0.09	0-14	-0.07	0.10
Dew Point Temp	2-11	-0.13	***	4-9	-0.12	**	12-13	0.10	***	11-14	0.21	***
Relative Humidity	9-9	-0.06	0.13	6-7	0.14	**	12-13	0.10	*	1-9	-0.15	***
Radiation	1-14	-0.22	***	2-5	-0.15	***	3-14	-0.16	***	12-12	0.10	***
Rainfall	1-3	0.04	0.30	0-13	-0.08	0.07	12-12	0.15	***	14-14	0.14	***
Cloud Amount	3-13	0.23	***	4-9	0.19	***	4-14	0.23	***	5-12	0.17	***
Wind speed	10-14	0.12	**	14-14	0.12	**	12-14	0.09	*	12-14	0.07	0.11
Sea level Pressure	12-14	-0.12	**	6-9	0.08	0.06	11-14	-0.16	***	11-14	-0.08	*

***: $p<0.001$, **:$p<0.01$, *: $p<0.05$

Table 4.8. Correlation coefficient estimates and correlation test between monthly global climatic indices and ILI proportion, influenza VPP in Hong Kong, 1998- 2008.

Weather Variables	Pearson			Partial Pearson			Spearman			Partial Spearman		
	lag	R^2	*P*	lag	R^2	*P*	lag	R^2	*P*	lag	R^2	*P*
						ILI proportion in GOPC setting						
MEI	0-3	-0.09	0.10	1-2	0.20	*	0-0	-0.14	0.06	0-0	-0.16	0.07
WP	1-3	0.34	***	1-3	0.38	***	1-3	0.31	***	1-3	0.26	***
PNA	1-3	0.30	***	1-3	0.32	***	1-3	0.22	*	1-2	0.21	***
PDO	0-0	0.21	*	0-0	0.16	0.06	1-2	0.16	0.06	1-1	0.11	0.09
SOI	1-1	-0.11	0.19	1-1	-0.16	0.06	0-0	0.15	*	0-0	0.07	0.08
						ILI proportion in GP setting						
MEI	1-3	0.14	0.06	1-1	-0.06	0.46	1-3	-0.24	**	1-3	-0.14	*
WP	1-3	0.34	0.07	1-3	0.17	*	1-3	0.19	***	1-2	0.10	0.07
PNA	1-3	0.30	0.15	1-3	0.21	*	1-3	0.17	**	1-3	0.12	0.12
PDO	0-0	0.21	0.23	0-0	0.20	**	1-3	-0.08	0.62	1-2	-0.09	0.50
SOI	1-3	-0.09	0.18	1-1	-0.17	*	1-3	0.20	**	1-3	0.23	***
						All virus strain VPP						
MEI	1-1	0.21	*	1-2	0.09	0.30	1-1	0.08	0.07	1-1	0.02	0.25
WP	1-3	0.20	*	1-3	0.24	**	1-3	0.18	*	1-3	0.17	*
PNA	1-3	0.22	**	1-3	0.18	*	0-0	0.13	**	0-0	0.10	0.07
PDO	0-0	0.32	***	0-0	0.22	**	0-0	0.29	***	0-0	0.20	**
SOI	1-1	-0.20	*	1-1	-0.15	0.07	1-1	-0.12	***	1-1	-0.10	0.08
						H3N2 subtype VPP						
MEI	1-2	0.40	***	1-1	0.16	0.06	1-2	0.27	**	1-2	0.11	0.08
WP	1-3	0.19	*	1-3	0.25	0.07	1-3	0.11	0.06	1-3	0.11	0.07
PNA	1-2	0.20	*	1-2	0.10	0.25	0-0	0.09	>0.5	0-0	0.06	0.78
PDO	0-0	0.36	***	0-0	0.16	0.06	0-0	0.27	***	0-0	0.16	0.08
SOI	1-3	-0.38	***	1-3	-0.15	0.07	1-3	-0.28	***	1-3	-0.13	0.09

***: $p<0.001$, **:$p<0.01$, *: $p<0.05$

Table 4.9. Significant statistical correlations between monthly global climatic indices and influenza epidemic morbidity impacts in Hong Kong, 1998-2008.

Summarized epidemic variables	PNA in preceding month		Average PNA from preceding 2 month		Average PNA from preceding 3 month	
	Correlation coefficient	*P*	Correlation coefficient	*P*	Correlation coefficient	*P*
Duration of epidemics	0.578	0.039	0.646	0.017	0.637	0.019
Cumulative positive virus proportion	0.573	0.041	0.672	0.012	0.646	0.017
Cumulative ILI count	0.475	0.101	0.578	0.038	0.574	0.040

Table 4.10. ARIMA model coefficient estimates and summary for lagged crude weather variables and influenza VPP in Hong Kong, 1998-2008.

ARIMA Model order	Fit		AR		MA		Weather variables			X2 test
	Residual	AIC	Est.	SE	Est.	SE	Variable	Est.	SE	
ARIMA(0,1,0)	0.34	1003.2								
ARIMA(0,1,1)	0.33	996.2			-0.11	0.04				
ARIMA(0,1,3)	0.32	972.4			-0.16	0.04				
					0.04	0.04				
					0.19	0.04				
Univariate										
ARIMA(0,1,3)	0.31	960.1			-0.17	0.04	AH	-117	38.5	**
					0.03	0.04				
					0.17	0.04				
ARIMA(0,1,3)	0.31	963.2			-0.17	0.04	Avg. TEMP	-0.14	0.04	**
					0.04	0.04				
					0.17	0.04				
ARIMA(0,1,3)	0.31	960.5			-0.17	0.04	MIN TEMP	-0.14	0.04	**
					0.03	0.04				
					0.18	0.04				
ARIMA(0,1,3)	0.31	964.8			-0.17	0.04	Max TEMP	-0.14	0.04	**
					0.04	0.04				
					0.17	0.04				
ARIMA(0,1,3)	0.32	966.8			-0.17	0.04	DEWP	-0.08	0.03	*
					0.03	0.04				
					0.17	0.04				
ARIMA(0,1,3)	0.31	963.6			-0.16	0.04	Rainfall	-0.03	0.01	**
					0.04	0.04				
					0.19	0.01				
Multivariate										
ARIMA(0,1,3)	0.31	955.0			-0.17	0.04	AH	-42.7	48.4	*
					0.03	0.04	MIN TEMP	-0.11	0.05	
					0.18	0.04				
ARIMA(0,1,3)	0.31	952.1			-0.17	0.04	MIN TEMP	-0.12	0.04	**
					0.03	0.04	Rainfall	0.025	0.01	
					0.18	0.04				
ARIMA(0,1,3)	0.31	944.1			-0.17	0.04	AH	-21.7	48.9	**
					0.03	0.04	Min Temp	0.11	0.05	
					0.18	0.04	Rainfall	-0.02	0.01	

***: p<0.001, **:p<0.01, *: p<0.05

Figure 4.1. The location of Hong Kong in relation to China and other countries in the region.

* download and access in April, 2011.
http://www.enchantedlearning.com/asia/china/mapquizprintout.shtml

Figure 4.2. Weekly influenza VPP and ILI proportion in Hong Kong, China, 1998-2008.

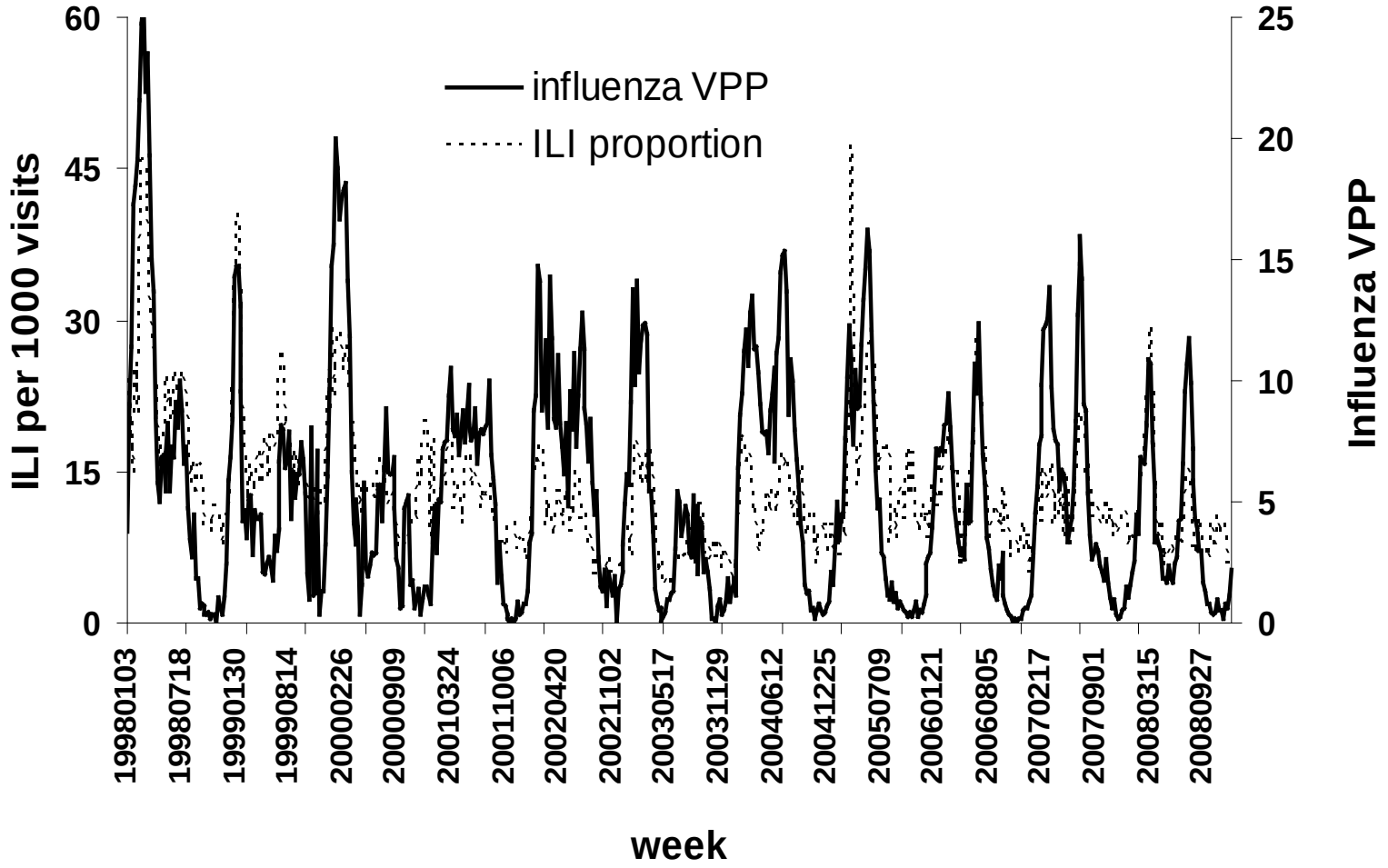

Figure 4.3. Average weekly ILI proportion and influenza VPP in Hong Kong, China, 1998-2008.

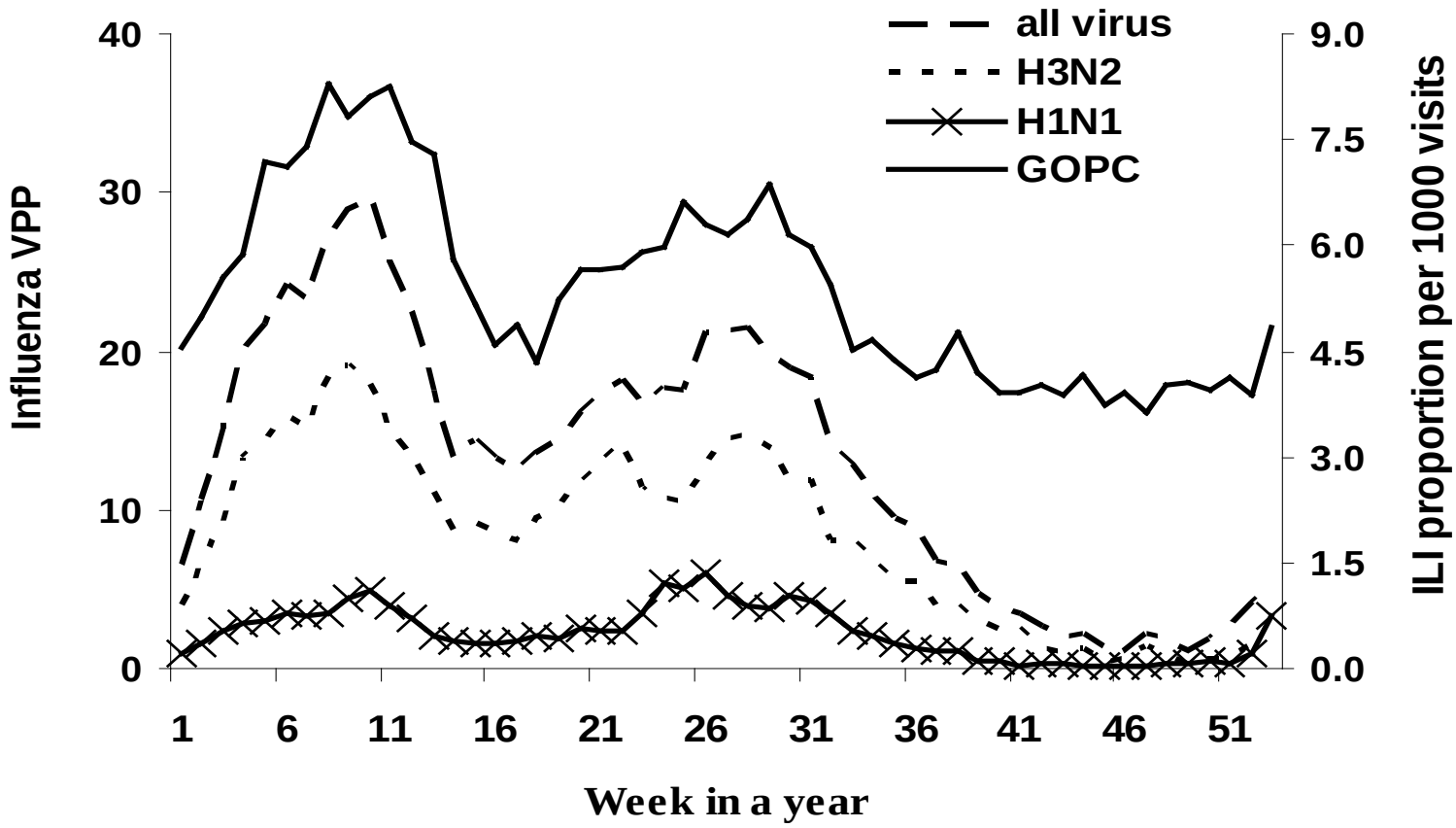

Figure 4.4. Average daily local weather variables (A. temperature and rainfall; B. RH and AH) in Hong Kong, China, 1998-2008.

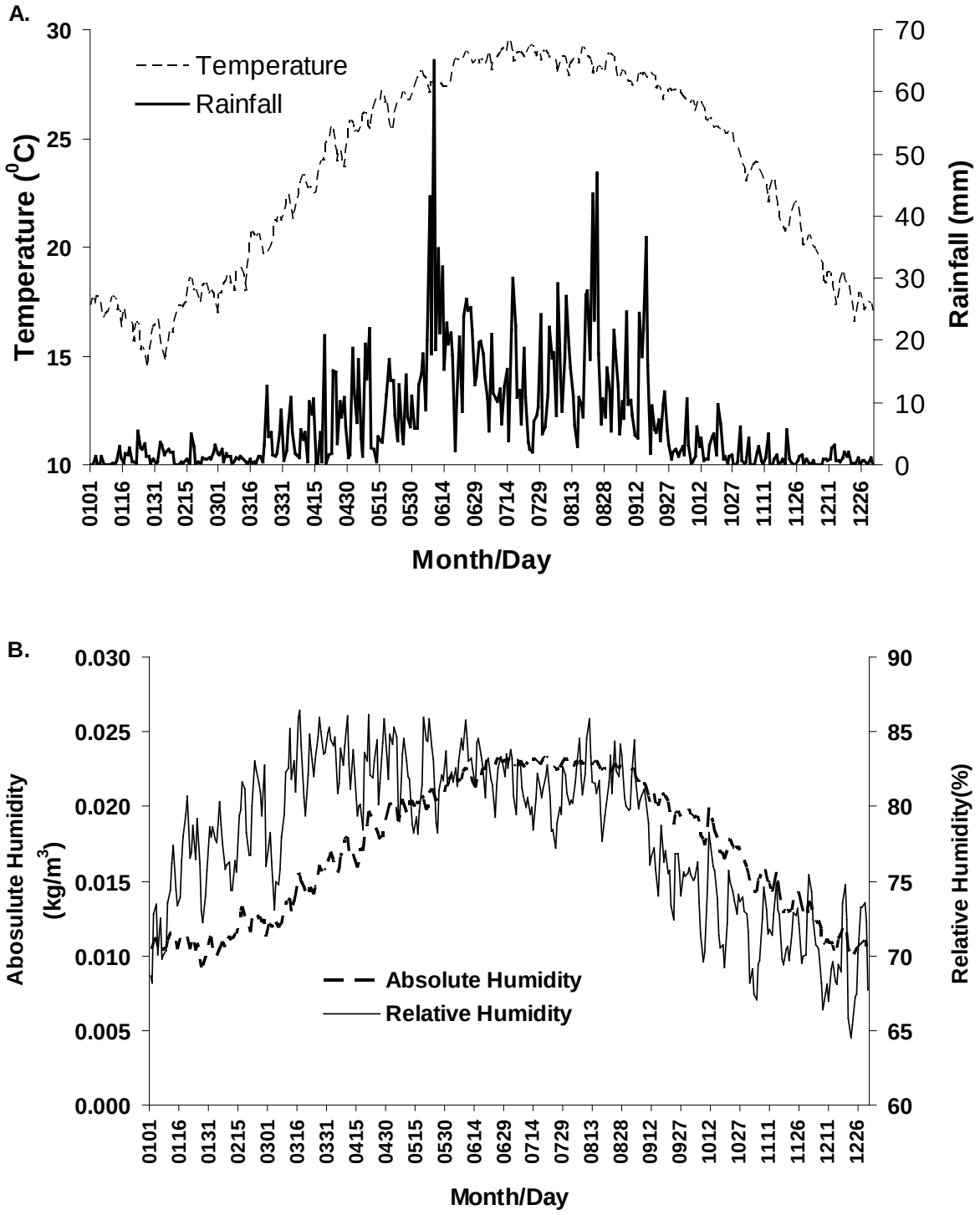

Figure 4.5. Monthly global climatic indices (A.MEI, PDO; B. WP, PNA) distribution between 1998 and 2008.

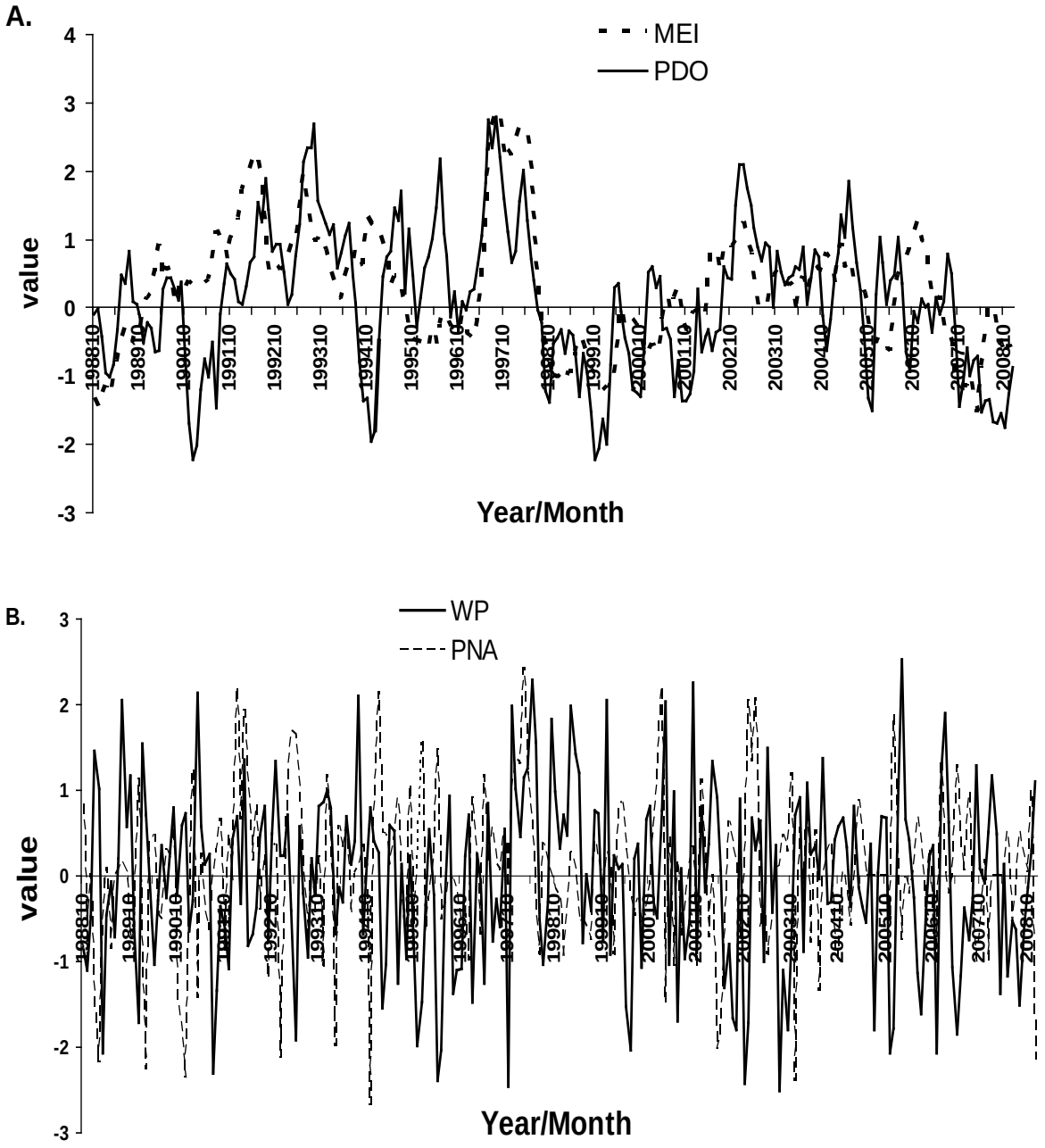

Figure 4.6. Influenza epidemic onsets based on weekly VPP (A) and ILI proportion (B) in Hong Kong, China, 1998-2008.

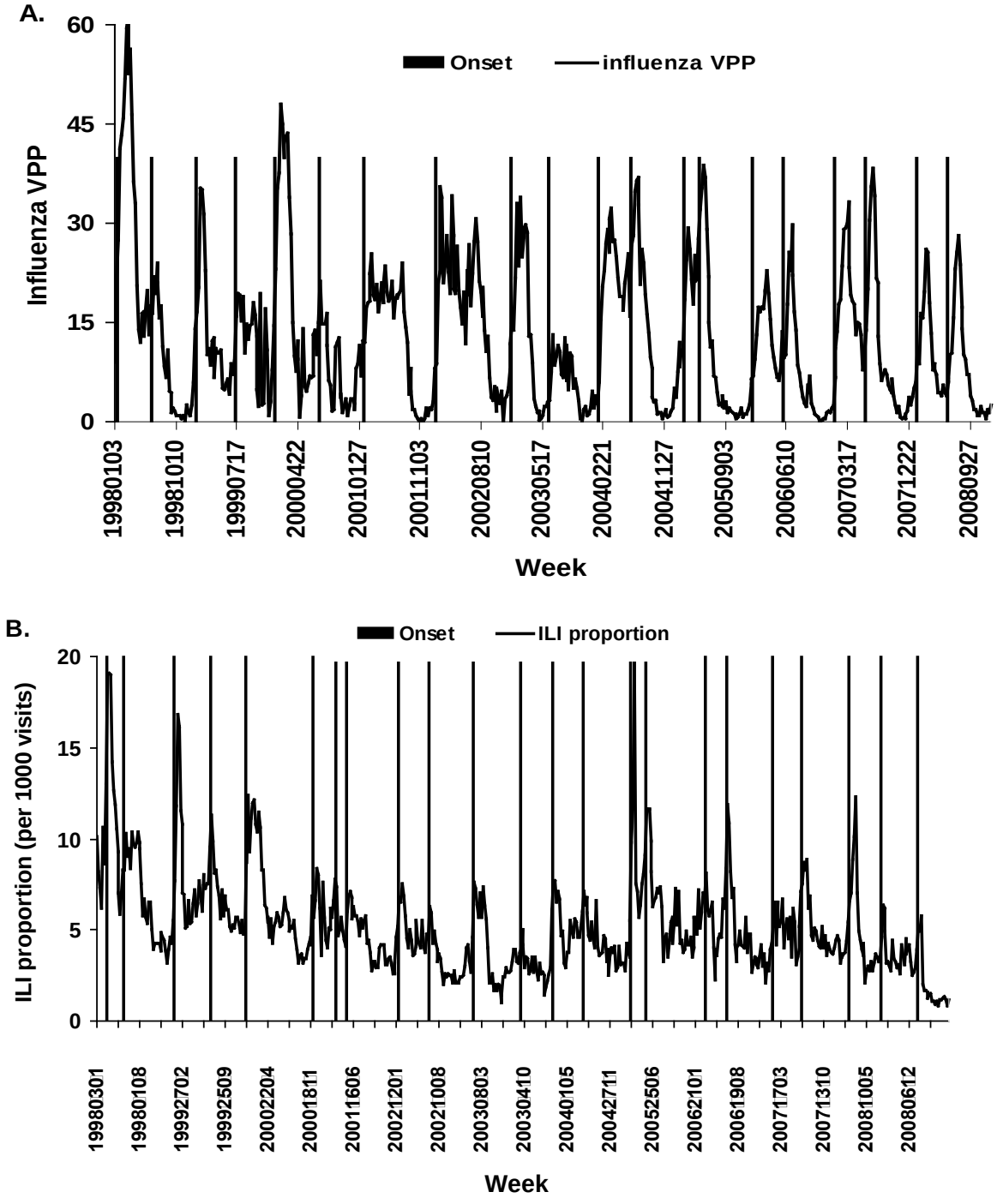

Figure 4.7. Cross correlation maps (A. Pearson approach; B, Partial Pearson approach) of weekly weather variables and all influenza strains VPP

(A)

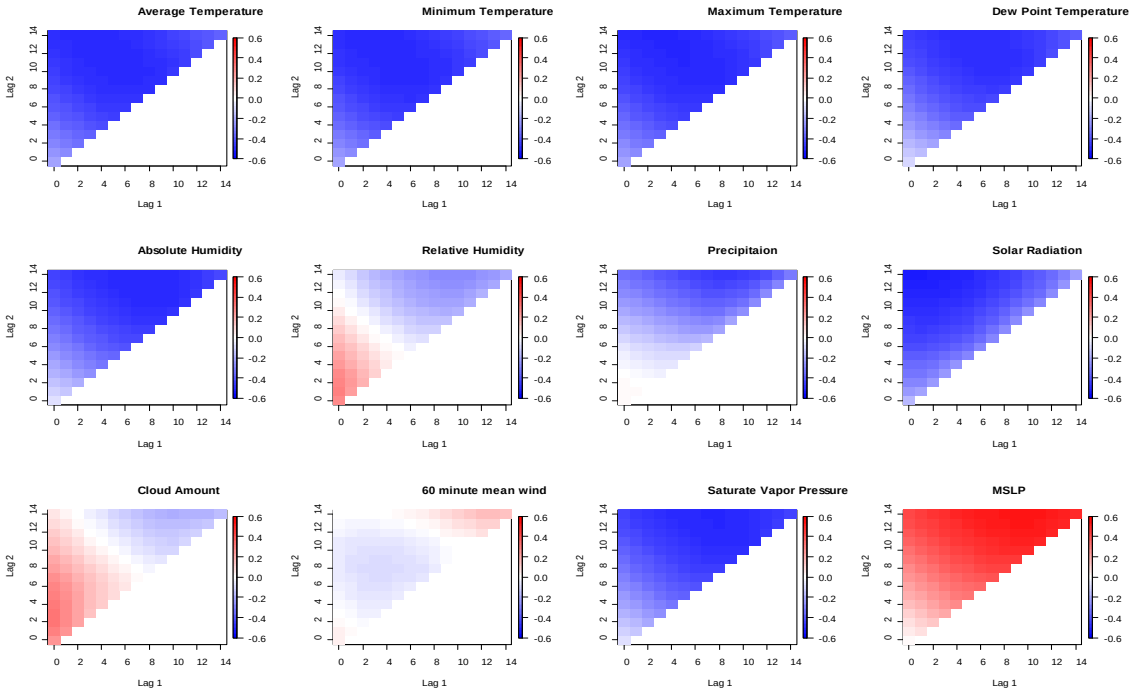

(B)

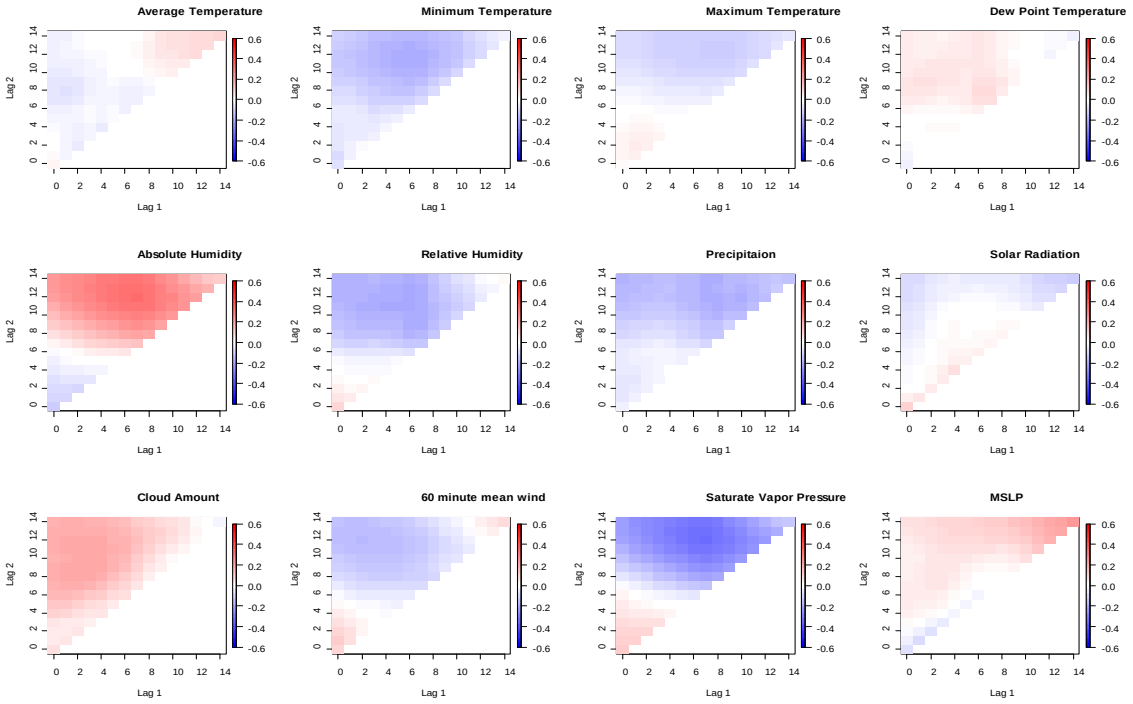

Figure 4.8. Cross correlation maps (A.Pearson approach; B. Partial Pearson approach) of weekly GOPC ILI proportion and weather variables.

(A)

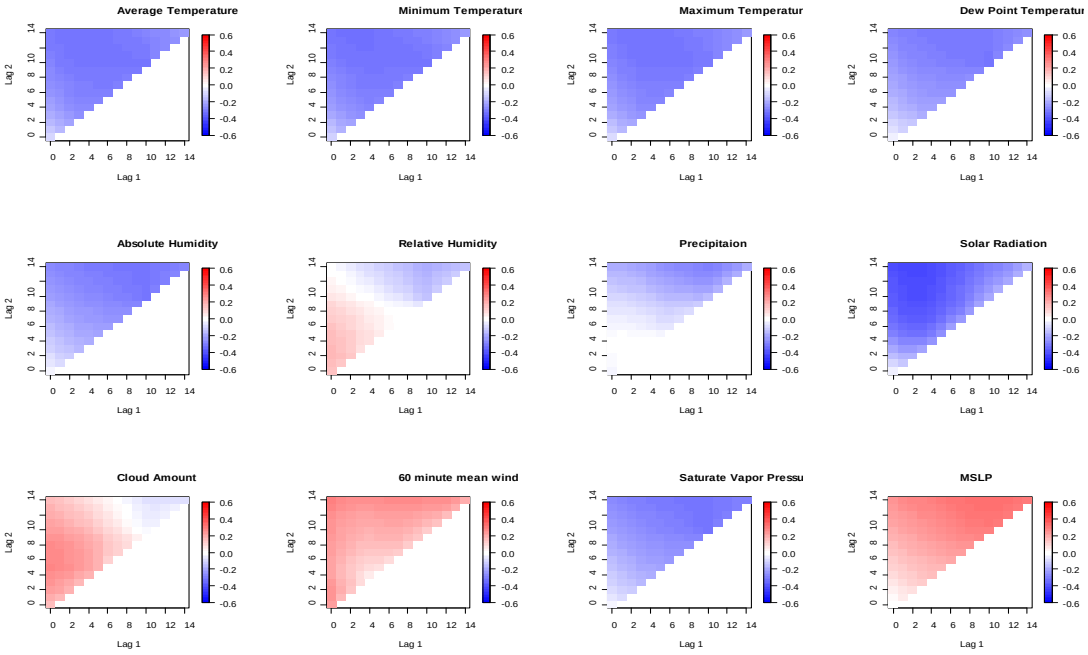

(B)

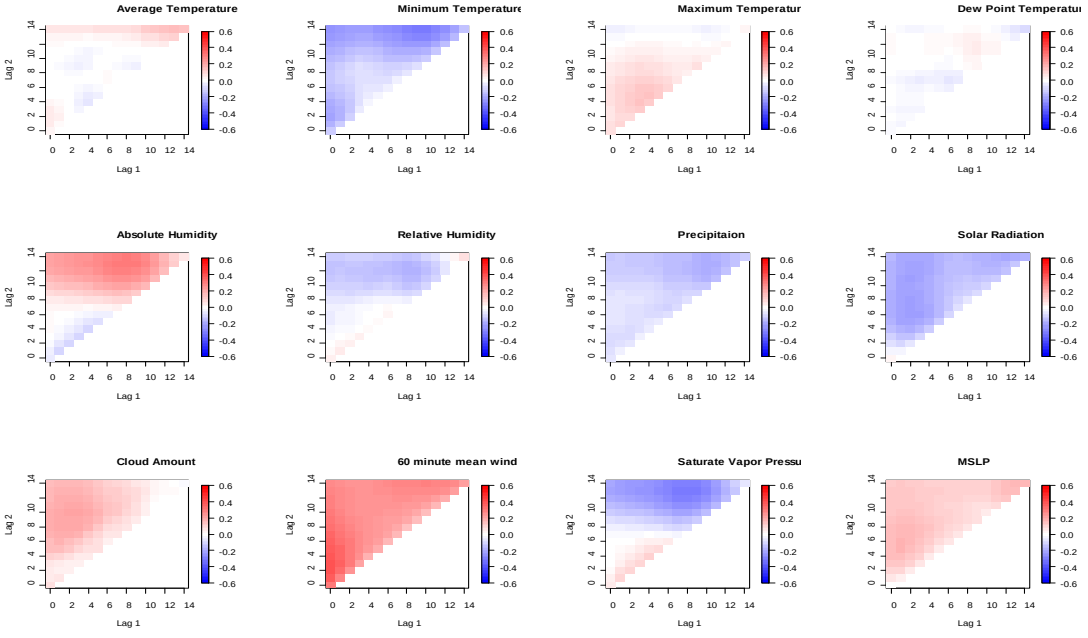

Figure 4.9. Cross correlation maps (A. Pearson approach; B. Partial Pearson approach) of weekly weather variable anomaly and all types of influenza VPP.

(A)

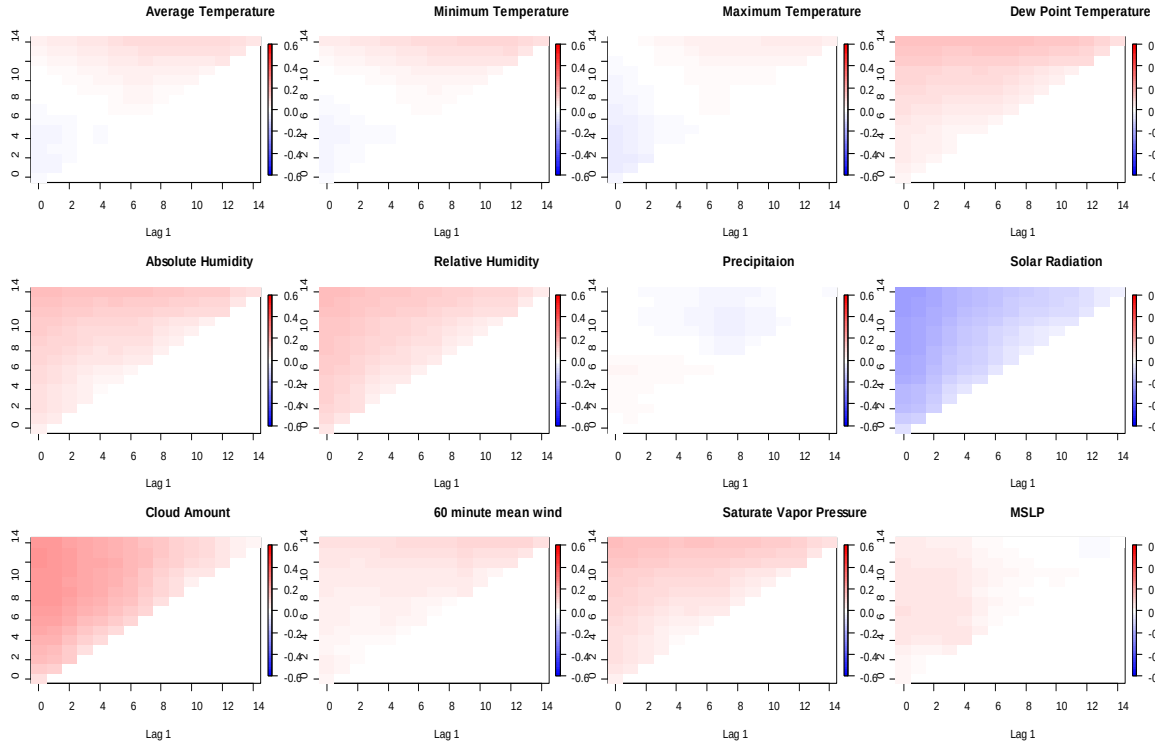

(B)

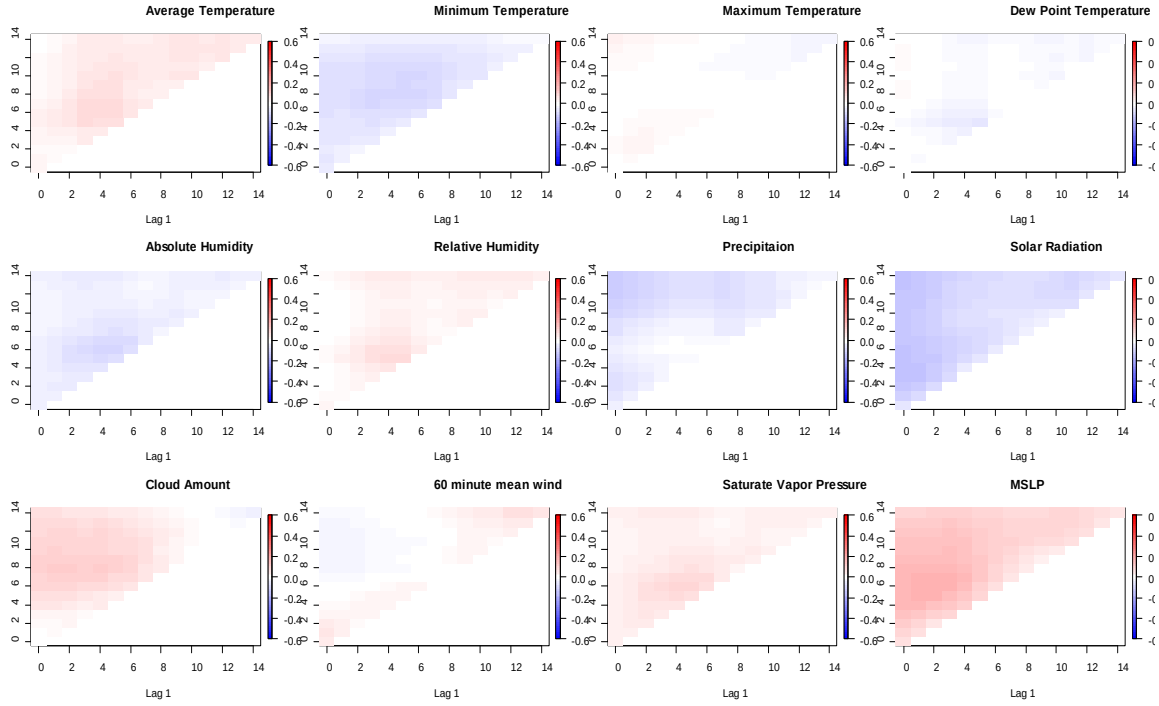

Figure 4.10. Influenza epidemic onset and absolute humidity anomaly in Hong Kong, China, 1998-2008.

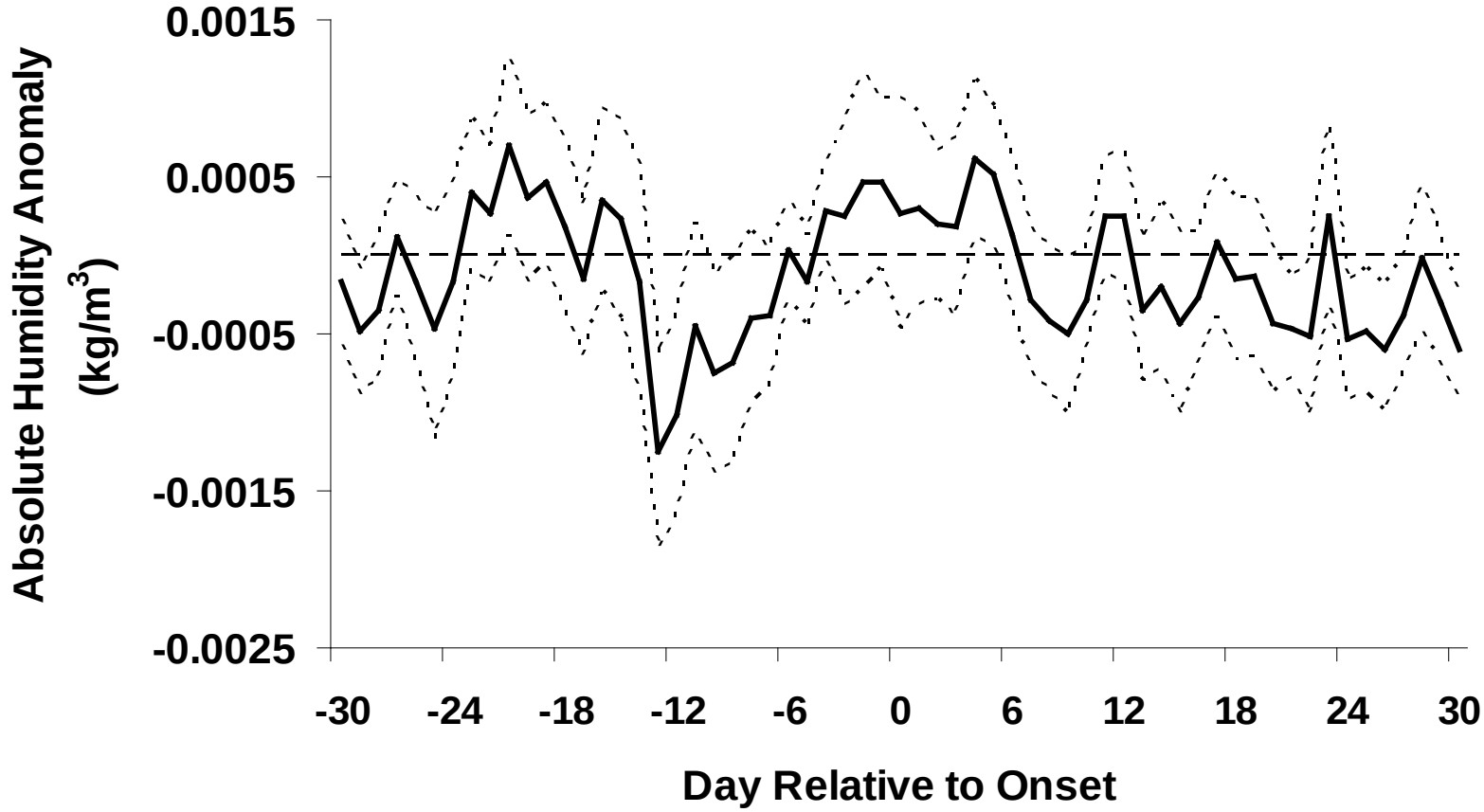

Figure 4.11. Observed and fitted weekly influenza VPP in Hong Kong, China, 1998-2008.

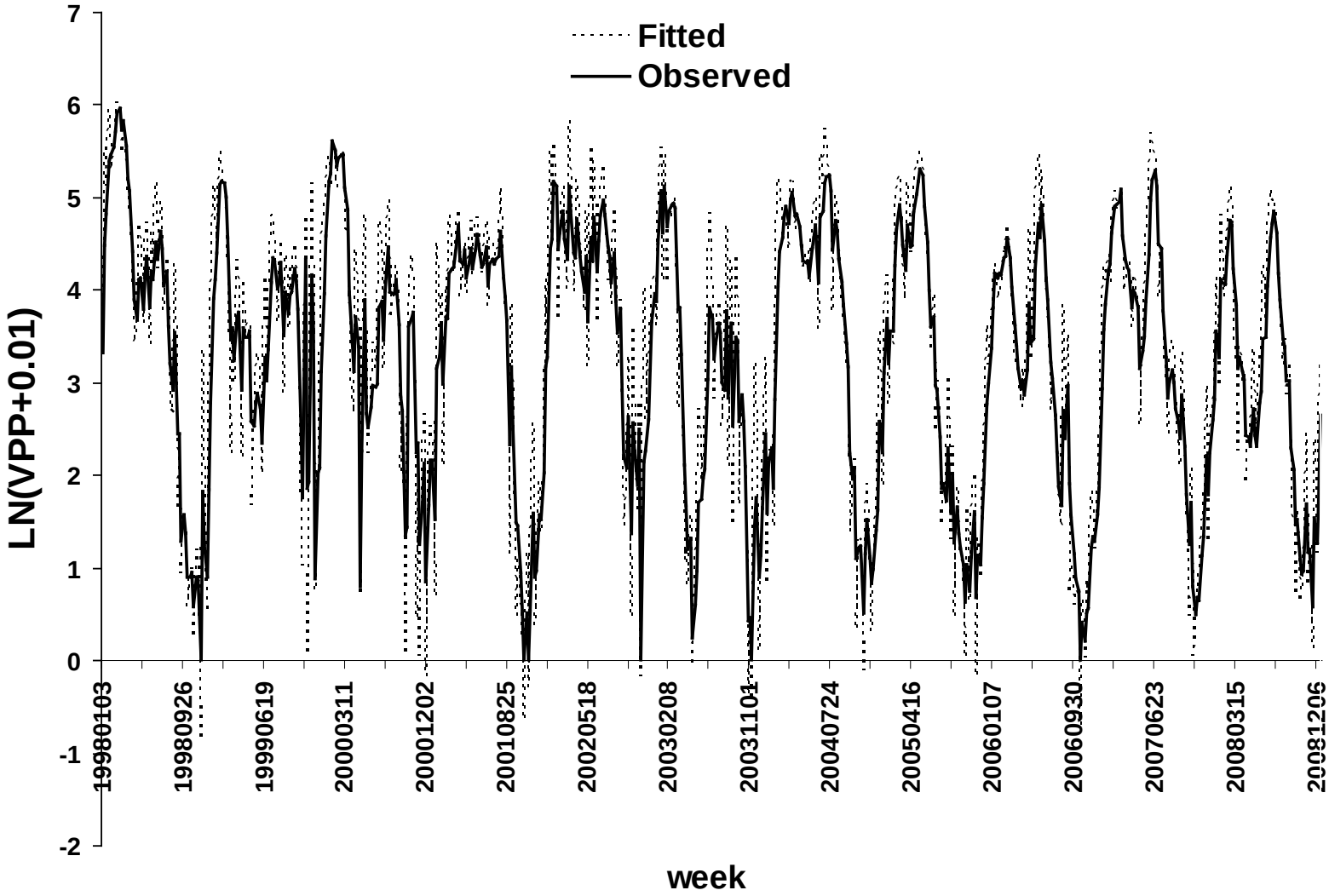

REFERENCES

1. Brammer TL, Murray EL, Fukuda K, Hall HE, Klimov A, Cox NJ. Surveillance for influenza--United States, 1997-98, 1998-99, and 1999-00 seasons. *MMWR Surveill Summ.* 2002 Oct 25;51(7):1-10.

2. Marc J W Sprenger, Paul G H Mulder, Walter E P Beyer, Roel Van Strik, and Nic Masurel. Impact of influenza on mortality in relation to age and underlying disease, 1967–1989. *Int. J. Epidemiology*, 1993;22(2):334-340.

3. Fleming DM, Zambon M, Bartelds AI, de Jong JC. The duration and magnitude of influenza epidemics: A study of surveillance data from sentinel general practices in England, Wales and The Netherlands. *Eur J Epidemiol* 1999; 15: 467–473.

4. Cox NJ, Subbarao K. Global epidemiology of influenza: past and present. *Ann Rev Med* 2000;51: 407–421.

5. Viboud C, Alonso WJ, Simonsen L. Influenza in tropical regions. *PLoS Med.* 2006;3(4): e89.

6. Julian W. Tang, Karry L. K. Ngai, Wai Y. Lam, Paul K. S Chan. Seasonality of influenza A(H3N2) virus: A Hong Kong perspective (1997–2006). *PLoS ONE* 2008;3(7): e2768. doi:10.1371/journal.pone.0002768.

7. Brian S. Finkelman1, Cecile Viboud, Katia Koelle, Matthew J. Ferrari1, Nita Bharti1, Bryan T. Grenfell. Global patterns in seasonal activity of influenza A/H3N2, A/H1N1, and B from 1997 to 2005: viral coexistence and latitudinal gradients. *PLoS ONE* 2007;2(12): e1296. doi:10.1371/journal.pone.0001296

8. Kennedy F. Shortridge. Is China an influenza epicenter? *Chin Med J* 1997;110(8):637-641.

9. Stuart-Harris CH, Schild GC, Oxford JS.. Influenza. The Viruses and the Disease, pp. 118–38. Victoria, Can.: Edward Arnold. 1985; 2nd ed.

10. Shortridge KF, Stuart-Harris CH (1982) An influenza epicentre? Lancet 2:812–813.

11. Shortridge KF, Zhou NN, Guan Y, et al.. Characterization of avian H5N1 influenza viruses from poultry in Hong Kong. *Virology* 1998;252:331–42.

12. Ku AS, Chan LT. The first case of H5N1 avian influenza infection in a human with complications of adult respiratory distress syndrome and Reye's syndrome. *J Paediatr Child Health.* 1999 Apr;35(2):207-9.

13. Colin A. Russell, Terry C. Jones, Ian G. Barr, et al. The global circulation of seasonal influenza A (H3N2) Viruses. *Science* 2008:Vol. 320, no. 5874:P340-346.

14. Center for Health Protection. Sentinel Surveillance. Available: http://www.chp.gov.hk/. Accessed 2006 Dec 11.

15. Cowling BJ, Wong IO, Ho LM, Riley S, Leung GM. Methods for monitoring influenza surveillance data. *Int J Epidemiol*. 2006;35:1314–21. DOI: 10.1093/ije/dyl162.

16. Viboud C, Pakdaman K, Boe¨lle PY, Wilson ML, Myers MF, et al. Association of influenza epidemics with global climate variability. *Eur J Epidemiol* 2004;19: 1055–1059.

17. Park AW, Glass K. Dynamic patterns of avian and human influenza in east and southeast *Asia. Lancet Infect Dis* 2007;7: 543–548.

18. Lofgren E, Fefferman NH, Naumov YN, Gorski J, Naumova EN. Influenza seasonality: underlying causes and modeling theories. *J Virol* 2007;81: 5429–5436.

19. Anders HS. Atmospheric pressure and epidemic influenza in Philadelphia. *Phila. Med. J.*, 1902; pp. 178–80.

20. Eccles R. An explanation for the seasonality of acute upper respiratory tract viral infections. *Acta Otolaryngol* 2002;122:183-191.

21. Babin SM. Weather and Climate effects on disease back ground levels. *Johns Hopkins Appl. Technical. Digest* 2003;24(1):343-348.

22. Du Prel JB, Puppe W, Grondahl B, Knuf M, Weigl JA, et al. Are meteorological parameters associated with acute respiratory tract infections? *Clin Infect Dis.* 2009;49: 861–868.

23. Mitsuyoshi Urashima, Nahoko Shindo, and Nobuhiko Okabe. A seasonal model to simulate influenza oscillation in Tokyo. *Jpn. J. Infect. Dis.*, 2003;56:43-47.

24. Lowen AC, Mubareka S, Steel J, Palese P. Influenza virus transmission is dependent on relative humidity and temperature. *PLoS Pathog* 2007;3: 1470–1476.

25. Jeffrey Shaman, and Melvin Kohn. Absolute humidity modulates influenza survival, transmission, and seasonality. *PNAS*, March 3, 2009; vol. 106; 9:3243–3248.

26. Jeffrey Shaman, Virginia E. Pitzer, Ce´ cile Viboud, Bryan T. Grenfell, Marc Lipsitch. Absolute humidity and the seasonal onset of influenza in the continental United States. *PLoS Biology*, 2010, Vol. 8, Issue 2; e1000316.

27. David N. Fisman. Seasonality of infectious diseases. *Annu. Rev. Public Health*. 2007.28:127-143.

28. Anselin L. Local indicator of spatial association –LISA. *Geogrphical Analysis*. 1995;27:93-115.

29. Dowell SF, Whitney CG,Wright C, Rose CEJ, Schuchat A. Seasonal patterns of invasive pneumococcal disease. *Emerg. Infect. Dis.* 2003;9:573–79.

30. Talbot TR, Poehling KA, Hartert TV, Arbogast PG, Halasa NB, et al. Seasonality of invasive pneumococcal disease: temporal relation to documented influenza and respiratory syncytial viral circulation. *Am. J. Med.* 2005;118:285–91.

31. Cannell JJ, Vieth R, Umhau JC, Holick MF, Grant WB, et al.. Epidemic influenza and vitamin D. *Epidemiol. Infect.* 2006;134:1129–40.

32. Sharon Greene. Influenza-associated mortality in the United States: spatio-temporal patterns related to climate and virus subtype. Doctoral dissertation. Ann Arbor, University of Michigan, 2008.

33. Hong Kong Observatory. http://www.hko.gov.hk/lrf/enso/enso-front.htm, accessed July 2010.

34. Wintertime East Asian Jet Stream and Its Association with the Asian-Pacific Climate. Yang Song, Lau K.-M., Kim K.-M. http://ntrs.nasa.gov/archive/nasa/casi.ntrs.nasa.gov/20000053089_2000036046.pdf, accessed July 2010.

35. Variations of the surface temperature in Hong Kong during the last century. Xiaoli Ding, Dawei Zheng, Song Yang. *Int. J. Climatol.* 2002; Vol 22, Issue 6, P 715–730.

36. http://www.cpc.ncep.noaa.gov/data/teledoc/pna.shtml, accessed July 2010.

37. http://www.cpc.noaa.gov/data/teledoc/wp.shtml, accessed July 2010.

38. Mantua NJ, Hare SR, Zhang Y, et al. A pacific interdecadal climate oscillation with impacts on salmon production. *B AM METEOROL SOC* 1997;78:1069-1079.

39. http://www.hko.gov.hk/climate_change/pdo_e.htm, accessed July 2010.

40. http://www.hko.gov.hk/wxinfo/climat/climahk.htm, accessed July 2010.

41. Jeffrey Shaman, Edward Goldstein, and Marc Lipsitch. Absolute humidity and pandemic versus epidemic influenza. *Am J Epidemiol.* 2011;173:127–135.

42. http://www.cdc.noaa.gov/ClimateIndices/Analysis/, accessed July 2010.

43. Curriero FC, Shone SM, and Glass GE. Cross correlation maps: a tool for visualizing and modeling time lagged associations. *Vector Borne Zoonotic Dis* 2005;5: 267-75.

44. RM Epan, RF Epan. The thermal denaturation of influenza virus and its relationship to membrane fusion. *Biochem. J.,* 2002;365:841-848.

45. Lowen AC, Steel J, Mubareka S, Palese P. High Temperature (30 C) blocks aerosol but not contact transmission of influenza virus. *J. Virol.* 2008;82: 5650–5652

46. Flahault A, Viboud C. Pakdaman K, Boelle P-Y, Wilson ML, Myers M, et al. Association on influenza epidemics in France and the USA with global climate variability. In: Kawaoka Y, editor. Proceeding of the International Conference on Options of the Control of Influenza V Held in Okinawa, Japan, October 7-11, 2003, International Congress Series 1263. San Diego, CA: Elservier Inc.,2004:73-7.

47. Eric H. Y. Lau, Benjamin J. Cowling, Lai-Ming Ho, and Gabriel M. Leung. Optimizing use of multistream influenza sentinel surveillance data. *Emerg. Infect. Dis.* 2008;Vol. 14, No. 7.

48. Radina P. Soebiyanto, Farida Adimi, Richard K. Kiang. Modeling and predicting seasonal influenza transmission in warm regions using climatological parameters. *PLoS ONE,* 2010;Vol.5:3;e9450.

49. D S Hui, J Woo, E Hui et al. Influenza-like illness in residential care homes: a study of the incidence, aetiological agents, natural history and health resource utilization. *Thorax* 2008;63;690-697;doi:10.1136/thx.2007.090951

50. Monto AS, Gravenstein S, Elliott M, Colopy M, Schweinle J. Clinical signs and symptoms predicting influenza infection. *Arch Intern Med* 2000;160:3243–3247.

51. El Nino and Human Health. Kovats RS. Bulletin of the World Health Organization 2000;78(9):1127-1133.

52. Gouveia N, Hajat S, Armstrong B. Socioeconomic differentials in the temperature mortality relationship in Sao Paula, Brazil. *Int J Epidemiol* 2003;32:390-397.

53. Kalkstein LS, Greene JS. An evaluation of climate/mortality relationships in large US cities and the possible impacts of a climate change. *Environ Health Perspect* 1997;105:84-93.

CHAPTER 5

REFLECTIONS ON THE POTENTIAL EFFECT OF ENVIRONMENT ON HUMAN INFLUENZA TRANSMISSION AND THE ASSOICATION BETWEEN CLIMATE AND INFLUENZA

SUMMARY OF MAJOR FINDINGS AND IMPLICATIONS

Annual influenza epidemics and potential pandemics are of great public health concern (1,2). Influenza virus is transmitted among humans through the environment, including air and fomites. In order to understand how human influenza virus transmission is environmentally mediated and to help inform the effective intervention strategies, we examined the role of the environment in influenza transmission, the temporal dynamics of the relative importance of different transmission modes, and the climatic factors that are associated with human influenza. The analyses set forth in this dissertation contribute to these objectives. We assess the different levels of details and heterogeneities by developing environmentally mediated influenza transmission models using mathematical compartmental models, agent-based models (ABM) and time series statistical models.

Chapter 2 developed an environmentally mediated influenza infection transmission system (EITS) deterministic compartmental model and its stochastic counterpart. This model showed that environment plays an important role in the influenza transmission process at population level. Previous influenza transmission

models assumed an instantaneous symmetric contact processes rather than pathogen transmission through the environment (3,4). Some studies considered the environmental effects in population infection transmission but lacked human activity details (5,6). The EITS model structure is relatively novel in the sense that pathogen transmission is explicitly formulated by parameterizing detailed human activities in the environment. We found that the environmental persistence ratio ($\rho N / \mu$, where μ is the pathogen elimination rate, ρ is the rate humans pick up pathogens, and N equals population size), an indicator of the importance of pick-up compared to environmental elimination of pathogens from the environment, indicates whether transmission is density dependent (low ratio), frequency dependent (high ratio), or in between. We also observed that the environmental contamination ratio (α / γ, where α is the pathogen deposit rate and γ is the recovery rate), a measure of the pathogen deposition magnitude from an infectious individual, reflects the probability of outbreak occurrence. These insights provide both a theoretical context to examine the role of the environment in pathogen transmission and a framework to interpret environmental data to inform environmental interventions.

Chapter 3 builds upon previous works by constructing a more detailed environmentally mediated influenza agent based model for an enclosed abstract venue and demonstrated the pre-unrecognized temporal dynamics of the relative importance of different influenza transmission modes over the course of epidemics. We found that the influenza virus particle dissemination and persistence processes were associated with the temporal variation of the relative importance of different influenza transmission modes. The temporal variation of the relative importance of different influenza transmission modes originates from the different dissemination and persistence assumptions for

different transmission modes. Changing dissemination and persistence model conformations can significantly influence this temporal variation. Model parameters, such as movement rate, surface touching rate and virus die off rate can mediate this temporal variation. These findings help convince researchers and public health policy makers to pay attention to the non-recognized phenomenon, and might point out new scientific directions for research in population based infection transmission.

Chapter 4 examined the seasonal patterns of influenza disease in an Asian subtropic metropolitan region and demonstrated the associations between influenza morbidity and local weather variables and global climate indices. Based on 11 years long time, better quality dataset, we confirmed a biannual epidemic pattern in 9 of the 11 study period years in Hong Kong, China. A new predominant influenza virus strain replacement generally was related to the second epidemic peak generally in early summer. Furthermore, we found significant statistical associations between influenza morbidity (virus positive proportion and influenza-like illness (ILI) proportion) and local weather variables/global climate indices. Absolute humidity (AH) was found to be the most significant one among all local weather variables. The negative AH anomaly is significantly related to the onset of influenza epidemics. This work is the first to observe statistical association between absolute humidity and influenza by using human influenza morbidity data.

We expect the results reported in this dissertation to contribute to building a better scientific basis for controlling influenza epidemics and the understanding of environmentally mediated influenza transmission system. By integrating environmental microbial transfer models into traditional population transmission dynamics, our results

strengthen infection disease epidemiological theory. These new influenza models are more realistic than previous ones, with direct, instantaneous contact among individuals and environment. Our findings concerning the importance of environment in human influenza transmission system, the temporal dynamics of the relative importance of different influenza transmission modes, and the relationship between climate and influenza could open new venues for influenza research. We provided scientific suggestions for improving public health surveillance of environmental exposures, infections, diseases and outbreaks, data collection and analysis for disease control purposes. Although we did not focus on specific intervention strategies, this work could help public health policy makers to develop influenza preparedness plans and rethink about the application of some non-pharmaceutical interventions such as hand washing, wearing masks, and environmental decontamination.

POTENTIAL LIMITATIONS

The relevant data from our literature review were not adequate for model parameterization in out research. For uninformed model parameters, such as virus die off rate on surfaces and in air, hand touching surface rate, transfer efficiency, and HID_{50} on upper respiratory track, we either tried the similar parameter from other pathogen studies or explored the wide parameter space. If future research indicates a significant difference from the parameter values we use here, the relative importance of different influenza transmission modes might change. Nevertheless, the observed impact of environment in human transmission infection and the temporal dynamics of the relative importance of different transmission modes should not be significantly biased.

The compartmental models in Chapter 2 provide useful insights but lack of details. The agent-based models in Chapter 3 capture a higher level of heterogeneity, but sometimes, it is nontrivial to explain the results. Overall, we use an assembly of models from a compartmental model to an agent base model, which handled different levels of heterogeneity. We believe these approaches are complementary in their ability to answer our research questions.

The influenza morbidity measurements used in our work were indicators based on ILI subpopulations from influenza surveillance systems rather than true influenza prevalence or incidence based on the general population. Sensitivity and specificity issues cannot be avoided when using these measurements. However, influenza VPP and ILI proportions can present true influenza dynamics and are among of the best available influenza indicators (7).

SUGGESTIONS FOR FUTURE RESEARCH

Inclusion of Multiple Transmission Modes in Deterministic Compartmental Models

Choice of different modeling approaches could be complex and problematic. If the model is too simple, it could ignore the important aspects from reality and may lead to wrong inferences. If the model is too complex, it could become impossible to accurately parameterize using available data (8). The compartmental models are computationally efficient and can provide insights into disease transmission processes and suggestions for disease control strategies. Classic compartmental models formulate instantaneous symmetric contact processes rather than pathogen transmission through the environment (3).

In Chapter 2, as a first step to examine the environmentally mediated influenza transmission theoretically, an ordinary difference equation based deterministic compartmental model was developed. Although, in real world, influenza transmission among humans operates through multiple transmission modes simultaneously, we formulated each transmission mode separately for respiratory, frequently touched surfaces and infrequently touched surfaces transmission; in order to simplify and better understand each transmission mode. To examine relative importance of different influenza transmission modes and to provide potential effective public health intervention suggestions, more detailed reality and multiple transmission modes should be incorporated in compartmental models for future work. As in some previous studies on water-borne transmitted infections (5), multiple transmission modes models could simulate epidemics with more realistic assumptions, and provide better references. Compartmental models with multiple transmission modes enable us to study the relative importance of different transmission modes in a computationally efficient way comparing to agent-based model.

Consideration of Multiple Influenza Virus Strains and Human Immunity Status in Deterministic Compartmental Model

As described in Chapter 4, the temporal pattern of influenza cases can appear as a single unimodal peak, a single wide plateau-shaped peak, or as double peaks in tropic/subtropic regions due to co-circulation of different influenza virus strains. Influenza seasonality has been modeled in many different ways. Seasonality of infectious diseases has been formulated as sinusoidal term of transmission probability

(9,10). Weber *et al.* and Earn *et al.* used a time term to formulate the seasonal transition, and they suggested that a realistic seasonal function is more important than explicit modeling heterogeneous transmission (11,12). Shamman *et al.* has considered a transmission probability based on absolute humidity (AH) to model influenza mortality in North America (13). Lin *et al.* concluded that herd immunity can lead to sustained oscillations in a system with three interacting influenza A strains (14). Hay *et al.* noted that moderate levels of cross-immunity among antigenically diverse pathogens could lead to sustained cyclical or chaotic dynamics (15). However, these previous investigations did not include weather variables as drivers of influenza morbidity while considering data on multiple influenza strains.

Future research could incorporate multiple influenza strains, seasonal weather drivers such as AH, and host immunity status. This type of deterministic compartmental model could not only simulate the findings from real data, but also could help us understand whether a specific type of seasonality appears to be based on weather force and strain genetic variation conditions.

Consideration of Heterogeneity of Environment Surfaces and Non-random Movement in the Agent Based Model (ABM)

ABM is a natural extension of ODE models and may deal with population and environmental heterogeneity better in influenza transmission. Influenza transmission is affected by multiple factors such as individual immunity status, social connection, pathogen features, and environmental factors. Environmental venue factors include venue size and venue locus connection patterns. Pathogen factors may involve

survivability, dose-response, and dispersion of virus particles. Population factors can encompass population density, human picking up and depositing, and human movement patterns within the venue. The EITS agent based model developed in Chapter 3 captures specific aspects of reality and certain degrees of heterogeneity. However, in order to make the mechanism behind the temporal dynamics of the relative importance of different influenza transmission modes clearer, we intentionally avoided some realistic complexities. Specifically, the model is limited to capture heterogeneity of surface locus and non-random movement patterns in reality, which could be important in determining the relative importance of different influenza transmission modes.

Future environmentally mediated influenza ABMs might include these extra complexities. The environmental locus could be classified as individual locus and public locus. An individual locus refers to places like an individual workstation, where individuals spend most of their time and touch the surface at relative high frequency. A public locus refers to places like cafeterias, restrooms or other sites where many people come and stay for a relatively short time period. Individuals touch public locus surfaces at relative low frequency, but the total touching by all people on these surfaces is high. Individuals can move between individual locus and public locus based on their daily schedule. In this way, individuals do not expose to viral particles in public place all the time as simulated in the ABM reported in Chapter 3. We can study the importance of global and local high frequency touched surfaces as described in Chapter 2. This model conformation might help to provide useful suggestions on where and how often to apply environmental decontamination interventions.

Consideration of Multiple Venues and Movement Patterns among Them in Influenza Agent Based Model

The ABM developed in Chapter 3 simulates influenza infection transmission inside a single abstract venue such as an open office complex or conference room. In reality, influenza transmission and disease epidemics happen in multiple venues such as schools, households, and clinics (16). Venues usually have different roles in infection transmission processes. Some venues directly connect and disseminate infection to many other venues, some contribute to explosive epidemics, some sustain chains of transmission over a longer term, others provide key bridges between venues, and some are dead ends that do not contribute to sustained chains of transmission. When confronting emerging infections affecting multiple venues, field epidemiologists have to make effective public health decisions in a limited time. These public health decisions regarding influenza infections usually include choosing the correct specific venues to control, cutting off venue connections, employing the appropriate control strategies at the right time, focusing on specific population groups and so on. Potential interventions that have been suggested for influenza controlling include hand washing, mask use, environment decontamination, ultraviolet radiation, and increased airflow exchange. Practically, there are no clear guidelines on how to make these decisions. Scientifically, the theoretical basis for investigating the choice of actions in realistic multiple venue settings is inadequate.

To provide scientific suggestions regarding how to determine the most important venues, specific characteristics of venues and venue connection patterns, human movement flow among multiple venues, environmentally mediated ABMs in multiple

venues should be considered in future work. This multiple venue ABM captures the specific aspects of reality that single venue models ignore such as venue connection pattern, and detailed human movement patterns among venues. This multiple venue model could help clarify various theoretical venue connection patterns and evaluate differences in focused interventions on specific venues. The multiple venue models could help us examine specific control decisions and provide principles to choose places where large numbers of individuals expose environmental contamination or to focus control on sites that act to disseminate infection to other sites.

Inclusion of Weather Variable Effects in the Agent Based Infection Transmission Model

The ABM developed in Chapter 3 simulates environmentally mediated influenza transmission in indoor environments. The impact of weather variables on influenza transmission and on the outbreak probability was not considered in previous ABM. Previous studies and our work in Chapter 4 have shown that absolute humidity (AH) is associated with influenza transmissibility and influenza outbreak probability (15,17). Absolute humidity seems to be an important determinant of virus survival in air. By including AH, temperature in environmentally mediated model analyses, we can examine how raising and lowering the virus survival in air affects the timing of respiratory transmission. Given the delayed nature of respiratory transmission mode compared to droplet spray mode postulated in Chapter 3, a transient period of low absolute humidity might modify the temporal variation of the relative importance of different influenza transmission modes.

Consideration of Influenza Morbidity Measurement Based on Different Population Groups

The work in Chapter 4 analyzed influenza morbidity data, which may have inaccuracies because of the diagnosis of ILI and the selective submission of isolates from diagnosed ILI cases that relies on physician reporting as part of the existing influenza surveillance system. There are inconsistences of reporting, because physicians tend to over-report during epidemic periods and under-report during non-epidemic periods (18). Clinical symptoms and severity are different among different influenza types, and vary by age group. The public health reporting system commonly captures data on individuals with particular behavior patterns and access to medical services in the surveillance system (19). Physician-collected specimens usually have low capacity to present population-based disease prevalence (20). Therefore, population-level influenza virological data will be better to provide more precise measures.

However, comprehensive, ongoing population influenza viral surveillance is not practical and not available. An alternative involving influenza virological surveillance, that covered all outpatients and inpatients with ILI in local hospitals, could be a more accurate data source (21). Based on the assumptions concerning the stability and representability of the patient population being seen in the hospital, similar analyses using such hospital-based virological data might be further generalized and could be useful to confirm our findings.

REFERENCES

1. CDC. Flu in the United Staes. http://ww.cdc.gov/flu/. National Center for Infectious Disease, 2009.

2. Kilbourne ED: Influenza New York: Plenum Press; 1987.

3. Anderson RM, May RM. Infectious Diseases of Humans Dynamics and Control. Oxford University Press; 1992.

4. Diekmann O, Heesterbeek JAP. Mathematical Epidemiology of Infectious Diseases. John Wiley & Sons. Inc.; 2000.

5. Joseph N.S. Eisenberg, et al., Disease Transmission Models for Public Health Decision Making: Analysis of Epidemic and Endemic Conditions Caused by Waterborne Pathogens. *Environ Health Perspect* 2002;110(8):783:90.

6. Richard I. Joh, HaoWang, Howard Weiss, Joshua S. Weitz. Dynamics of Indirectly Transmitted Infectious Diseases with Immunological Threshold. *Bull Math Biol*. 2009;71: 845–862. DOI 10.1007/s11538-008-9384-4.

7. Monto AS, Gravenstein S, Elliott M, Colopy M, Schweinle J. Clinical signs and symptoms predicting influenza infection. *Arch Intern Med* 2000;160:3243–3247.

8. Koopman, JS. Modeling Infection Transmission. *Annu. Rev. Public Health*. 2004; 25: 303-326.

9. Simonsen L, Clarke MJ, Williamson GD, et al. The impact of influenza epidemics on mortality: introducing a severity index. *Am J Public Health* 1997;87:1944–50.

10. Donald R. Olson, Lone Simonsen, Paul J. Edelson and Stephen S. Morse. Epidemiological evidence of an early wave of the 1918 influenza pandemic in New York City. *PNAS* 2005; vol.102 no. 31, p1059-11063. doi: 10.1073/pnas.0408290102

11. Weber A, Weber M, Milligan P. Modeling epidemics caused by respiratory syncytial virus (RSV). *Math. Biosci* 2001;128(4);845-859.

12. Earn DJD, Rohani P, Bolker BM, Grenfell BT. A simple model for complex dynamical transitions in epidemics. *Science* 2000;287:667-670.

13. Jeffrey Shaman, Virginia E. Pitzer, Ce´ cile Viboud, Bryan T. Grenfell, Marc Lipsitch. Absolute Humidity and the Seasonal Onset of Influenza in the Continental United States. *PLoS Biology*, 2010, Vol. 8, Issue 2; e1000316.

14. Lin J, Andreasen V, Levin SA. Dynamics of influenza A drift: The linear three-strain model. *Math. Biosci* 1999;162:33-51.

15. Hay SI, Myers MF, Burke DS, Vaughn DW, Endy T, Ananda N, et al. Etiology of interepidemics perods of mosquito-born disease. *PNAS* 2000;97(16):9335-9339.

16. Eubank S, Guclu H, Kumar VSA, et al. Modelling disease outbreaks in realistic urban social networks. *Nature.* 2004;429:180-184.

17. Jeffrey Shaman, and Melvin Kohn. Absolute humidity modulates influenza survival, transmission, and seasonality. *PNAS*, 2009; vol. 106; 9:3243–3248.

18. Fleming DM, Zambon M, Bartelds AIM. Population estimates of person presenting to general practitioners with influenza-like illness, 1987-96: A study of the demography of influenza-like illness in sentinel practice networks in England and Wales, and in The Netherlands. *Epidemiol Infect* 2000;124:245-253.

19. Hajat S, Anderson HR, Atkinson RW, Haines A. Effects of air pollution on general practitioner consultations for upper respiratory diseases in London. Occup Environ Med 2002;59;294-299.

20. Monto AS, Koopman JS, Ira M. Longini J. Tecumseh study of illness: XIII. Influenza infection and disease, 1976-1981. *Am J of Epidemiol.* 1985;121(6):811-822.

21. Paul K.S. Chan, H.Y. Mok, T.C. Lee, Ida M.T. Chu, W.Y. Lam, Joseph J.Y. Sung. Seasonal influenza activity in Hong Kong and its association with meteorological variations. *J. Med. Virol.* 2009;1797-1806, 81(10).